Aus der Klinik für Allgemein-, Viszeral- und Transplantationschirurgie

der Chirurgischen Universitätsklinik

der Ruprecht-Karls-Universität Heidelberg

Direktor: Prof. Dr. med. Dr. h.c. mult. M.W. Büchler

Glutamine-Dependent de novo Synthetic Asparagine via ATF4/ASNS/eIF4F Complex Axes for Homeostatic Regulation in Hepatocellular Carcinoma responding to Endoplasmic Reticulum (ER) Stress

Inauguraldissertation

zur Erlangung des Doctor scientiarum humanarum

der Medizinischen Fakultät

der Ruprecht-Karls-Universität Heidelberg

vorgelegt von

Kai Wei

aus Volksrepublik China

2019

Dekan: Herr Prof. Dr. med. Andreas Draguhn
Doktormutter: Frau Prof. (apl.) Dr. med. Katrin Hoffmann

Dedicated to my Family, Teachers and Friends

DECLARATION

I hereby declare that this PhD. thesis is the result of my own work under the supervision of Prof. (apl.) Dr. med. Katrin Hofmann, and I used no other than the indicated references and resources. All the information that has been taken directly or indirectly from other sources is indicated as such.

Heidelberg, 01.06.2019

KAI WEI

LIST OF CONTENT

LIST OF ABBREVIATIONS

Abbrevations	Full name
4EBP1	4E-binding protein 1
A	Alanine
AKT	Protein Kinase B
ASCT2	Alanine, Serine, Cysteine Transporter 2
ASNS	targets asparagine synthetase
ATF4	activating transcription factor-4
ATF6	activating transcription factor-6
ATF6f	transcriptional activator domain of ATF6
ATP	adenosine triphosphate
BCA	bicinchoninic acid assay
BSA	Bovine Serum Albumin
bZIP	basic Leu zipper
c-Myc	a family member of regulator genes and proto-oncogenes Myc
C/EBPα	CCAAT enhancer binding protein-α
C/EBPβ	CCAAT enhancer binding protein beta
Caspase-8	apoptosis-Related Cysteine Peptidase 8
cDNA	Complementary deoxyribonucleic acid
CHOP	C/EBP-homologous protein
Cocl2	Cobalt(II) chloride
CRISPR/Cas9	clustered regularly interspaced short palindromic repeats
CTLA-4	cytotoxic T-lymphocyte-associated antigen 4
D	Aspartic acid
DAPI	4′,6-diamidino-2-phenylindole
DEB-TACE	TACE with drug-eluting beads
DEPC	Diethyl pyrocarbonate
DMEM	Dulbecco's Modified Eagle Medium
DMSO	dimethyl sulfoxide
dNTP	deoxynucleoside triphosphate
DTT	Dithiothreitol
E	Glutamic acid
EDTA	Ethylenediaminetetraacetic acid
eIF1	eukaryotic translation initiation factor 1
eIF1A	eukaryotic translation initiation factor 1A
eIF2	eukaryotic Initiation Factor 2
eIF2a	Eukaryotic translation initiation factor 2a
eIF3	eukaryotic translation initiation factor 3
eIF4E	eukaryotic initiation factor 4E
eIF4F	eukaryotic initiation factor 4F
eIF4G	eukaryotic translation initiation factor 4G
eIF5	eukaryotic translation initiation factor 5
eIFs	eukaryotic translation initiation factors
EMT	epithelial-mesenchymal transition
ER	Endoplasmic reticulum
ERAD	ER-associated degradation
ERK	Extracellular signal-Regulated Kinases

Ets	Transcription factor E-twenty six
FACS	Fluorescence-activated cell sorting
FADD	Fas-associated protein with death domain
FBS	fetal bovine serum
FC	fold change
FCS	Fetal Calf Serum
FITC	Fluorescein isothiocyanate
G	glucose
GAPDH	glyceraldehyde 3-phosphate dehydrogenase
GCN2	general control nonderepressible 2
GDC	Genomic DNA Control
GFP	green fluorescent protein
GLS1	glutaminase I
GTP	guanosine-5'-triphosphate
HCC	Hepatocellular carcinoma
HCl	Hydrochloric acid
HIF-1α	hypoxia-inducible factor 1-alpha
HPG	L-homopropargylglycine
IC50	half maximal inhibitory concentration
IF	immunofluorescence
IRE1	inositol-requiring protein-1
LC-MS	Liquid chromatography–mass spectrometry
LDS	Lithium dodecyl sulfate
MAPK	mitogen-activated protein kinase
MEK	Mitogen-activated protein kinase kinase
MNK	MAP kinase interacting serine/threonine kinase
mTOR	Mammalian target of rapamycin
mTOR	mammalian target of rapamycin
mTORC1	mTOR complex 1
mTORC2	mTOR complex 2
MTT	3-(4,5-dimethylthiazol-2-yl)-2,5-diphenyltetrazolium bromide
N	asparagine
Nacl	Natriumchlorid
NAD+	nicotinamide adenine dinucleotide
NADP+	nicotinamide adenine dinucleotide phosphate
NADPH	nicotinamide adenine dinucleotide phosphate
NEAA	unnecessary amino acids
NF-κB	nuclear factor kappa-light-chain-enhancer of activated B cells
NSCLC	Non-small-cell lung carcinoma
OD	optical density
P	Proline
p-4EBP1	phosphorylated 4E-binding protein 1
p-AKT	phosphorylated protein kinase B
p-eIF4E	phosphorylated eukaryotic initiation factor 4E
p-mTOR	phosphorylated mammalian target of rapamycin
p-TSC2	phosphorylated tuberous Sclerosis Complex 2
p70 S6K	Ribosomal protein S6 kinase beta-1

p70S6K1/2	Ribosomal protein S6 kinase beta-1/2
PAGE	polyacrylamide gel electrophoresis
PBS	Phosphate Buffered Saline
PCR	Polymerase chain reaction
PD-1	anti-programmed cell death protein 1
PD-L1	anti-programmed cell death protein ligand 1
PDCD4	Programmed Cell Death 4
PERK	protein kinase RNA (PKR)-like ER kinase
PI	propidium iodide
PI3K	Phosphoinositide 3-kinase
PIC	pre-initiation complex
PKR	protein kinase RNA
PLA	Proximity Ligation Assay
PS	phosphatidylserine
Q	glutamine
qPCR	Quantitative PCR
RAF	Rapidly Accelerated Fibrosarcoma
RAS	Rat Sarcoma
Reg	Regorafenib
RFA	radiofrequency ablation
RIDD	IRE1-dependent mRNA decay
RIPA	Radioimmunoprecipitation assay
RNA	Ribonucleic acid
S1P	site 1 protease
S2P	site 2 protease
SDS	sodium dodecyl sulfate
shRNA	Short hairpin RNA
Sir t1	Silent mating type information regulation 2 homolog- 1
Sir t2	Silent mating type information regulation 2 homolog- 2
Sir t3	Silent mating type information regulation 2 homolog- 3
siRNA	Small interfering RNA
SIRT	selective internal radiation therapy
SLC	solute carrier family of proteins
SLC1A5	solute Carrier Family 1 Member 5
SLC38A2	solute Carrier Family 38 Member 2
Sor	Sorafenib
Sp1	specificity protein 1
spectrila	L-Asparaginase
Stat3	Signal Transducer And Activator Of Transcription 3
sXBP1	Spliced X box-binding protein 1
TACE	trans-arterial chemoembolization
TAE	trans-arterial embolization
TARE	Trans-arterial radioembolization
TBS	Tris-buffered saline
TBST	TBS+Tween
TC	a ternary comp
TCA cycle	tricarboxylic acid cycle
TKI	tyrosine kinase inhibitor
TKIs	tyrosine kinase inhibitors

TSC2	tuberous Sclerosis Complex 2
UPR	unfolded protein response
UTR	untranslated region
V9302	(S)-2-Amino-4-(bis(2-((3-methylbenzyl)oxy)benzyl)amino)butanoic acid
XBP1	X box-binding protein 1

LIST OF IMAGES AND FIGURES

1. INTRODUCTION

1.1 Hepatocellular Carcinoma

Hepatocellular carcinoma (HCC) is the fifth most common tumor and the second most common cause of cancer-related death worldwide(Torre *et al.*, 2015). The male-to-female predominance is greater than 2:1(Bruix *et al.*, 2011). East and South Asia plus sub-Saharan Africa are the regions of highest incidence, followed by Southern Europe and North America. Overall the numbers of HCC are increasing worldwide since it is clearly linked to the metabolic syndrome and NASH (Bruix *et al.*, 2011; Heimbach *et al.*, 2018; Siegel and Zhu, 2009).

1.2 Treatment of Hepatocellular Carcinoma

Multiple treatment options are available for HCC including curative resection, liver transplantation, radiofrequency ablation (RFA), trans-arterial embolization (TAE)/trans-arterial chemoembolization (TACE), radioembolization, systemic targeted agents like Sorafenib and Regorafenib, and recent immune checkpoint inhibitors such as anti-PD-1/PD-L1 or CTLA-4 antibodies. The treatment of HCC depends on the tumor stage, patients` performance status, and liver function. Despite those plenty treatment options, the prognosis of HCC is dismal with 5-year overall survival rates of 18%(Altekruse *et al.*, 2012).

Due to its high recurrence rate and resistance to most known treatment options it requires a multidisciplinary approach.

1.2.1 Surgical treatment

Surgical resection is the optimal treatment for a small number of patients with single nodules, good liver function and no underlying cirrhosis. Only patients with well-compensated cirrhosis, Child-Pugh class A, are considered the candidates for surgical resection based the concerning of high risk of post-operative hepatic decompensation(Beard *et al.*, 2013; Bhoori

et al., 2007). If stringent pre-operative selection criteria are followed, the patients have nearly 70% five-year survival but with a high risk of recurrence. Early tumor recurrence within two years of surgery is mainly related to local invasion and intrahepatic metastasis. Late recurrence, occurring more than two years after surgery, is mainly related to de novo tumor formation(Cucchetti *et al.*, 2009; Mazzaferro *et al.*, 2006; Xia *et al.*, 2010). For the patients with early-stage HCC, surgical resection is the recommendable approach treatment, which should be weighed against the availability and the response rate of other local ablative therapies like radiofrequency ablation.

1.2.2 Radiofrequency Ablation

RFA, the most effective local ablative therapy, is considered a standard treatment for the patients with early stage (BCLC 0-A) tumors when they are not suitable for surgery(Livraghi *et al.*, 2008). Compared with surgical resection, RFA is less invasive, lower complication rates and shorter hospital duration with inexpensive consumption. However, RFA is size and tumor location-dependent, in patients with tumor > 3 cm but < 5 cm in size, or with tumor close to important blood vessels, the success rate of RFA alone is decreased.

1.2.3 Trans-Arterial Embolization and Trans-Arterial Chemo-Embolization

TAE and TACE are widely used as a standard treatment for the patients with intermediate-advanced stage HCC, especially for unresectable patients. Improved survival has been demonstrated, compared to the best placebo care(European Association For The Study Of The *et al.*, 2012; Forner *et al.*, 2012). However, the heterogeneity of different tumor burden, the chemo-resistance from liver cancer, the risk of TACE/TAE- associated complications, and the lack of standardized chemical therapy regimen for TACE limited the application of conventional TAE and TACE(Lanza *et al.*, 2016; Raza and Sood, 2014). The usage of TACE with drug-eluting beads (DEB-TACE) in recent years diminishes the amount of

chemotherapeutic agent that reaches the systemic circulation and increases the local concentration of the drug and the antitumor efficacy, which is superior to the conventional TACE(Bonomo *et al.*, 2010; Song *et al.*, 2012).

1.2.4 Trans-Arterial Radioembolization

Recently, Trans-Arterial Radioembolization (TARE) or Selective Internal Radiation Therapy (SIRT) is an emerging modality that has achieved promising results for intermediate-advanced HCC(Sangro *et al.*, 2011; Shah *et al.*, 2011; Sieghart *et al.*, 2013). In contrast to TAE and TACE, TARE achieves cell death by local radiation damage via smaller 35 μm diameter implantable radioactive microspheres being delivered into the tumor arteries, which considered to be a form of brachytherapy with no significant embolic effect(Salem *et al.*, 2011; Sangro *et al.*, 2011; Sangro *et al.*, 2012). Currently, the most popular radioembolization technique uses microspheres coated with Y90 b-emitting isotope (TheraSphere and SIR Sphere) and is investigated in phase II clinical trials (Mazzaferro *et al.*, 2013).

1.2.5 Liver transplantation

Liver transplantation for HCC has the goal to eliminate the tumor itself as well as the tumor-generating environment of cirrhosis and providing the widest surgical margin possible. Therefore, it not only reduces true recurrences but also protect from de novo tumorigenesis(Sapisochin and Bruix, 2017). It is the best treatment option for patients with early-stage tumor. However, the shortage of available organ donors imposes the application of restrictive criteria to secure the optimal use of the available livers (Mazzaferro *et al.*, 1996).

1.2.6 Systemic Therapy

The vast majority of HCC patients is diagnosed in an advanced stage with impaired liver function. For those patients and patients with recurrent disease after local therapies systemic treatment options are needed. Sorafenib, the first FDA approved multikinase inhibitor for patients with advanced HCC, was shown to prolong survival in SHARP and Oriental trials (Cheng *et al.*, 2009; Llovet *et al.*, 2008). However, Sorafenib does not show the same effect in all HCC patients, and the average prolongation of overall survival was just 3.8 months (Llovet *et al.*, 2008). More and more studies demonstrated that small-molecule target inhibitors resistance occurred in cancer treatment, including HCC resistance to Sorafenib (Berasain, 2013; Ebos *et al.*, 2009; Paez-Ribes *et al.*, 2009; Zhai and Sun, 2013). Recent studies demonstrated that the second-line agent Regorafenib can bring survival benefits to patients with acquired Sorafenib resistance (Bruix *et al.*, 2017; Wilhelm *et al.*, 2011). However, Regorafenib is not suitable for the treatment of patients with primary Sorafenib resistance, and a second-line treatment for this subgroup of patients remains an unmet need (Bruix *et al.*, 2017). For these reasons, an effective treatment with a well-tolerated pharmaceutical profile is requested for advanced HCCs.

With the recent FDA approval of the second line anti-programmed cell death protein 1 (PD-1)/anti-programmed cell death protein ligand 1 (PD-L1) or cytotoxic T-lymphocyte-associated antigen 4 (CTLA-4) inhibitor, immunotherapy might be a potential novel treatment option for patients with HCC (Calderaro *et al.*, 2016; El-Khoueiry *et al.*, 2017; Makarova-Rusher *et al.*, 2015; Truong *et al.*, 2016). However, there is increasing evidence on the occurrence of adaptive resistance and treatment costs are extremely high. To justify and monitor the treatment with these agents appropriate biomarkers need to be established (Koyama *et al.*, 2016).

1.3 Endoplasmic reticulum (ER) stress and tumor

Various treatments would trigger endoplasmic reticulum (ER) stress within the tumor cells. The ER is the organelle in which transmembrane proteins and proteins that are going to be secreted are synthesized and folded (Hetz, 2012). Many stressful conditions on cells, including hypoxia, nutrition deprivation, inflammation, infections, and changes in cell microenvironment, challenge the folding capacity of the cell and promote ER stress (Hetz, 2012; Hetz *et al.*, 2015). The unfolded protein response (UPR), a homeostatic signaling network, buffers and orchestrates the recovery of ER function. However, when this fails, ER stress will result in apoptosis(Hetz, 2012; Hetz *et al.*, 2015; Ron and Walter, 2007; Walter and Ron, 2011).

1.3.1 The mechanism of unfolded protein response (UPR)

Three different classes of ER stress sensors have been identified, each one is a distinct arm of the UPR that is mediated by inositol-requiring protein-1 (IRE1), activating transcription factor-6 (ATF6) or protein kinase RNA (PKR)-like ER kinase (PERK) (Ron and Walter, 2007). Theses distinct branches of the UPR regulate the expression of numerous genes that maintain homeostasis in the ER or induce apoptosis if ER stress remains unmitigated (Walter and Ron, 2011).

1.3.1.1 IRE1

The IRE1 branch is the most conserved branch of the UPR in eukaryotes from yeast to mammals(Mori, 2009). This multidomain protein is a kinase and also an endoribonuclease, under ER stress conditions, it dimerizes and autotransphosphorylates. The RNAse activity of IRE1 can participate in RNA degradation to reduce protein synthesis, a process known as regulated IRE1-dependent mRNA decay (RIDD) (Hollien and Weissman, 2006). Active IRE1α processes the mRNA encoding the transcription factor X box-binding protein 1

(XBP1), excising a 26-nucleotide-long intron that shifts the coding reading frame of this mRNA, resulting in the formation of spliced XBP1 (sXBP1), which translocate to the nucleus to induce the upregulation of its target genes, the protein products of which operate in ER-associated degradation (ERAD), the entry of proteins into the ER and protein folding (Acosta-Alvear *et al.*, 2007; Calfon *et al.*, 2002; Lee *et al.*, 2002; Yoshida *et al.*, 2001).

1.3.1.2 ATF6

ATF6 is a transmembrane protein with a cytoplasmic portion that has a basic Leu zipper (bZIP) transcription factor and is localized at the ER in unstressed cells (Haze *et al.*, 1999; Zhang *et al.*, 2006). Under ER stress, ATF6 are delivered to the Golgi apparatus, where it is processed by site 1 protease (S1P) and S2P. ATF6 then releases its cytosolic domain fragment (ATF6f) to target UPR proteins, such as chaperones, and to control the upregulation of genes encoding ERAD components and also XBP1(Shen *et al.*, 2002; Walter and Ron, 2011; Yamamoto *et al.*, 2007; Ye *et al.*, 2000).

1.3.1.3 PERK

PERK, an ER-located transmembrane kinase, oligomerizes and phosphorylates itself and the ubiquitous translation initiation factor Eukaryotic translation initiation factor 2a (eIF2a), indirectly inactivating eIF2 and inhibiting mRNA translation to reduce the flux of protein entering the ER to alleviate ER stress (Harding *et al.*, 2009; Marciniak *et al.*, 2004; Tsaytler *et al.*, 2011). When phosphorylation of eIF2α is inhibited, PERK leads to the selective translation of the mRNA encoding the transcription factor ATF4. ATF4 controls the levels of pro-survival genes that are related to redox balance, protein synthesis and secretion, amino acid synthesis and transport, and the autophagy gene that is related to the pro-apoptotic transcription factor C/EBP-homologous protein (CHOP) (Ameri and Harris, 2008; Han *et al.*, 2013; Harding *et al.*, 2003; Schroder and Kaufman, 2005).

1.3.2 UPR involvement in intra-and extra-cellular environment adaption

Recent studies demonstrated that cancer cells with constitutive or acquired resistance to the small-molecule tyrosine kinase inhibitor (TKI) Sunitinib are also resistant to ER stress-triggered cell death (Holohan *et al.*, 2013; Pi *et al.*, 2014; Salaroglio *et al.*, 2017; Visioli *et al.*, 2014). ATF4, a biomarker of a poor prognosis in breast cancer, is involved in leading to autophagy completion and inducing cell death resistance (Notte *et al.*, 2015). It is discussed to be the potential mechanism of combined TKI and ER stress-triggered cell death resistance. Previous work has suggested both, pro- and anti-oncogenic roles for ATF4. One hand, ATF4 promotes tumor growth and metastasis in fibrosarcoma xenograft mice; upregulates genes correlated with poor prognosis; and targets the asparagine synthetase (ASNS) regulated asparagine biosynthesis which contributes to apoptotic suppression in Non-small-cell lung carcinoma (NSCLC) (DeNicola *et al.*, 2015; Dey *et al.*, 2015; Ye *et al.*, 2010). Furthermore, ATF4 maintains the serine dependent cell cycle by upregulating serine biosynthetic enzymes upon starvation (Gwinn *et al.*, 2018; Ye *et al.*, 2012). In contrast, ATF4 inhibits tumor growth in neuroblastoma and targets genes of CHOP promoted apoptosis (Qing *et al.*, 2012). Among them, ATF4 regulates the expression of genes involved in multiple amino acid synthesis and transport pathways (Gwinn *et al.*, 2018; Ye *et al.*, 2012).

1.4 Amino acid and tumor

Tumor cells show an increased nutrition uptake to support macromolecular biosynthesis and cell proliferation (Cantor and Sabatini, 2012; Hanahan and Weinberg, 2011; Ward and Thompson, 2012). In particular, it is becoming more apparent that amino acid metabolism is critical to support cellular functions via alterations in pathways, such as the Mammalian target of rapamycin (mTOR) pathway that couples amino acid availability to cell growth and autophagy (Jewell *et al.*, 2013). Many amino acids cannot be synthesized by the cell, and therefore their uptake is essential for protein biosynthesis and cell viability (Eagle, 1955).

Among these essential amino acids are glutamine and asparagine, on which tumor cells exhibit increased dependency (DeBerardinis *et al.*, 2007; Krall *et al.*, 2016).

1.4.1 Glutamine metabolism in cancer

Glutamine is the most abundant and highly consumed amino acid in the plasma. It is a well-known nutrient used by tumor cells to increase proliferation as well as survival under metabolic stress conditions (Hensley *et al.*, 2013; Yang *et al.*, 2009). The evolutionarily redundant families of transporters expressed on the cancer cell surface known as the solute carrier family of proteins (SLC), such as SLC1A5 and SLC38A2, have been implicated to sequester glutamine from the extra cellular space (Hassanein *et al.*, 2015; Jeon *et al.*, 2015; Pochini *et al.*, 2014; Schulte *et al.*, 2018). The functions of glutamine include its conversion to glutamate as a metabolic intermediate to be channeled into the TCA cycle, its function as a precursor for the biosynthesis of nucleic acids, certain amino acids, and glutathione, as well as its role as regulator in cellular redox homeostasis through a variety of mechanisms (Altman *et al.*, 2016b; Lu *et al.*, 2010). Therefore, therapeutic suppression of the glutamine metabolism is considered recently to be an attractive anticancer strategy (Choi and Park, 2018).

1.4.2 Asparagine metabolism in cancer

The biosynthesis of asparagine is tightly linked to the glutamine/glutamate and TCA cycle metabolism (Krall *et al.*, 2016; Tsun and Possemato, 2015). Its de novo synthesis requests the unidirectional and ATP-dependent ASNS activity that synthesizes asparagine utilizing nitrogen from glutamine in the cytoplasm. There the TCA cycle intermediate oxaloacetate and glutamate derived nitrogen mitochondrial aspartate can be transported (Milman and Cooney, 1979; Safer *et al.*, 1971).

Unlike other amino acids, Asparagine, which is abundant in the circulation, is only used for protein and nucleotide biosynthesis, and cellular pathways regulation. It is never an intermediary metabolite, but a mediator in cellular homeostasis. This is the potential mechanism through which asparagine suppresses the apoptosis (Ubuka and Meister, 1971; Zhang *et al.*, 2014). The importance of asparagine for tumor growth has been demonstrated by the effectiveness of extracellular L-asparaginase in treating leukemia. Here the asparagine is depleted from the circulation by converting it to aspartate (Broome, 1963; Clavell *et al.*, 1986). Notably, although asparaginase is effective as a therapeutic for cells that obtain the majority of their asparagine from the environment, cancer cells that are capable of synthesizing asparagine de novo via ASNS are less responsive to asparaginase therapy (Lorenzi *et al.*, 2008). Future studies on the clear mechanism of apoptosis suppression of asparagine and application of asparagine depletion on cancer treatment are expected.

1.5 Protein synthesis and tumor

Increasing evidence suggests that dysregulation of the protein synthesis plays a pivotal role in tumorigenesis. Protein biosynthesis is strictly regulated by multiple steps, which occur principally during transcription and translation (Kafri *et al.*, 2016). In eukaryotes, protein translation takes place in the cytoplasm, where ribosomes assemble amino acids into polypeptides following the decoded mRNA, and is divided into four phases: initiation, elongation, termination and recycling (Vincent *et al.*, 2016). The 5'cap structure of mRNA consists of a 7-methylguanosine residue, which is critical for the recognition by ribosomes. There are two different patterns of eukaryotic translation initiation: cap-dependent initiation and cap-independent initiation. Over 90 % of mRNAs are translated through cap-dependent initiation in eukaryotic cells (Walters and Thompson, 2016). Inhibition of cap-dependent initiation is crucial for the translational control cancerous cells under chemotherapy; because

initiation is the rate-limiting step of the eukaryotic translation of most of the mRNA (Vincent *et al.*, 2016).

The eukaryotic initiation factor-4F (eIF4F) complex plays a key role in the regulation of the translation process. Many studies demonstrated that the abnormal expression or activation of eIF4F complex is closely related to tumor formation and development (Oblinger *et al.*, 2016; Pelletier *et al.*, 2015). The eIF4F complex is composed of the cap-binding protein eIF4E regulated by mTOR dependent factor 4E-binding protein 1(4EBP1), the RNA helicase eIF4A, and the multidomain adaptor protein eIF4G (Gingras *et al.*, 1999; Hsieh *et al.*, 2010; von der Haar *et al.*, 2004) (Figure 1).
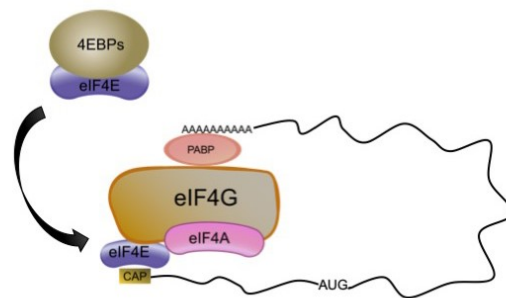
Figure 1. The structure of eIF4F complex. The eIF4F complex consists of three proteins: the cap-binding protein eIF4E, the DEAD box RNA helicase eIF4A, and the scaffolding protein eIF4G. 4EBP1, which is binding with eIF4E initially, negatively regulates eIF4E. Phosphorylation of 4EBP1 dissociates from eIF4E, allowing translation initiation complex formation at the 5' end of messenger RNAs. (Own Created Image)

1.5.1 eIF4F Complex and protein translation

In eukaryotes a set of initiation factors (eIFs) are required to dissociate the 40S and 60S ribosomal subunits, to recruit the mRNA and initiator tRNA to the 40S subunit, and to promote the joining of the 60S subunit so that elongation can commence(Dever, 2002). First,

a ternary complex (TC) is build up with eIF2 (including α, β and γ subunits), initiator tRNA and guanosine-5'-triphosphate (GTP). Next, the 43S pre-initiation complex (PIC) is assembled with the 40S ribosome subunit, TC and eIFs (eIF1, eIF1A, eIF3, eIF5), while eIF4F complex assembled with eIF4E (a 5′mRNA cap-binding subunit), eIF4G (a scaffolding protein) and eIF4A (a RNA helicase). The combination of 43S PIC and eIF4F complex leads to formation of 48S initiation complex, which recruits mRNA with eIF4E and the interaction of eIF4G–eIF3. After identification of the initiation codon, 48S initiation complex released eIFs and combined with 60S ribosome subunit. This process is facilitated by eIF4A, with the requirement for its ATP independent helicase activity directly proportional to the amount of secondary structure in the 50-untranslated region (UTR). In addition, UTR during this process must be melted for scanning. Finally, the formation of the 80S ribosome symbolizes the stop of initiation and the launch of elongation (Lopez-Lastra *et al.*, 2005; Malys and McCarthy, 2011).

1.5.2 Regulations of eIF4f Complex

The eIF4F complex is located at the convergence of several cell signaling pathways involved in carcinogenesis, including the Pi3K/AKT/mTOR pathway and the RAS/RAF/MEK/ERK/MNK/MAPK pathway. In addition, other oncogenic factors, such as c--Myc, NF-κB, C/EBPα, C/EBPβ, Sp1, Ets and HIF-1α, also regulate the expression of different subunits of the eIF4F complex (Malka-Mahieu *et al.*, 2017; Mishra *et al.*, 2015). For instance, the c-Myc transcription factor, one of the most frequently activated oncogenes in human cancers, increases the transcription of all genes encoding components of the eIF4F complex (eIF4E, eIF4A, and eIF4G), thereby controlling the protein translation(Bhat *et al.*, 2015). HIF-1α activates eIF4E via the hypoxia response elements in its proximal promoter region(Yi *et al.*, 2013). Other transcription factors can also regulate the transcription of the

individual components of the translation complex following stimulation by various growth factor pathways.

1.5.2.1 PI3K/AKT/mTOR signaling pathways regulates 4EBP1

mTOR, a macromolecular serine/threonine kinase, exists as a convergence of major signaling pathways and regulates cell growth, cell survival, apoptosis, autophagy and tumorigenesis. There are two different complexes in the mTOR family: mTOR complex 1 (mTORC1) and mTOR complex 2 (mTORC2), which share the same catalytic subunit(Laplante and Sabatini, 2012). mTORC1, the key molecule of PI3K/AKT/mTOR signaling pathways, regulates protein synthesis, cell growth, cell proliferation and autophagy. mTORC2 impacts on cell survival, cytoskeletal regulation and degradation of newly synthesized peptides by mainly activating Akt (Huang and Fingar, 2014; Oh and Jacinto, 2011). The major downstream regulators of mTORC1 are 4EBP1 and p70S6K1/2 (Bhat *et al.*, 2015; Laplante and Sabatini, 2012). 4EBP1 negatively regulates eIF4E. Phosphorylation by mTORC1 leads to 4EBP1 dissociation from eIF4E, allowing translation initiation complex formation at the 5' end of messenger RNAs. Activated PDCD4, the downstream molecule of p70S6K, leads to its dissociation from eIF4A and amplification of eIF4F complex (Suzuki *et al.*, 2008). Recent evidence suggests that the amino acid levels can communicate to mTORC1 by a lysosome-based signaling system (Jewell *et al.*, 2013). The mTOR pathway is activated in most cancers. Recent studies confirm that the mTORC1/4E-BP1 axis is a pivotal pathway in mRNA translation, during tumorigenesis (Hsieh *et al.*, 2012).

1.5.2.2 MAPK signaling pathway regulates interaction of eIF4E and eIF4G.

In the MAPK pathway, ERK influences the translation via the activation of the RSK kinases that target PDCD4 and S6, independently of the S6K kinases (Buxade *et al.*, 2008). MNK, downstream of ERK, controls the phosphorylation of eIF4E on a single site (Ser209) through

its interaction with eIF4G. Mitogens and stress up-regulated the mRNA translation via phosphorylation of eIF4E by Mnk (Buxade *et al.*, 2008). Increasing evidence links the eIF4E phosphorylation and high eIF4G expression with tumorigenesis, invasion, and metastatic progression in cancer (Topisirovic *et al.*, 2004; Wendel *et al.*, 2007).

1.5.3 eIF4f Complex and tumorigenesis

The cap-dependent initiation plays a pivotal role in tumorigenesis(Jewell *et al.*, 2013). The quantity of eIF4E is crucial to form the eIF4F complex and maintain protein synthesis initiation. Redundant eIF4E can be simultaneously hijacked by malignant cells for tumorigenesis (Pelletier *et al.*, 2015; Truitt *et al.*, 2015). Phosphorylation of eIF4E up-regulates cell survival and growth cycle proteins, thereby promotes epithelial-mesenchymal transition (EMT), tumor invasion and metastasis (Robichaud *et al.*, 2015). High expression of eIF4A and eIF4G can be detected in most cancers (Akcakanat *et al.*, 2014; Liang *et al.*, 2014).

1.5.4 eIF4f Complex and resistance to anticancer therapies

Recently, it has been demonstrated that the activity of the eIF4F complex contributes to drive resistance to many types of therapies used as treatment in cancer. eIF4E overexpression or amplification promotes resistance to mTOR inhibitors in colon cancer and TKIs as well as cisplatin in breast cancer (Ilic *et al.*, 2011; Martinez *et al.*, 2015; Zindy *et al.*, 2011). The eIF4A-inhibitory protein PDCD4 can also contribute to chemoresistance against paclitaxel and doxorubicin (Bourguignon *et al.*, 2009). In addition, eIF4B, initiation eIF4A cofactors, is overexpressed in cisplatin/fluorouracil-resistant gastric tumors (Kim *et al.*, 2011). Likely, in a BRAF(V600)-mutated context, resistance to anti-BRAF and anti-MEK therapies is associated with a prominently active eIF4F complex (Boussemart *et al.*, 2014).

1.6 Aim of this study

I.   To investigate the role of endogenous and exogenous cellular stress induced UPR on the cellular homeostatic system.

II. To evaluate the effects of ER stress on amino acids metabolism, especially of Glutamine and Asparagine in hepatocellular cancer cells.

III. To study the role of exogenous Asparagine on the recovery function of Glutamine-deprived cells.

IV. To explore the mechanism of Glutamine-dependent Asparagine involved in ER stress for cellular homeostasis.

V.   To assess the introduction of therapeutic targeting of amino acids metabolism in therapies-resistant hepatocellular cancer cells.

2. MATERIALS AND METHODS

2.1 Materials
2.1.1 Instruments

Name	Company
Rotor 45 Ti	Beckman Coulter, Krefeld
Rotor SW60 Ti	Beckman Coulter, Krefeld
Ultracentrifuge	Beckman Coulter,Krefeld
FACS Calibur	Becton-Dickinson, Heidelberg
Power supply PS 9009	Bio-Rad, California, U.S.A
Cell chamber Neubauer improved	Brand, Wertheim
Confocal microscope	Carl Zeiss LSM710
Thermo-mixer	Eppendorf, Hamburg
Magnetic stirrer 3000	Heidolph,Keilheim
Steril hood	Heraeus, Hanau
Tabletop centrifuge	Heraeus, Hanau
Centrifuge Biofuge fresco	Heraeus, Hanau, Hanau
Pipettus-Akku	Hirschmann, Eberstadt
Water-bath	Julabo, Seelbach
Rotor GSA	Kendro, USA
Ph-Meter-761 Calimatic	Knick, Berlin
Incubator for cell culture	Labotect, Göettingen
Microscope DMBRE	Leica,Bensheim
Odyssey® CLx Imaging System	LI-COR Biosciences, Lincoln, NE, U.S.A.
LightCycler® 480 Instrument II	Roche, Basel, Schwitzerland
Weighing scale RC210 D	Sartorius, Göettingen
QTRAP® 6500 LC-MS/MS System	SCIEX, England,UK

Gas Chromatograph-Mass Spectrometry	Shimadzu, Kyoto, Japan
Whirlmixer Vortex Genie	Si Inc, New York, USA
Spot Flex Camera	Visitron System, Germany

2.1.2 Miscellaneous material

Name	Company
Parafilm	American Nat.Can,Greenwich,Great
Needles	BD Biosciences, Heidelberg
Syringes	BD Biosciences, Heidelberg
Cell culture flasks $25cm^2$, $75cm^2$	Greiner, Frickenhausen
Cell culture 96-well, 24-well, 6-well plates	Greiner, Frickenhausen
Cell culture 10 cm plates	Greiner, Frickenhausen
Cryovials	Greiner, Frickenhausen
Falcon tubes 15ml, 50ml	Greiner, Frickenhausen
Centrifuge tube 20ul, 100ul, 500ul, 1000ul	Greiner, Frickenhausen
Petri dishes	Greiner, Frickenhausen
Cover slides	R.Langenbrinck, Emmendingen
Sterile filter 0.2 μm	Renner, Darmstadt
Pipette tips	Sarstedt, Numbrecht

2.1.3 Chemicals and reagents

Name	Company
Dako Antibody Diluent, background reducing	Agilent Technologyies, USA
Dako Fluorescence Mounting Medium	Agilent Technologyies, USA
V9302 ASCT2 antagonist	AOBIOUS INC, USA
Sodium hydrogen carbonate	AppliChem, Darmstadt
rtStar™ First-Strand cDNA Synthesis Kit	Arraystar, USA
Arraystar SYBR® Green Real-time qPCR Master Mix	Arraystar, USA
Ecotainer® Sterile Water for Irrigation	B. Braun, Germany
PI	BD biosciences,USA
Bindinmg buffer	BioVision, USA
Tris-base	Carl Roth GmbH, Germany
Tris-hydrochlorid	Carl Roth GmbH, Germany
Natriumchlorid	Carl Roth GmbH, Germany
TWEEN-20	Carl Roth GmbH, Germany
Phosphatase Inhibitor Tablets	Carl Roth GmbH, Germany
Ethanol ≥99,8 %, mit ca. 1 % MEK	Carl Roth GmbH, Germany
Ethanol ≥70 %, mit ca. 1 % MEK	Carl Roth GmbH, Germany
Aceton ≥99,5 %,	Carl Roth GmbH, Germany
Roticlear	Carl Roth GmbH, Germany
Paraformaldehyde	Carl Roth GmbH, Germany
Potassium carbonate	Carl Roth GmbH, Germany
L-ASPARAGINE:H2O (13C4, 99%)	Eurisotop,UK
Sodium chloride	Fluka, Buchs, Switzerland
WhatmanTM 3mm CHR Blotting Paper Sheets	GE Healthcare, UK

AmershamTM Protran® Western blotting membranes, nitrocellulose	GE Healthcare, UK
Liquid nitrogen	Heidelberg, Germany
Cy2 AffiniPure Goat Anti-Mouse IgG (H+L)	Jackson ImmunoResearch, USA
Normal goat serum	Jackson ImmunoResearch, USA
Cy3 AffiniPure Goat Anti-Rabbit IgG (H+L)	Jackson ImmunoResearch, USA
IRDye® 800CW Goat anti-Rabbit IgG(H+L)	LI-COR Biosciences, USA
IRDye® 680RD Goat anti-Mouse IgG(H+L)	LI-COR Biosciences, USA
Spectrila	Medac, Germany
Dimethylformamide	Merck, Darmstadt
Potassium chloride	Merck, Darmstadt
Sodium acetate	Merck, Darmstadt
Calcium chloride	Merck, Darmstadt
Formaldehyde	Merck, Darmstadt
Sodium hydrogen phosphate	Merck, Darmstadt
Bovine Serum Albumin (BSA)	PAA, Pasching, Austria
Hydrochloric acid (HCl)	Riedel-de Haen, Seelze
Sodium hydroxide	Riedel-de Haen, Seelze
Protease Inhibitor Cocktail Tablets	Roche Diagnostics GmbH, Germany
Phosphatase Inhibitor Tablets	Roche Diagnostics GmbH, Germany

shRNA Plasmid Transfection Reagent	santa cruz biotechnology, USA
shRNA Plasmid Transfection Medium	santa cruz biotechnology, USA
Control shRNA Plasmid-A	santa cruz biotechnology, USA
Puromycin dihydrochloride	santa cruz biotechnology, USA
eIF4A shRNA Plasmid (h)	santa cruz biotechnology, USA
eIF4G shRNA Plasmid (h)	santa cruz biotechnology, USA
eIF4E shRNA Plasmid (h)	santa cruz biotechnology, USA
4EBP shRNA Plasmid (h)	santa cruz biotechnology, USA
Asparagine synthetase Double Nickase Plasmid	santa cruz biotechnology, USA
CREB-2 Double Nickase Plasmid	santa cruz biotechnology, USA
Plasmid Transfection Medium	santa cruz biotechnology, USA
UltraCruz® Transfection Reagent	santa cruz biotechnology, USA
Sorafenib	selleckchem,USA
Regorafenib	selleckchem,USA
Albumin Bovine Fraction V, pH 7.0	SERVA Electrophoresis GmbH, Germany
Methanol	Sigma-Aldrich, USA
DAPI(4′,6-diamidino-2-phenylindole)	Sigma-Aldrich, USA
Thiazolyl Blue Tetrazolium Bromide	Sigma-Aldrich, USA
RIPA Buffer	Sigma-Aldrich, USA
Dulbecco's Phosphate Buffered Saline	Sigma-Aldrich, USA
DMSO (Dimethyl sulfoxide)	Sigma-Aldrich, USA
Eosin Y	Sigma-Aldrich, USA
Hematoxylin	Sigma-Aldrich, USA
2-Propanol	Sigma-Aldrich, USA

Triton-X100	Sigma-Aldrich, USA
Glucose	Sigma-Aldrich, USA
Asparagine	Sigma-Aldrich, USA
Aspartic acid	Sigma-Aldrich, USA
Alanine	Sigma-Aldrich, USA
Glutamic acid	Sigma-Aldrich, USA
Proline	Sigma-Aldrich, USA
Cobalt chloride	Sigma-Aldrich, USA
Phenylmethylsulphonylfluoride	Sigma-Aldrich, USA
PI	Sigma-Aldrich, USA
Glutamine	Sigma-Aldrich, USA
PageRulerTM Prestained Protein Ladder,10 to 180 kDa	Thermo Scientific, USA
SpectraTM Multicolor High Range Protein Ladder	Thermo Scientific, USA
Trypsin-EDTA (0.25%)	Thermo Scientific, USA
PierceTM BCA Protein Assay Kit	Thermo Scientific, USA
LDS Sample Buffer (4X)	Thermo Scientific, USA
Sample Reducing Agent (10X)	Thermo Scientific, USA
Tris-Glycine SDS Sample Buffer (2X)	Thermo Scientific, USA
4-12% Bis-Tris Protein Gels, 1.0 mm, 12-well	Thermo Scientific, USA
4-12% Tris-Glycine Mini Gels, 12-well	Thermo Scientific, USA
MOPS SDS running buffer (20×)	Thermo Scientific, USA
Tris-Glycine SDS running buffer (10×)	Thermo Scientific, USA
Transfer Buffer (20×)	Thermo Scientific, USA
Tris-Glycine Transfer Buffer (25×)	Thermo Scientific, USA
Lipofectamine 2000 Transfection Reagent	Thermo Scientific, USA

CHOP siRNA	Thermo Scientific, USA
Opti-MEM™ I Reduced Serum Medium	Thermo Scientific, USA
TRIzol™	Thermo Scientific, USA

2.1.4 Cell culture medium and supplements

Name	Company
Fetal bovine serum	Biochrom GmbH, Germany
Penicillin/Streptomycin	Biochrom GmbH, Germany
Dulbecco's Modified Eagle Medium (DMEM)	Sigma-Aldrich, USA
DMEM, no glucose	Thermo Scientific, USA
DMEM, high glucose, no glutamine	Thermo Scientific, USA
DMEM, high glucose, NEAA, no glutamine	Thermo Scientific, USA
DMEM, high glucose, no glutamine, no methionine, no cystine	Thermo Scientific, USA

2.1.5 Buffers and solutions

MTT solution	1. 100mg MTT
	2. 20ml PBS
TBS buffer (10×)	1. 24.2g Tris base
	2. 80g Nacl
	3. adjust pH to 7.6 using HCl.
	4. total volume: 1000 ml high purity water

Phosphatase Inhibitor solution (10×)	one of Phosphatase Inhibitor Cocktail Tablets dissolved in 1ml RIPA Buffer
Protease Inhibitor solution (25×)	one of Protease Inhibitor Cocktail Tablets dissolved in 2ml PBS
Cell Lysis Buffer	Phosphatase Inhibitor solution (10×), Protease Inhibitor solution (25×) and RIPA buffer were mixed at a ratio of 5:2:43
In suit Wash Buffer A	1. 8.8 g NaCl 2. 1.2 g Tris base 3. 0.5 ml Tween 20 4. adjust pH to 7.4 using HCl 5. total volume: 1000 ml high purity water.
In suit Wash Buffer B	1. 5.84 g NaCl 2. 4.24 g Tris base 3. 26.0 g Tris-HCl 4. adjust pH to 7.5 using HCl 5. total volume: 1000 ml high purity water.
0.5% BSA solution	10g Albumin Bovine Fraction V+200ml TBST (0.1%)
Freezing medium	10% DMSO in FCS
PBS (10x)	1. 1.37 M NaCl 2. 100mM Na2HPO4 3. 27 mM KCl 4. 18mM KH2PO4 5. 4. adjust pH to 7.4 using HCl 6. total volume: 1000 ml high purity water.
PI	100mg Propidium iodide+100ml high purity water

2.1.6 Kits

Name	Company
NADPH Determination Kit	Abcam,USA
NuRNA^{TM} Human Central Metabolism PCR Array	Arraystar, USA
AnnV-FITC Apoptosis Kit	Bioversion,UK
ATP Determination Kit	Invitrogen, Karlsruhe
Duolink® In Situ PLA® Probe Anti-Mouse MINUS	Sigma-Aldrich, USA
Duolink® In Situ PLA® Probe Anti-Rabbit PLUS	Sigma-Aldrich, USA
Click-iT® HPG Alexa Fluor® Protein Synthesis Assay Kits	Thermo Scientific, USA

2.1.7 List of antibodies

Name	Company
NF-kB p105/p50 Rabbit mAb	Abcam,USA
HIF 1a, Rabbit mAb	Abcam,USA
sir t1(E104), Rabbit mAb	Abcam,USA
sir t2, Rabbit mAb	Abcam,USA
sir t3, Rabbit mAb	Abcam,USA
NF-KB p65(E379), Rabbit mAb	Abcam,USA
stat3(EPR787Y), Rabbit mAb	Abcam,USA
ETS1, Rabbit mAb	Abcam,USA
Akt (pan) (C67E7) RabbitmAb	Cell Signaling Technology, USA
Phospho-Akt (Ser473) Antibody	Cell Signaling Technology, USA
mTOR (7C10) Rabbit mAb	Cell Signaling Technology, USA
Phospho-mTOR (Ser2448) (D9C2) XP® Rabbit mAb	Cell Signaling Technology, USA

Tuberin/TSC2 (D93F12) XP®RabbitmAb	Cell Signaling Technology, USA
Phospho-Tuberin/TSC2 (Ser939) Antibody	Cell Signaling Technology, USA
Phospho-Tuberin/TSC2 (Thr1462) (5B12) Rabbit mAb	Cell Signaling Technology, USA
4E-BP1 (53H11) Rabbit mAb (for Western Blot)	Cell Signaling Technology, USA
eIF4E (C46H6) Rabbit mAb (for Western Blot)	Cell Signaling Technology, USA
eIF4G Antibody	Cell Signaling Technology, USA
Phospho-eIF4E (Ser209) Rabbit mAb	Cell Signaling Technology, USA
IRE1α (14C10) Rabbit mAb	Cell Signaling Technology, USA
PDI (C81H6) Rabbit mAb	Cell Signaling Technology, USA
CHOP (L63F7) Mouse mAb	Cell Signaling Technology, USA
PERK (D11A8) Rabbit mAb	Cell Signaling Technology, USA
GAPDH (14C10) Rabbit mAb	Cell Signaling Technology, USA
Phospho-4E-BP1 (Thr37/46) (236B4) Rabbit mAb	Cell Signaling Technology, USA
eIF4A (C32B4) Rabbit mAb	Cell Signaling Technology, USA
ASCT2 (D7C12) Rabbit mAb	Cell Signaling Technology, USA
c-Myc (D84C12) Rabbit mAb	Cell Signaling Technology, USA
p44/42 MAPK (Erk1/2) (137F5) Rabbit mAb	Cell Signaling Technology, USA
Caspase-8 (1C12) Mouse mAb	Cell Signaling Technology, USA
FADD Antibody,Rabbit mAb	Cell Signaling Technology, USA
Mnk1 (C4C1) Rabbit mAb	Cell Signaling Technology, USA
C/EBP-beta	Cell Signaling Technology, USA
Asparagine synthetase (SC67-07) Rabbit mAb	Novusbio, UK
eIF4E antibody (A-10) (for in situ PLA)	Santa Cruz Biotechnology, USA
4E-BP1 antibody (R-113) (for in situ PLA)	Santa Cruz Biotechnology, USA

p70 S6 kinase α Antibody (Thr 389)	Santa Cruz Biotechnology, USA
CREB-2 Antibody (C-20) Rabbit mAb	Santa Cruz Biotechnology, USA
SP2	Santa Cruz Biotechnology, USA

2.1.8 Clinical samples

A total of twenty-five human-derived specimens were utilized for this thesis, in all of which there were primary HCC specimen and the corresponding nontumor liver specimen. The specimens were independently collected from our own liver tissue bank. Due to the medical secrecy, the national and federal data protection law confidential data of patients are protected. The data collection and evaluation was carried out anonymously in accordance with § 3 (6) Landesdatenschutzgesetz Baden-Württemberg. Tissue collection after inormed consent was allowed according to the Ethics Committee of the Medical Faculty of the University of Heidelberg. All patient related data data were pseudonymous data only. After collection, all specimens were stored at -80°C. Before tissue sections were prepared, all selected frozen tissues were immersed in O.C.T gel immediately after being removed from the freezer and subsequently solidified into blocks using dry ice. The blocks were then stored at -80°C.

Frozen tissue sections were prepared using a Leica machine (CM1950). The sections were sliced to a thickness of 6.0μm and then immersed in 99.9% acetone for 10 minutes for fixation and immediate permeation. The slides were dried at room temperature for 30 minutes and subsequently stored at -20°C. For each experiment group, the paired specimens were sliced and stained under the same conditions and at the same time. Clinicopathological characteristics of the patients are shown in table 1.

Table1. The clinicopathologic features of HCC patients treated by radical operation

Characteristic	N = 26
Gender	
Male	16
Female	10
Age	63.19 ± 13.09
AFP (ng/ml)	
<400	11
≥400	15
Tumor size(cm)	
<3	4
3-5	10
≥5	12
Tumor number	
Single	13
Multiple	13
Child-Pugh class	
A	25
B	1
BCLC stage	
0	1
A	13
B	12
TNM stage	
I	10
II	6
III	10

2.2 Method
2.2.1 Cell culture

Both human HCC cell lines, Huh7 (European Collection of Cell Cultures) and HepG2 (Toni Lindl GmbH, Munich, Germany), were cultured in DMEM supplemented with 10% (v/v) FBS and 100μg/ml penicillin/streptomycin in a humidified atmosphere of 95% O_2 and 5% CO_2 at 37℃. Cells grew adherently and, when confluent, were detached with trypsin for sub-culturing. All cell lines were exchanged for new thawing cell lines if passaged was performed more than 50 times.

2.2.2 Drugs

Sorafenib and Regorafenib were obtained from Selleckchem, USA. The stock solution was prepared with DMSO, at a concentration of Sorafenib 50mM, Regorafenib 50mM. Chloride hexahydrate (Cocl2) was obtained from Sigma-Aldrich, USA; V-9302 was obtained from AOBIOUS INC, USA; and Spectrila (Asparaginase) was from Medac, Germany. The stock solution was prepared with phosphate buffered saline, at a concentration of Cocl2 10mM, V-9302 100mM. and Spectrila 2500U/ml. Ultimate concentrations of all solvents in the medium were no more than 0.1%.

2.2.3 Nutrition Deprivation and Stimulation

For cell culture in supplementation with glucose and glutamine at normal concentration or low concentration which more closely reflects plasma glutamine levels in previous studies(Birsoy *et al.*, 2014; Gwinn *et al.*, 2018; Le *et al.*, 2014). Glucose and Glutamine deprivation was performed that Cell were passaged into new experimental plates and overnight with normal DMEM Medium before separately changed into DMEM, no glucose Medium and DMEM, high glucose, no glutamine Medium from Thermo Scientific, USA. For experiments involving low glucose, low glutamine, unnecessary amino acids(NEAA) and asparagine pre-loading, cells were incubated with 0.45g/l glucose in DMEM, no glucose Medium; 0.4 mM glutamine in DMEM, high glucose, no glutamine Medium, DMEM; high glucose, NEAA, no glutamine; 0.45 mM asparagine in normal DMEM Medium or DMEM, high glucose, no glutamine Medium. 0.4mM Alanine, 0.4 mM Aspartic acid, 0.4 mM Glutamic acid, and 0.4 mM Proline were added into EM, high glucose, no glutamine Medium respectively for cell culture. Cobalt (II) Chloride hexahydrate (CoCl2) is a chemical inducer of hypoxia-inducible factor, which was added to normal DMEM Medium as Hypoxia condition.

2.2.4 In situ Proximity Ligation Assay (PLA assay)

In situ Proximity Ligation Assay, a new method for detecting the combination of two target proteins, was first reported in 2006(Soderberg *et al.*, 2006). There are three crucial reactions in the course of this procedure:

a. The binding of proximity probes: Two probes (PLA probe MINUS and PLA probe PLUS) must first bind to two different primary antibodies from different species (one is from rabbit and the other one is from mouse).

b. Circularization and ligation of connector oligonucleotides: The ligation solution, which contains two oligonucleotides, is added to tissue sections. During the catalysis reaction of ligase, the oligonucleotides hybridize with two PLA probes and will often bind with each other to form a closed circle if the two probes are in close proximity (5-10 nm).

c. Amplification and detection:

The amplification solution contains nucleotides, polymerase and oligonucleotides which have been labeled with fluorescence. The ligated circle, formatted with two probes, then becomes the template for rolling-circle amplification (RCA) and one of two probes acts as a primer. The labeled oligonucleotides hybridize to form RCA products and the resulting signal can be easily visualized via fluorescence microscopy.

PLA assay for HCC cell lines:

In this project, the interactions of eIF4E:eIF4G and eIF4E:4E-BP1 in cell lines and tissue were detected via in situ PLA method using a Duolink$^{®}$ PLA$^{®}$ assay kit.

The protocol for the PLA assay in HCC cell lines was as follows:

1. Cell seeding and treatments: All cancer cells were isolated by 0.25% trypsin and resuspended at a concentration of 2.5×10^4/ml in DMEM medium, then pipetted into 8-well culture slides (800μl/well), whereas 400μl into the well of controls. The cell-culture slides were maintained in a humidified atmosphere of 5% CO2 at 37°C 24 hours after cell seeding, the medium in each well was renewed with 600μl of additional treatments whereas control groups renewed with 600μl of DMEM. DMSO in each well was balanced between the groups and was diluted to less than 0.1%.

2. Fixation of cells: After treatment, each well was gently washed with cool PBS twice. After that, cancer cells in each well were fixed with 600μl of 4% paraformaldehyde solution for 10 minutes at room temperature.

3. Permeabilization of cell membranes: After fixation and wash, cancer cells were permeabilized with 0.05% Triton-x100 solution (diluted in PBS) for 10 minutes. The walls of chambers (or wells) were detached from slides subsequently.

4. Blocking: One drop of Duolink blocking solution was added to each sample on the slides. Afterwards, all slides were maintained in a preheated humidified chamber at 37°Cfor 30 minutes.

5.Primary antibodies: Anti-eIF4E, eIF4G, and 4E-BP1 antibodies were diluted in antibody solvent (from the PLA kit) at the concentration of 1:200 and incubated with the cells overnight at 4°C.

6. Probes: After rinsing for 2×5 minutes with Wash Buffer A, PLA MINUS, and PLA PLUS probes were mixed with the antibody solvent (1:5) and incubated on slides for 1.0 hour at 37°C in the humid environment.

7. Ligation: After rinsing for 2 × 5 minutes with Wash Buffer A, the ligation solvent and ligase were mixed with ddH$_2$O (Ligation solvent 1:5, Ligase 1:40). Then, the solution was incubated with the cells for 0.5 hour at 37°C in the humid environment.

8. Amplification and detection: After rinsing for 2 × 2 minutes with Wash Buffer A, the amplification solution (which contains nucleotides, polymerase, and oligonucleotides that had been labeled via fluorescence) was added to the cells and incubated at 37°C in a humid environment. The amplification time varied for the different cell lines; for SW620 and SW480 cells, the time was 75 minutes, while for HT29 and HCT116 cells, it was 80 minutes.

9. Mounting: After rinsing for 2 × 10 minutes with Wash Buffer B, the cell nuclei were stained with DAPI for 5 minutes. The slides were rinsed with Wash Buffer B for an additional 5 minutes and subsequently allowed to dry at room temperature in the dark. The sections were mounted using Dako Mounting Medium and left in the cool room overnight to solidify.

10. Detection: The number of PLA signals was detected using a fluorescence microscope (Leica Leitz DMRB) and counted via semi-automated image analysis with a free BolbFinder Software (http://www.cb.uu.se/~amin/BlobFinder/). The number of signals was analyzed using Graphpad Prism 6.0 via unpaired T test statistics method. Significance was set at P < 0.05.

2.2.5 Cell viabilities and MTT assay

The half maximal inhibitory concentration (IC50) value of various drugs was determined in the setting of MTT assay experiments from 24, 48 and 72 hours. The usage of concentration of Sorafenib and Regorafenib were from 0~40uM, Cocl2 from 0~20uM, V-9302 from

0~80uM and Spectrila from 0~1000U/ml. Then cell viabilities were performed from 0 to 6 days to assess the cellular proliferation.

This assay was performed as follows:

1. Cell lines were seeded in a 96-well plate at a density of 5 x 10^3 cells/well for MTT assay, at a density of 1 x 10^3 cells/well for cell proliferation assessment in DMEM medium.

2. After 24 hours, the cells were treated with either normal medium (for the control group) or the indicated concentrations of additional treatments (for the experiment groups). The volume of medium per well is 200µl.

3. At different time points respectively, 10µl of MTT (5mg/ml, 0.5%) was added into each well and the wells were subsequently incubated for 4 hours at 37°C.

4. The medium was discarded after incubation and 200µl if MTT solution was subsequently added to every well.

5. Cell viability was observed as absorbance at 590nm and with a reference filter of 620nm. The data was analyzed using Graphpad Prism 6.0 using one-way ANOVA statistical method. Significance was set at $P < 0.05$.

2.2.6 Click-iT® HPG Alexa Fluor® Protein Synthesis Assay

Click-iT® HPG (L-homopropargylglycine) is an amino acid analog of methionine containing an alkyne moiety. Similar to 35S-methionine, Click-iT® HPG is added to cultured cells and the amino acid is incorporated into proteins during active protein synthesis. Detection of the incorporated amino acid utilizes a chemo selective ligation or click reaction between an azide and alkyne, where the alkyne-modified protein is detected with either Alexa Fluor® 488 azide.

1. Pre-incubation

Cells was plated into 8-well culture slides at desired density of 2 x 10^4 cells/well and allowed to recover overnight before additional treatment. After cells as desired to be treated, Click-iT® HPG by diluting 1:1000 in pre-warmed L-methionine-free medium for a 50 μM final working solution was added 100 μL/well, followed 30 minutes incubation.

2. Cell Fixation and Permeabilization

After incubation, medium containing Click-iT® HPG was removed, followed by cell wash with PBS. Then 100 μL/well 3.7% formaldehyde in PBS was added to incubate for 15 minutes at room temperature. In the end, after washed with 3% BSA in PBS twice, 100 μL/well of 0.5% Triton® X-100 in PBS was added into samples and incubated for 20 minutes at room temperature.

3. Detection

After removing the permeabilization buffer and cells was washed twice with 100 μL/well 3% BSA in PBS before prepared Prepare Click-iT® reaction cocktail, which contains 1X Click-iT® HPG reaction buffer, Copper (II) Sulfate (CuSO4), Alexa Fluor® azide, and 1X Click-iT® HPG buffer additive was be put into each well. Incubation was 30 minutes at room temperature, protected from light. Then cells were washed once with 100 μL per well of Click-iT® reaction rinse buffer.

4. DNA Staining

HCS NuclearMask™ Blue Stain solution was diluted 1:2000 in PBS to obtain a 1X HCS NuclearMask™ Blue Stain working solution, which was then added into the each well

for 30 minutes incubation at room temperature, protected from light. After cells were washed twice with PBS, the slides were proceeded to Imaging and Analysis.

5. Imaging and analysis

Each slide was mounted with Duolink in Situ Mounting Medium and covered by a 24x50mm coverslip. Samples was signals was detected using a fluorescence microscope (Leica Leitz DMRB) and Nascent protein synthesis is assessed by determining signal intensity in the fluorescent channel in the ring around the nucleus as defined by NuclearMask^{TM} Blue Stain.The expressions were detected using a microscope and counted via semi-automated image analysis with a free ImageJ Software (http://imagej.nih.gov/ij/). The number of signals was analyzed using Graphpad Prism 6.0 via unpaired T test statistics method. Significance was set at $P < 0.05$.

2.2.7 Proteins extraction

1. Cells were seeded in 6-well plates at a density of 1 x 10^6 cells/well. After treatment, the cells were lysed using a lysis buffer before being aspirated. The cells were washed twice with ice cold PBS and kept on ice.

2. After aspiration with PBS, 100µl of lysis buffer was added into each well before the wells were incubated for 15 minutes. Afterwards, the adherent cells were scraped from the plates using a plastic cell scraper, and then centrifuged at 13,000 rmp for 15 minutes in a centrifuge pre-cooled to 4°C.

3. After removal from the centrifuge, the tube was cooled on ice before the supernatant was transferred to a fresh tube and the pellet was discarded. The proteins were stored in -80°C.

2.2.8 BCA Protein Assay

The BCA protein assay was conducted as follows:

1. Five microliters of each standard or unknown protein lysis was pipetted into a

   96-well plate.

2. Working Reagent was prepared by mixing BCA Reagent A with BCA Reagent

   B in a ratio of 50:1. Next, 200μl of the Working Reagent was added to each well

   before the plate was thoroughly mixed on a plate shaker for 30 seconds.

3. Afterwards, the plate was maintained in a 37°C incubator for 30 minutes.

4. The optical density of each well was measured with MultiskanTM FC Microplate

   Reader (Thermo Fisher scientific, USA) at 570nm wavelength with a reference of

   620nm, after the plate turning cool at room temperature.

5. The concentration of each sample was calculated in line with simultaneously

   measured Diluted Albumin Standards

2.2.9 Western Blot

The Western Blot test was performed as follows:

1. Protein preparation

   Proteins from each group were mixed with LDS loading buffer and sample reducing

   buffer. Then, the proteins were denatured using 4-12% Bis-Tris SDS- PAGE gel at

   70°C for 10 minutes and denatured using 4% Tris-Glycine SDS- PAGE gel at 85°C

   for 2 minutes.

2. SDS-PAGE gel selection

Twenty microliters of the protein solution were loaded into each well. To detect proteins that were between 10 and 130 KD, 4-12% Bis-Tris SDS-PAGE gel was used, while 4% Tris-Glycine SDS-PAGE gel was used for proteins between 130 and 300 KD.

3. Protein running time

For 4-12% Bis-Tris SDS-PAGE gel, the running time was 50 minutes at 200V and for 4% Tris-Glycine SDS-PAGE gel, the running time was 1.5 hours at 125V.

4. Protein transfer

Proteins were transferred to a nitrocellulose membrane (0.45μm pore size). For 4-12% Bis-Tris SDS-PAGE gel, the transfer time was 1.5 hours at 40V and for 4% Tris-Glycine SDS-PAGE gel, the transfer time was 2 hours at 25V.

5. Blocking

After transfer, the NC membrane was rinsed with ddH_2O, followed by TBST (0.1% Tween20) for 5minutes. Then, via gentle rotation, the membrane was blocked using 5% BSA for 1.0 hour at room temperature.

6. Primary antibodies

The membrane was sliced into more than one band, according to the size of the target proteins after blocking. All primary antibodies were diluted using the blocking solution to a concentration of 1:1000, before being incubated overnight at 4°C.

7. Secondary antibodies

Membranes were incubated with fluorescence-labelled, IRDye secondary antibodies. Primary antibodies were discarded, and the membranes were rinsed in TBST (0.1% Tween20) for 3 × 10 minutes before being incubated with the appropriate IRDye secondary antibodies at a concentration of 1:10000 for 1.0 hour at room temperature.

8. Signal detection

The membranes were rinsed in TBST (0.1% Tween20) for 3 × 10 minutes and then visualized using an Odyssey CLx scan machine (LI-COR Bioscience). The results were obtained using Image Studio Software (LI-COR Bioscience). The Western Blot experiment for each protein was performed at least three times with independently prepared protein lysates at varying time points.

2.2.10 Immunofluorescence (IF)

The signal expressions of target proteins were assessed in the same tumor and nontumor liver tissues. The immunofluorescence (IF) was evaluated as follows:

1. Preparation of tissue sections: Tissue sections stored in -20°C were rinsed in the cool TBST (0.1% Tween20 + TBS) for 2 × 5 minutes, followed by cool PBS for 1 × 5 minutes.

2. Blocking: For every reaction area, the tissue sections were blocked with 100μl of 10% pure goat serum and incubated for 1.0 hour at room temperature.

3. Primary antibodies: Blocking solution was aspirated onto the sections and 50μl of primary antibody diluent was added to each reaction area. The primary antibodies were used at the following concentration of primary antibodies 1:100. The primary antibodies were incubated overnight at 4°C.

4. Secondary antibodies: Sections were rinsed in TBST for 3 × 5 minutes. Fluorescent-conjugated secondary antibodies (Cy2 and Cy3) were diluted with DAKO Antibody Diluent to a concertation of 1:400. To each reaction area, 50μl of secondary antibody diluent was added and the samples were incubated at room temperature for 1.0 hour.

5. Slides were rinsed in TBST for 2 × 5 minutes and the tissues were incubated with DAPI (1:1000) for 10 minutes at room temperature. To each reaction area, 100μl of the reaction diluent was added.

6. The sections were mounted using Dako Mounting Medium and left to solidify in the cool room overnight.

7. Detection

The expressions of proteins were detected using a microscope and counted via semi-automated image analysis with a free ImageJ Software (http://imagej.nih.gov/ij/). The strength of signals was analyzed with Graphpad Prism 6.0 using paired (Tumor vs corresponding Nontumor) T test statistical methods. Significance was set at $P < 0.05$.

2.2.11 NuRNA^{TM} Human Central Metabolism PCR Array

NuRNA^{TM} Human Central Metabolism PCR Array is specifically designed for rapid, accurate, and systematic expression profiling of 373 enzymes or protein factors in the core metabolic pathways as well as key metabolite transporters, for studying cell metabolism, metabolic regulation, and metabolic changes in biological processes or diseases.

1. TRIzol RNA Isolation

   1.1. cell was washed rinsed with ice cold PBS once, before was lysed directly in a culture dish by adding 1 ml of TRIZOL Reagent per 3.5 cm diameter dish and scraping with cell scraper. Vortex thoroughly.

1.2. The samples were incubated for 5 minutes at room temperature to permit the complete dissociation of nucleoprotein complexes, then via Centrifuge to remove cell debris. The supernatant was transferred to new tube.

1.3. 0.2 ml of chloroform was added into per 1 ml of TRIZOL Reagent. Samples were vortexed vigorously for 15 seconds and incubated at room temperature for 2 to 3 minutes. After samples were centrifuged at 12,000 x g for 15 minutes at 2 C, the mixture was separated into lower red, phenolchloroform phase, an interphase, and a colorless upper aqueous phase. RNA remains exclusively in the aqueous phase.

1.4. The upper aqueous phase was transfered carefully without disturbing the interphase into fresh tube.

1.5. RNA was precipitated from the aqueous phase by mixing with isopropyl alcohol.0.5 ml of isopropyl alcohol was used into per 1 ml of TRIZOL Reagent for the initial homogenization. Samples were incubated at room temporary for 10 minutes and centrifuged at 12,000x g for 10 minutes at 4°C. The RNA precipitate formed a gel-like pellet on the side and bottom of the tube.

1.6. The supernatant was removed completely. The RNA pellet was washed once with 75% ethanol, before being added at least 1 ml of 75% ethanol per 1 ml of TRIZOL Reagent used for the initial homogenization. The samples were mixed by vortexing and centrifuge at 7,500 x g for 5 minutes at 4 °C. All leftover ethanol was removed.

1.7. RNA pellet was dried for 10 minutes before was avoided to dry completely as this will greatly decrease its solubility. RNA was dissolved in DEPC-treated water by passing solution a few times through a pipette tip.

1.8. 1 µl of RNA with 39 µl of DEPC-treated water was dilute 1:40. 10 µl microcuvette was taken OD at 260 nm and 280 nm to determine sample concentration and purity. The A260/A280 ratio should be from 1.8 to 2.0. Apply the convention that 1 OD at 260 equals 40 ng /ul RNA.

2. First-strand cDNA synthesis

   2.1. The following components was mixed: Oligo(dT)18, or Random Primers 1.0 µL, dNTP Mix 1.5 µL, RNA Spike-in 1.0 µL, and Template Total RNA 10.5 µL into a 200 uL PCR tube for each sample.

   2.2. The mixed solution above was incubate in a thermal cycler at 65°C for 5 min, then immediately chilled on ice for at least 1 min, followed spin down briefly.

   2.3. The following components were added: 5 × RT Reaction Buffer 4.0 µL, 0.1 M DTT 1.0 µL, RNase Inhibitor 0.6 µL and Reverse Transcriptase 0.4 µdirectly to the product from STEP 2. The final volume will be 20 L.

   2.4. Then it was incubated at 25°C for 5~10 min, followed by 60 min at 50°C.

   2.5. It was terminated the reaction at 85°C for 5 min, follow kept the finished First Strand cDNA Synthesis reaction on ice until the next step.

3. Perform qPCR for the PCR array

   3.1. The cDNA was diluted in Nuclease-free Water. If 1.5 µg input RNA is used with rtStar™ First-Strand cDNA Synthesis Kit, the dilution factor is 1:80. The diluted cDNA is used as the qPCR template in Wells for assays on the Transcripts, Housekeeping gene Internal Controls, and Spike-in External Controls.

   3.2. For GDC Controls, 1 µL NRT (mock cDNA synthesis reaction without the reverse transcriptase) sample or 1 µL RNA sample (without cDNA synthesis), 5 µL SYBR Green Master Mix, and 4 µL Nuclease-free Water were combined, followed by Mix well and spin down.

3.3. For Blank Controls, 25 µL SYBR Green Master Mix and 25 µL Nuclease-free Water were combined, then was mixed well and spin down.

3.4. The qPCR Mix was prepared: Arraystar SYBR Green Master Mix 2010 µL, diluted cDNA template 1600 µL, and ddH$_2$O 390 µL. There are total of 384 wells of PCR reactions. Some extra volumes have been included for liquid dispensing loss.

3.5. The 384-Well PCR Array was loaded. 10 uL aliquot of the cocktail from STEP 4 was added into each well, except the control wells. 10 uL aliquot of the GDC Mix from STEP 2 was added into well P23 to detect genomic DNA contamination. 10 uL aliquot of the Blank Mix from STEP 3 was added into wells P20~P22 and well P24.

3.6. The plate was centrifuged gently to remove bubbles.

3.7. The plate was kept on ice while set up the PCR program described in "Running Real-Time PCR Detection" below.

Cycles	Temperature	Time
1	95°C	10 minutes
40	95°C	10 seconds
	60°C	1 minutes
Melting curve analysis		

4. Data pre-processing and data analysis

4.1. Before the data analysis was initiated, the RNA spike-in wells are compared. Outlier samples may be identified and considered for exclusion in the further data analysis.

4.2. The ΔCt for each RNA in the plate was calculated with equation：$\Delta Ct_{RNA} = Ct_{RNA} - averag(Ct_{HKS})$ Where average (Ct HKs) is the geometric mean of the Ct values derived from the multiple HK genes. These most stably expressed housekeeping reference genes were selected from a broad range of samples by our stringent algorithm that evaluates the optimal properties and the number for endogenous controls.

4.3. The ΔΔCt for each RNA was calculated：$\Delta\Delta Ct = \Delta(sample\ 1) - \Delta Ct(sample\ 2)$, between samples. Or $\Delta\Delta Ct = \Delta Ct\ (group\ 1) - \Delta(group\ 2)$, between group averages .

4.4. Then ΔΔCt was converted to fold change (FC): $Fold\ Change = 2^{-\Delta\Delta Ct}$

By convention, if the fold change is greater than 1, the result is reported as a fold up-regulation. If the fold change is less than 1, its negative inverse (-1/FC) is reported as a fold down-regulation.

When comparing profiling differences between two groups (such as disease versus control) with biological replicates, the statistical significance of the difference can be estimated as p-value by t-test. RNAs having fold changes ≥2 and p-values ≤0.05 are selected as the significantly differentially expressed RNAs.

Fold change is related to biological effect size. Ranking by fold change is preferred over p-value. qPCR as commonly used in confirmation has a limit of quantification of 0.5 ΔCt, which is equivalent to approximately 1.5-fold change.
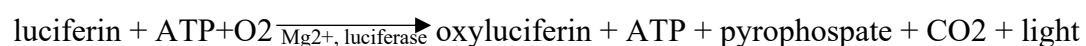
2.2.12 Gene Set Enrichment Analysis

Genevestigator is a high quality, manually curated and well annotated compendium of expression data collected from a variety of public repositories, including Gene Expression

Omnibus and ArrayExpress(Hruz *et al.*, 2008). Data from Genevestigator was normalized, quality controlled, and annotated manually. In brief, Affymetrix expression array data used for this study was normalized using the MAS5 algorithm, with global scaling set to a target value of 1000. The quality of the arrays was assessed using various Bioconductor packages, including AffyQCReport and SimpleAffy. Sample descriptions were annotated using the Genevestigator application ontologies for anatomical parts, stage of development, and experimental perturbations. Novel reference gene candidates used for experimental validation were obtained from RefGenes. The search algorithm identifies, for a chosen set of microarrays, those probe sets for which the standard deviation of signal intensities across these arrays is lowest.

Metascape (http://metascape.org/gp/index.html), a web resource compatible with all major browsers, sits on top of over 40 bioinformatics knowledgebases maintained by the scientific community, in which pathway enrichment analysis makes use of Gene Ontology, KEGG, Reactome, MSigDB, etc(Zhou *et al.*, 2019). Briefly, pairwise similarities between any two enriched terms are computed based on a Kappa-test score. The similarity matrix is then hierarchically clustered and a 0.3 similarity threshold is applied to trim the resultant tree into separate clusters. Metascape chooses the most significant (lowest p-value) term within each cluster to represent the cluster in bar graph and heatmap representations. The analysis provides other popular enrichment metrics in addition to p-values.

2.2.13 ATP Determination Assay

ATP Determination Assay is based on luciferase's requirement for ATP in producing light (emission maximum ~560 nm at pH 7.8) from the reaction:

$$\text{luciferin} + \text{ATP} + O_2 \xrightarrow{Mg^{2+}, \text{ luciferase}} \text{oxyluciferin} + \text{ATP} + \text{pyrophospate} + CO_2 + \text{light}$$

1. Cells was plated in 96-well plate at desired density of 5 x 10^3 and allowed to recover overnight before additional treatment.

2. 0.5 hour before the end of the treatment, the ATP standard and Luciferase Reagent from 20°C freezer were moved on ice to thaw.

3. All reagents from ATP Determination Kit were prepared.

4. The ATP standard reaction solution was made as follows (for 10mL): • 8.9ml dH2O • 500uL 20x reaction buffer • 100uL 0.1M DTT • 500uL 10mM D-Luciferin • 2.5uL firefly luciferase.

5. An appropriate volume of the ATP standard sample was put in the luminometer and measured the background luminescence.

6. The sample plates were spin down, and liquid was flicked off.

7. The desired amount of dilute ATP standard solution was added into the plates, follow it was measuerd by luminometer.

8. The background luminescence was subtracted, and the standard curve for a series of ATP concentrations was generated.

9. Followed the directions given in Standard Curve, ATP-containing samples were substituted for the ATP standard solutions.

10. The amount of ATP in the experimental samples was calculated from the standard curve.

2.2.14 NAPDH Determination Assay

Nicotinamide adenine dinucleotide (NAD+) and nicotinamide adenine dinucleotide phosphate (NADP+) are two important cofactors found in cells. NADH is the reduced form of NAD+. NAD forms NADP with the addition of a phosphate group to the 2' position of the adenyl nucleotide through an ester linkage. This NADPH probe is a chromogenic sensor that

has its maximum absorbance at 460 nm upon NADPH reduction. The absorption of the NADPH probe is directly proportional to the concentration of NADPH in the solution.

1. Cells was plated in 96-well plate at desired density of 5 x 10^3 and allowed to recover overnight before additional treatment.

2. 0.5 hour before the end of the treatment, the NAPDH kit from 20°C freezer was moved on ice to thaw.

3. NADPH reaction mixture was prepared by adding 1 ml of NADPH Probe into 4 mL NADPH Assay Buffer.

4. An appropriate volume of the NAPDH standard sample was put in the luminometer and measured the background luminescence.

5. The sample plates were spin down, and liquid was flicked off.

6. The mixture of 50 ul NAPDH standard solution and 50ul NADPH reaction mixture was added into the plates for one-hour incubation, follow it was measuerd by luminometer.

7. The background luminescence was subtracted, and the standard curve for a series of NAPDH concentrations was generated.

8. Followed the directions given in Standard Curve, NAPDH-containing samples were substituted for the NAPDH standard solutions.

9. The amount of NAPDH in the experimental samples was calculated from the standard curve.

2.2.15 Annexin V/ PI protocol apoptosis Assay

To distinguish between necrotic and apoptotic cells, the AnnexinV-APC and propidium iodide (PI) double staining was used. Annexin V is a member of the annexin family of intracellular proteins that binds to phosphatidylserine (PS) in a calcium-dependent manner. PS is normally only found on the intracellular leaflet of the plasma membrane in healthy cells, but during early apoptosis, membrane asymmetry is lost and PS translocates to the external

leaflet. Fluorochrome-labeled Annexin V can then be used to specifically target and identify apoptotic cells. To help distinguish between the necrotic and apoptotic cells， Propidium Iodide Solution (PI) is recommended to be used .Early apoptotic cells will exclude PI, while late stage apoptotic cells and necrotic cells will stain positively, due to the passage of these dyes into the nucleus where they bind to DNA.

1. Cells (1×10^6) were placed in 6-well plates to recover overnight before treatment.
2. The treated Cells was washed 1X with cold 1X PBS, followed the supernatant was removed.
3. Cells were re-suspended in 1X Binding buffer at a concentration of ~1×10^6 cells/mL, to prepare a sufficient volume to have 100 µL per sample.
4. Cells were stained 1x binding buffer (50µl) with 0.5 µl Annexin V-FITC and 1µg/ml PI .
5. Thereafter cells were incubated in the dark for 15 min at room temperature before evaluating staining with the FACS Calibur.
6. The data was analyzed with with a Flowjo Software (www.flowjo.com). The statistics was made with Graphpad Prism

   6.0 using T test statistical methods. Significance was set at P < 0.05.

2.2.16 Cell cycle Assay

PI intercalates into double-stranded nucleic acids and fluorescence. DNA staining with PI can be used to study the cell cycle. Relative DNA content shows the proportion of cells in G1, G2 and S phases. Meanwhile, a sub-G0/G1 peak in the fluorescence histogram that can be used to determine the relative amount of apoptotic cells in a sample based on the therapy the DNA is degraded by cellular endonucleases in nuclei of apoptotic cells containing less DNA than nuclei of healthy G0/G1 cells.

1. 1×10^{6} cells were seeded in 6-well plates and treated after overnight incubation.

2. Cells were harvested on ice after being washed by cold PBS.

3. Cold 70% ethanol was used to fixed cells for 30 minutes at 4 °C.

Cells washed with 2 x PBS were resuspended in 0.5 ml PBS containing 10 μg/ml RNase A and 20 μg/ml PI stock solution, transfer to FACS tubes and incubate at room temperature (RT) in the dark for 30 min.

4. Fluorescence activated cell was performed to detect DNA fraction to determine the respective different phases of cell cycle after PI staining in FACS Calibur.

5. The data was analyzed with with a Flowjo Software (www.flowjo.com). The statistics was made with Graphpad Prism 6.0 using T test statistical methods. Significance was set at $P < 0.05$.

2.2.17 Small interfering RNA (siRNA) transfection protocol

Chop were silenced by customized small interfering RNA (siRNA) or non-coding siRNA (Thermo Scientific, USA). Sequence (5'-> 3') GGAAACGGAAACAGAGUGGtt.

1. 1×10^{5} - 2×10^{5} cells were seeded in 6-well plates to 30-50% confluent after overnight incubation in normal medium without antibiotics.

2. For each transfection sample, oligomer-Lipofectamine 2000 complexes were as the following prepared:

   2.1. 3uL siRNA CHOP was added into 247 μl Gibco™ Opti-MEM™ I Reduced Serum Medium without serum and mixed gently.

   2.2. Lipofectamine 2000 gently was mixed before diluted 5 μl in 245 μl OptiMEM I Reduced Serum Medium, followed it incubated for 10 minutes at room temperature.

2.3. After the 5-minute incubation, the diluted siRNA CHOP with the diluted Lipofectamine 2000 were combined and mixed gently for 20 minutes incubation at room temperature

3. Cells were washed with 2X OptiMEM I Reduced Serum Medium before transfection.

4. The siRNA CHOP-Lipofectamine 2000 complexes was added into each well containing cells and medium.

5. Normal medium was changed at 6 hours after cells incubation at 37°C in a CO2 incubator for gene knockdown

6. Transferred cells were cultured from 24 to 72 hours for the next experiments.

2.2.18 Short hairpin RNA (shRNA) Transfection Protocol

shRNA eIF4A, shRNA eIF4E, shRNA eIF4G, and shRNA 4EBP1 were ordered from Santa Cruz biotechnology, USA. Whereas Control shRNA Plasmid was as a negative group.

1. 1.5×10^5 - 2.5×10^5 cells were seeded in 6-well plates to 50-70% confluent after overnight incubation in normal medium without antibiotics.

2. The transfection solution was prepared as followed:

2.1. Solution A: 10 μl of resuspended shRNA Plasmid DNA diluted into 90 μl shRNA Plasmid Transfection Medium for each sample.

2.2. Solution B: 1 μl of shRNA Plasmid Transfection Reagent was diluted with 99 μl shRNA Plasmid Transfection Medium for each sample

2.3. Solution A and Solution B were combined and mixed gently for 30 minutes incubation at room temperature.

3. Cells were washed 2x shRNA Transfection Medium until proceeded to transfection.

4. 0.8 ml shRNA Plasmid Transfection Medium and to well and 200 μl shRNA Plasmid DNA/shRNA Plasmid Transfection Reagent Complex (Solution A + Solution B) dropwise were added into well, covering the entire layer.

5. The plates were swirled gently to ensure that the entire cell layer was immersed in solution.

6. Cells were incubated for 6 hours at 37° C in a CO^2 incubator before 1 ml of normal growth medium containing 2 times the normal serum was added.

7. Transferred cells were further incubated for an additional 24 hours under normal conditions.

8. After 48 hours post-transfection, the medium was aspirated and replaced with fresh medium containing 1 μg/ml puromycin for selection of stably transfected.

9. The medium was replaced with fresh medium containing 1 μg/ml puromycin every 3 days until 2 weeks

10. Stable transfected cells were confirmed in Western blot analysis.

2.2.19 CRISPR/Cas9 Double Nickase Plasmid Transfection Protocol

Cas9 ATF4 and Cas9 ASNS were ordered from Santa Cruz biotechnology, USA. Whereas Control Double Nickase Plasmidwas as a negative group.

1. 2×10^5 cells were seeded in 6-well plates with antibiotic-free standard growth medium per well, 24 hours prior to transfection.

2. The transfection solution was prepared as followed:

   2.1. Solution A: 10 μl of Plasmid DNA diluted into 140 μl shRNA Plasmid Transfection Medium per each sample. The solution A was be stand for 5 minutes at room temperature.

   2.2. Solution B: 10 μl of UltraCruz® Transfection Reagen was diluted with Plasmid Transfection Medium to final volume to 150 μl for each sample. The solution B was be stand for 5 minutes at room temperature.

2.3. Solution A and Solution B were combined and mixed gently for 20 minutes incubation at room temperature.

3. Prior to transfection, Cells were washed 2x Plasmid Transfection Medium.

4. The 300 µl Plasmid DNA/UltraCruz® Transfection Reagent Complex (Solution A + Solution B) dropwise was added to each well.

5. The plates were swirled gently to ensure that the entire cell layer was immersed in solution.

6. Cells were incubated for 48 hours at 37° C in a CO^2.

7. After incubation, screen for GFP-positive cells was observed by using a fluorescence microscope (Leica Leitz DMRB) to confirm successfully-transfected cells.

8. Cells were proceeded with standard growth medium containing 1 µg/ml puromycin for 2 weeks to select successfully transfected cells. Medium was changed every 3 days.

9. Stable transfected cells were confirmed in Western blot analysis.

2.2.20 Statistics

Data represent mean ± SEM of different experiments, while "N" values in tables represent the number of patients with diagnosis HCC after radical liver resection and number of genes by performing NuRNA^{TM} Human Central Metabolism PCR Array. All the data were analyzed with Mann-Whitney U test by GraphPad, in which Two-way ANOVA determines how a response is affected by two factors, One-way ANOVA compares three or more unmatched groups, based on the assumption that the populations are Gaussian as well as the t test compares one variable between two group. with $p < 0.05$ considered statistically significant.
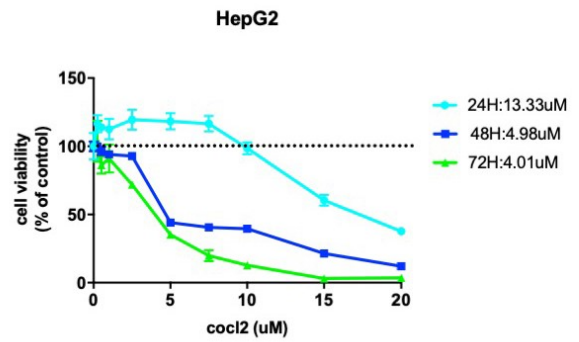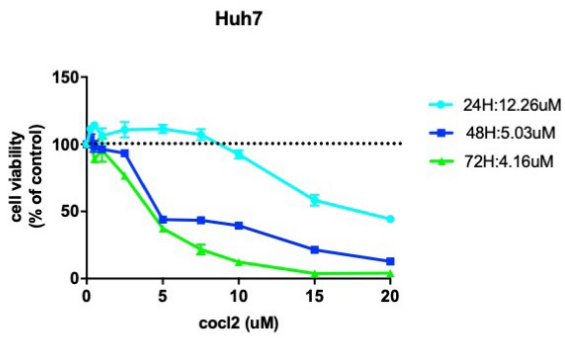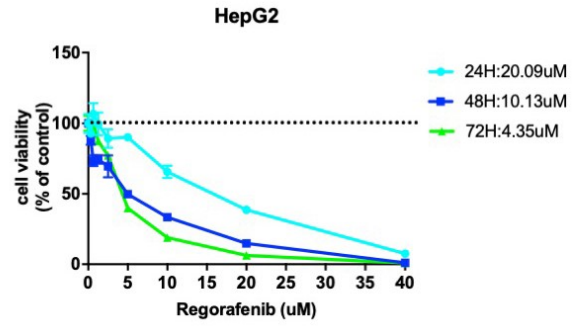
3. RESULTS

3.1 Resistance to endogenous and exogenous low concentration of cellular stress in Hepatocellular Carcinoma

To induce ER stress, Human Hepatocellular Carcinoma cell lines Huh7 and HepG2 were incubated with classic treatments, Sorafenib or Regorafenib (each 0~40uM) as exogenous stressful conditions; and with Cocl2 (0~20uM), a hypoxic conditions inducer, to confirm the half maximal inhibitory concentration (IC50) (Figure 2A). Notably, lower concentrations in contrast were demonstrated to promote the cell growth slightly. To i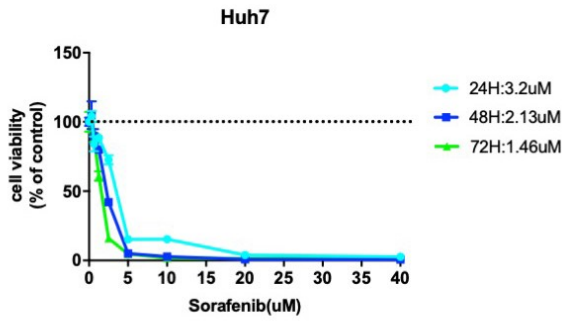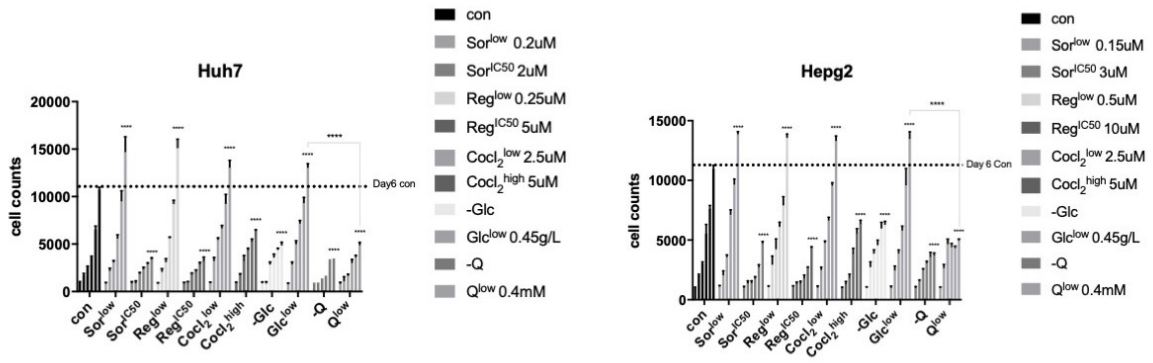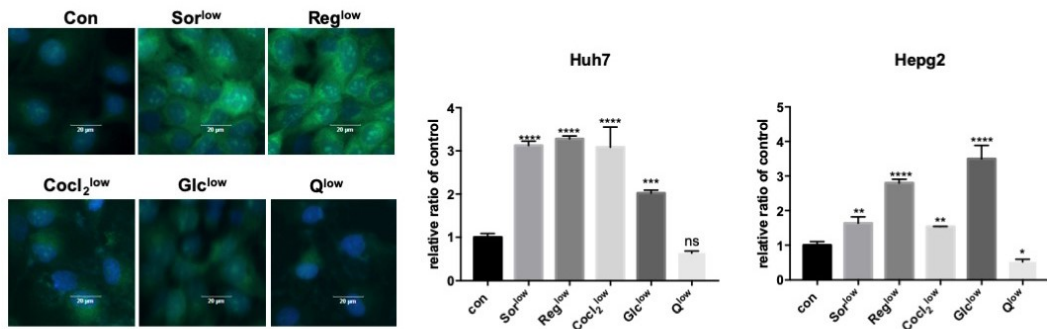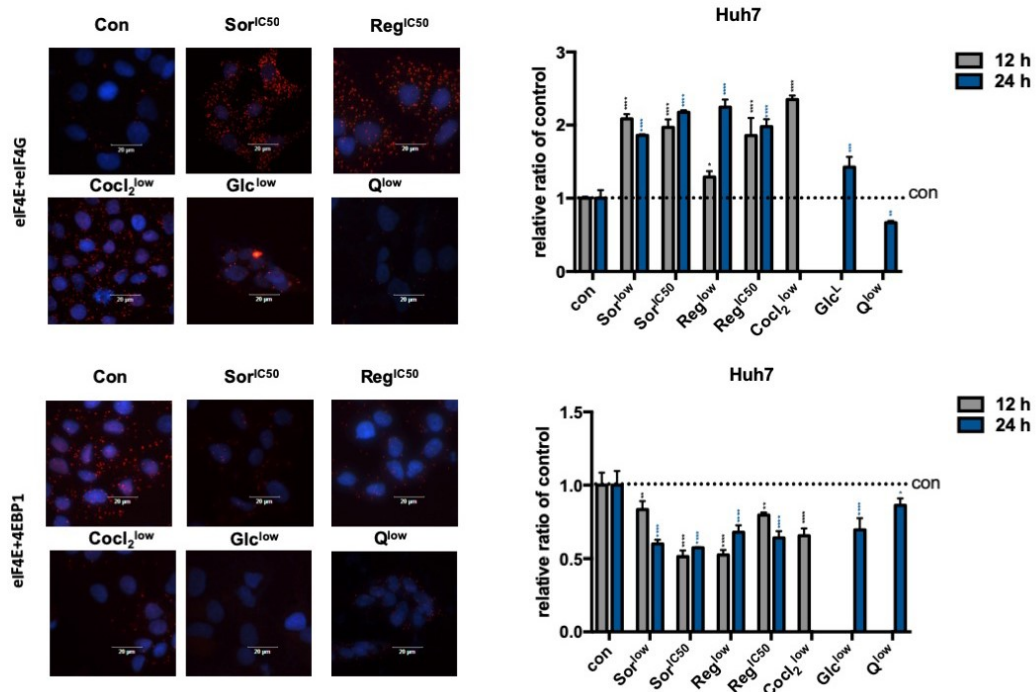nvestigate this concentration discrepancy of effects, cells were then grown for prolonged times to 6 days and cultured in 10- or 20-fold low and approximate IC50 drug concentrations as exogenous therapeutic stimulations and their growth was re-tested. At the same time the introduction of Cocl$_2$ at concentrations that caused hypoxic conditions on cells, and 10-fold lower concentration or the completed deprivation of Glucose and Glutamine in culture medium, were conducted as endogenous changes in tumor microenvironment. In Figure 2B, cells showed rapid cellular proliferation as a sign of resistance to low concentrations of cellular stress except under low concentration of glutamine condition. In contrast with other induced cellular stress conditions, low concentrations of glutamine arrested cell growth. Notably, two main hallmark of cancer metabolism—glucose and glutamine, were shown at low concentration a significant contrary tendency for HCC cells growth in current study. The glutamine abundant medium with a low concentration of glucose stimulated HCC cells proliferation, but the glucose abundant medium with a low concentration of glutamine lost this ability. Sorafenib or Regorafenib with IC50, and glucose or glutamine deprivation inhibited cell proliferation efficiently.
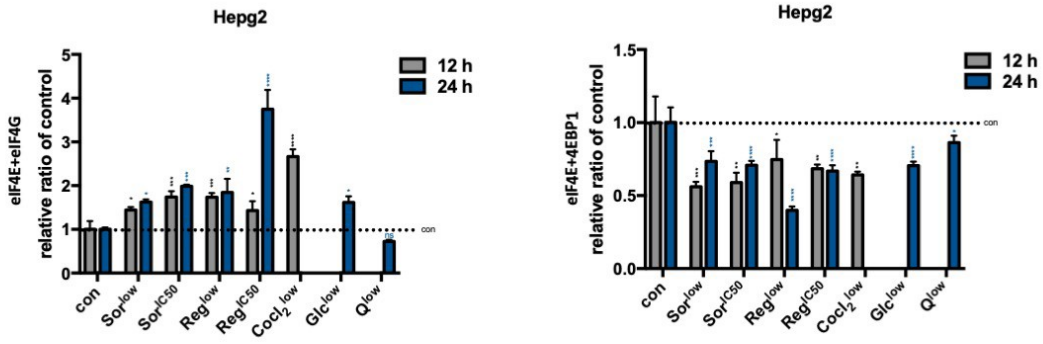
eIF4f complex regulated protein synthesis, the major metabolic event controlling cellular growth and proliferation, was observed in Figure 2C. However, glutamine with low concentration didn't support cellular protein biosynthesis adequately. To investigate further whether the eIF4f complex was involved in protein biosynthesis under different cellular stresses, PLA assay was introduced into the study (Figure 2D). The expressions of eIF4E-4EBP1 interactions were suppressed; phosphorylation of 4EBP1 dissociated eIF4E and associated eIF4E with eIF4G activation to mRNA translation. Among them, Sorafenib and Regorafenib with IC50 concentration were retained with the consideration of feasibility and effectivity for future translational medical study and were also observed to noninteraction of eIF4E-4EBP1 and active interaction of eIF4E-eIF4G like at its low concentration. Both the expressions of eIF4E-4EBP1 and eIF4E-eIF4G were down regulated in the presence of low concentration of glutamine. As shown in Figure 2E by using Western-Blot analysis, cells adapted to different cellular stressors by commonly expressing the subunits of eIF4F complex highly to continue protein translation. The phosphorylation of 4EBP1 and eIF4E was in correspondence with two activated classic arms of the UPR: PERK/CHOP and IRE1α. Low glutamine, however, stimulated the short-term activation of 4EBP1 and eIF4E, which were rapidly down regulated after 24 hours. This was in contrast to continuous UPR activation. Therefore, eIF4F complex modified protein synthesis was shown to be a response to the unfolded protein response and ER stress pathways. However, the maintenance of protein synthesis requests glutamine support.

A

B

Huh7

Hepg2

Legend:
- con
- Sor^{low} 0.2uM
- Sor^{IC50} 2uM
- Reg^{low} 0.25uM
- Reg^{IC50} 5uM
- Cocl$_2$^{low} 2.5uM
- Cocl$_2$^{high} 5uM
- -Glc
- Glc^{low} 0.45g/L
- -Q
- Q^{low} 0.4mM

Legend (Hepg2):
- con
- Sor^{low} 0.15uM
- Sor^{IC50} 3uM
- Reg^{low} 0.5uM
- Reg^{IC50} 10uM
- Cocl$_2$^{low} 2.5uM
- Cocl$_2$^{high} 5uM
- -Glc
- Glc^{low} 0.45g/L
- -Q
- Q^{low} 0.4mM

C Protein Synthesis Assay

Huh7

Hepg2

D PLA Assay

Huh7

Huh7

53

D
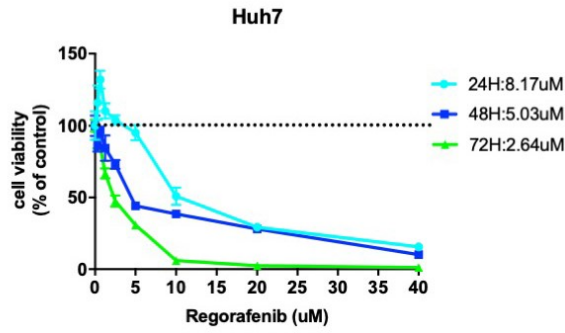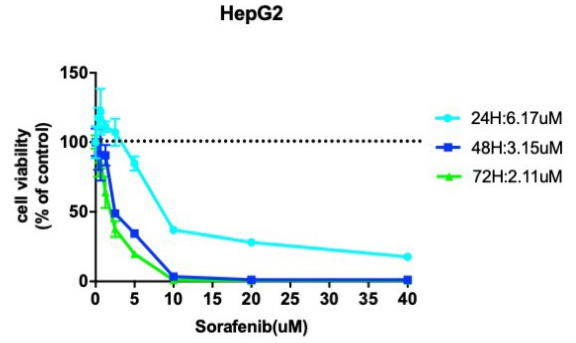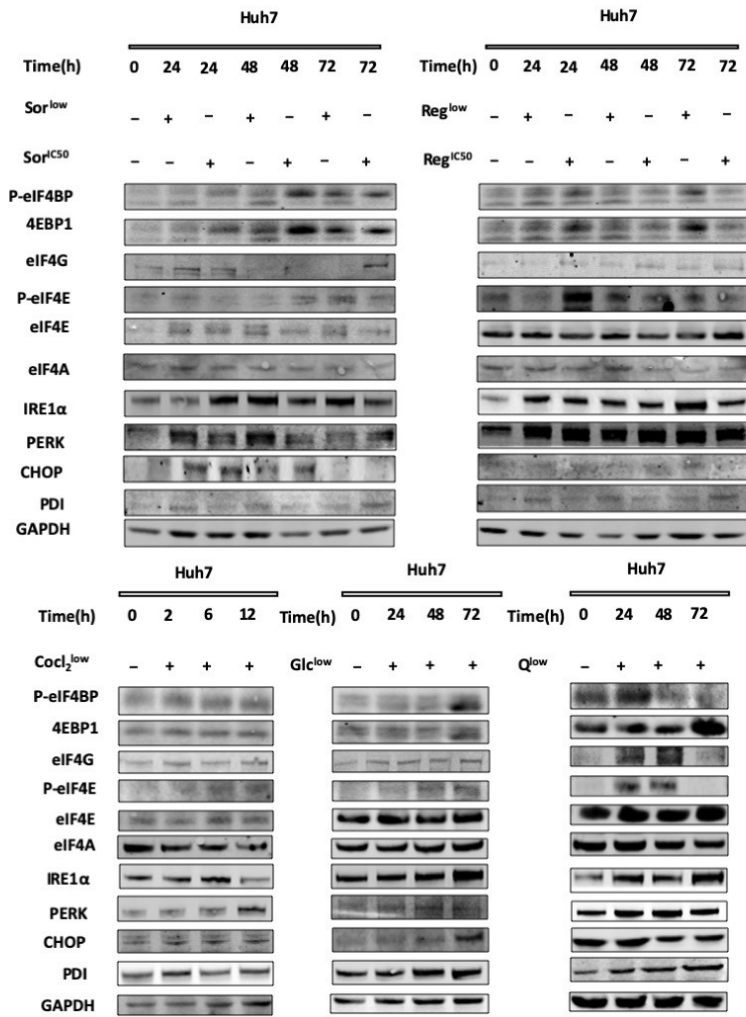
E
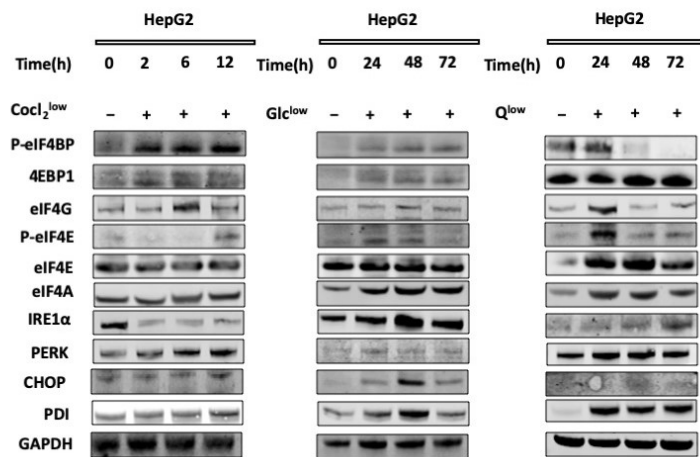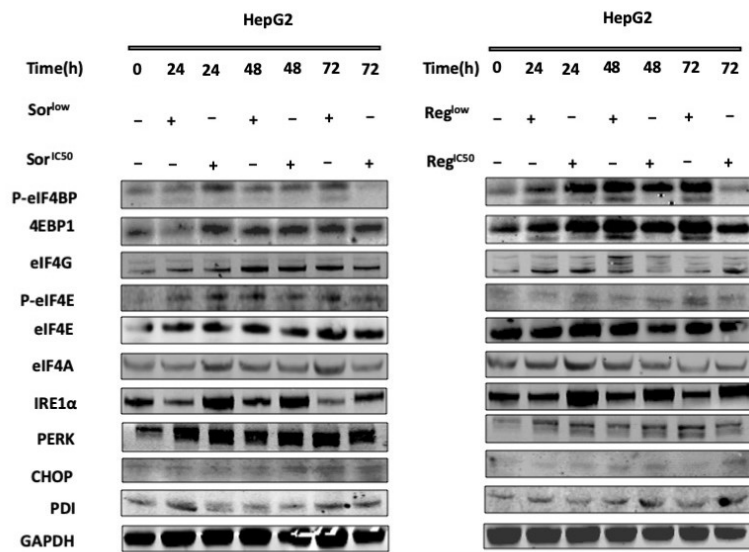
Figure 2. Adaptability and resistance to cellular stress in Hepatocellular Carcinoma. (A) The IC50 value of Sorafenib, Regorafenib and Cocl2 on HCC cell lines Huh7 and HepG2 for 24,48 and 72 hours. (B) Proliferation curves of Huh7 and HepG2 in the presence of various treatments from 0 to 6 days. (C) Protein synthesis ability of Huh7 and HepG2 treated by low concentration of Sorafenib (Sor), Regorafenib (Reg), glucose (Glc) and glutamine (Q) for 24 hours and Cocl2 for 12 hours. Green signal intensity in immunofluorescence reflected the level of new synthesized protein. Blue stain was binding with cell nuclear. Fluorescence was

detected by a Leica microscope at a magnification of 400x. (D) The detection of interaction and binding of eIF4E+eIF4G and eIF4E+4EBP1 in Huh7 and HepG2 treated by various treatments at 12 hours or 24 hours in PLA assay. Complex was visualized red, with nucleus dyed blue by DAPI. Fluorescence was detected by a Leica microscope at a magnification of 400x. (E) In Western Blot analysis, the expression of subunits of eIF4F complex and the phosphorylated forms; ER stress downstream IRE1α, PERK, CHOP and PDI in protein level from Huh7 and HepG2 treated by Sorafenib[IC50], Sorafenib[low], Regorafenib [IC50], Regorafenib[low] , glucose[low] and glutamine[low] at time-point: 24, 48 and 72 hours; and Cocl2^{low} at time-point: 2, 6 and 12 hours. P values were calculated by the Student's t-test: *P≤0.05; **P≤0.01; ***P≤0.001; ****P≤0.0001; ns, not significant.

3.2 Cancer cells increase the uptake and metabolism of glutamine in response to ER stress

The dramatic opposite cellular performance in the present of low glucose and low glutamine medium has drawn the focus of current study on cellular metabolism. Global amino acids regulation was shown to resistance to oxidative stress (Harding *et al.*, 2003). To define the metabolic changes in tumor cells experiencing ER stress response, the enzymatic and protein components in the core metabolic pathways and crucial metabolite transport systems were thus detected via PCR Array containing systematically profiles the expression of 373 transcripts encoding the enzymes or proteins in cell metabolism. Gene expression analysis after low concentration of Sorafenib, which mimics exogenous therapeutic stress, identified 280 genes up-regulated (Fold change [FC] = $2^{-(\Delta Ct \text{ cellular stress} - \Delta Ct \text{ con})}$, $Log_2FC > 1$) by at as. Low glucose was used as endogenous stress stimulant. 102 genes were up regulated ($Log_2FC > 1$) that all were in the lager gene set response to low Sorafenib treatment (Figure 3A-B), which indicated that facing ER stress response triggers cellular metabolism alteration. Analysis of 102 common genes in response to both low Sorafenib and low glucose, using the

gene annotation database provided by manufacturer (Supplementary table 1), revealed that genes were enriched in Nucleotide metabolism (19 genes), Citric acid (TCA) cycle (14 genes), Glycolysis (13 genes), Glutamine transporters and Glutaminolysis (10 genes), Fatty acid oxidation (10 genes), Pentose phosphate pathway (8 genes) and furthermore. Among them, 5 genes could be regard as two activated pathways. When the value of Log2 FC > 2 and a p value <0.05 was used as a cutoff, 36 genes from the low Sorafenib group and 76 genes from the low glucose group were determined as differentially expressed genes (Supplementary table2). The common 10 genes from the top 20 highest expression genes of both groups were picked up to investigate further (Table 2). Those indicated three gene enrichments in Glutamine transporters and Glutaminolysis, the rest in pathways of the TCA cycle, pentose phosphate pathway, lactate production and transporters, redox balance and fatty acid oxidation.

The essentiality of glutamine, but not glucose for maintaining cancer cells proliferation was demonstrated in the first part. 10 up-regulated genes therefore reflected the activated state of Glutamine transporters and Glutaminolysis pathway (Figure 3C). Among them, GLUD1 converts L-glutamate into α-ketoglutarate which is one intermediate products of TCA cycle, SLC1A5 and SLC1A6, the members of solute carrier family located on cell membrane, are responding for glutamine transportation (Plaitakis *et al.*, 2017; Pochini *et al.*, 2014). SLC1A5, as a classic glutamine transporter, was confirmed to be up-regulated at protein level under different stress conditions (Pochini *et al.*, 2014). (Figure 3D) Therefore, when facing extrinsic or intrinsic stressful changes, cancer cells increase the uptake and metabolism of glutamine in response to ER stress.

Gene enrichment and pathway analysis of the 102 genes with up expression in both low Sorafenib and low glucose group was conducted on a public database which comprises the core of most existing gene annotation portals, such as GO、KEGG、UniProt, DrugBank etc

(Zhou *et al.*, 2019). The analysis indicated gene enrichments in nucleotide metabolism, carbon metabolism, TCA cycle, purine metabolism Pentose phosphate pathway, fatty acid catabolic process, amino acid transport, etc. (Figure 3E). This revealed the possible metabolic pathways of glutamine.

D

E

GO:0055086: nucleobase-containing small molecule metabolic process
hsa01200: Carbon metabolism
R-HSA-71406: Pyruvate metabolism and Citric Acid (TCA) cycle
hsa00230: Purine metabolism
hsa00620: Pyruvate metabolism
hsa00030: Pentose phosphate pathway
GO:0006084: acetyl-CoA metabolic process
hsa05230: Central carbon metabolism in cancer
GO:0009062: fatty acid catabolic process
GO:0043648: dicarboxylic acid metabolic process
GO:1903825: organic acid transmembrane transport
GO:0051156: glucose 6-phosphate metabolic process
R-HSA-499943: Interconversion of nucleotide di- and triphosphates
hsa00640: Propanoate metabolism
R-HSA-425407: SLC-mediated transmembrane transport
GO:0009190: cyclic nucleotide biosynthetic process
GO:0019626: short-chain fatty acid catabolic process
GO:1901607: alpha-amino acid biosynthetic process
hsa01210: 2-Oxocarboxylic acid metabolism
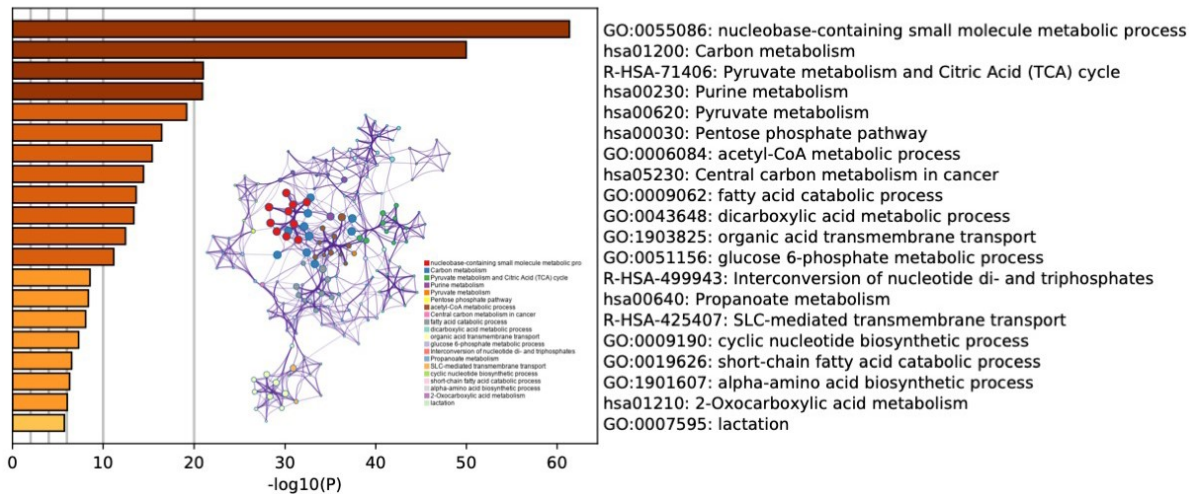GO:0007595: lactation

Figure 3. Increased uptake and metabolism of extracellular glutamine in response to ER stress. (A) The heatmap of the expression of 373 genes from both Sorafenib[low] treated group and glucose[low] treated group after 48 hours comparing with untreated group in cell line Huh7. (B) Venn diagram of overlap positive genes of both groups. The genes enrichment analysis of common 102 genes located in different metabolic pathways by using the gene annotation database provided by manufacturer. (C) The genes enrichment analysis in pathway of glutamine transporters and Glutaminolysis. (D) Western blots of cells expressing SCL1A5 in the presence of Sorafenib[IC50], Sorafenib[low], Regorafenib [IC50], Regorafenib[low] and glucose[low] at time-point: 24, 48 and 72 hours; and Cocl2^{low} at time-point: 2, 6 and 12 hours. (E) The genes enrichment analysis of common 102 genes by using web-analysis tool Metascape(Zhou *et al.*, 2019). Heatmap and Venn diagram was created by R language.

Table2. The common 10 genes from top 20 highest expression genes of both groups

Gene N = 10	Functions	Sor[low] Fold Change	P value	Glc[low] Fold Change	P value
L2HGDH	TCA cycle	804.867458	<0.0001	1350.91774	0.0004
TKTL2	Pentose phosphate pathway	471.988342	<0.0001	910.00087	<0.0001
GLUD1	Glutamine transporters and Glutaminolysis	399.653916	<0.0001	643.467786	0.0001
SLC1A5	Glutamine transporters and Glutaminolysis	124.725048	<0.0001	137.160772	<0.0001
SLC1A6	Glutamine transporters and Glutaminolysis	7.37481785	0.0005	1128.13509	<0.0001
SLC16A2	Lactate production and transporters	12.929615	0.0002	274.321543	<0.0001
SLC16A12	Lactate production and transporters	6.69278846	0.0007	145.989835	<0.0001
ME3	Redox balance	5.90774443	0.0009	179.73457	<0.0001
CPT2	Fatty acid oxidation	53.5423077	0.0007	113.750109	<0.0001
LIPF	Fatty acid oxidation	9.33472432	0.0004	160.866946	<0.0001

3.3 Glutamine-dependent de novo biosynthesis of Asparagine in cancer cells experiencing ER stress response

When glucose levels are low, cells commonly shift to glutaminolysis to maintain TCA cycle ATP and NADPH production (Lu *et al.*, 2010). To define whether the increased biosynthetic activity of cancer cells also requires a corresponding increase in the supply of ATP to maintain homeostasis under cellular stress, the intracellular ATP concentration in stimulated cells was measured. Analysis showed that it was down-regulated (Figure 4A), suggesting that the contribution of glutamine to ATP synthesis is not the cause of cellular adaption to ER stress response. In Figure 4B, no significant changes of cellular NAPDH level between the control and deferent cellular stress treated groups suggested that the increase of extracellular glutamine uptake was not used for the support of glutathione synthesis in redox balance.

Proliferating cells utilize the TCA cycle as the source of not only bioenergetic NADH and FADH2 equivalents, but also biosynthetic precursors (DeBerardinis *et al.*, 2007). In contrast to glucose which only supplies a carbon source for biosynthesis, glutamine supplies amino acids, including asparagine, and γ-nitrogen that rapidly proliferating cancer cells require for the synthesis of nucleic acids (Lu *et al.*, 2010). Asparagine is de novo synthesized from aspartate and glutamine by asparagine synthetase (ASNS), the transcriptional target of ATF4 (Ubuka and Meister, 1971). Like glutamine, asparagine has a critical role in nucleotide biosynthesis, and is a key coordinator for growth-promoting signals, such as the mTOR/4EBP1 pathway (Nicklin *et al.*, 2009; Zhang *et al.*, 2014). To test the hypothesis that de novo biosynthesis of asparagine may be up-regulated in correspondence with high exogenous glutamine uptake, ASNS, ATF4 as well as the AKT/mTOR/c-Myc cascades were investigated. It was observed that ATF4 up-regulated ASNS and the activation of mTOR pathway at protein level, which also occurred in the Sorafenib or Regorafenib IC50 concentration treatment groups (Figure 4C). In addition, depletion of glutamine resulted in

suppressed ASNS and mTORC1 signaling after a short time accumulation of 24 hours, which suggested that abundant glutamine is the prerequisite for asparagine de novo synthesis in cancer cells.
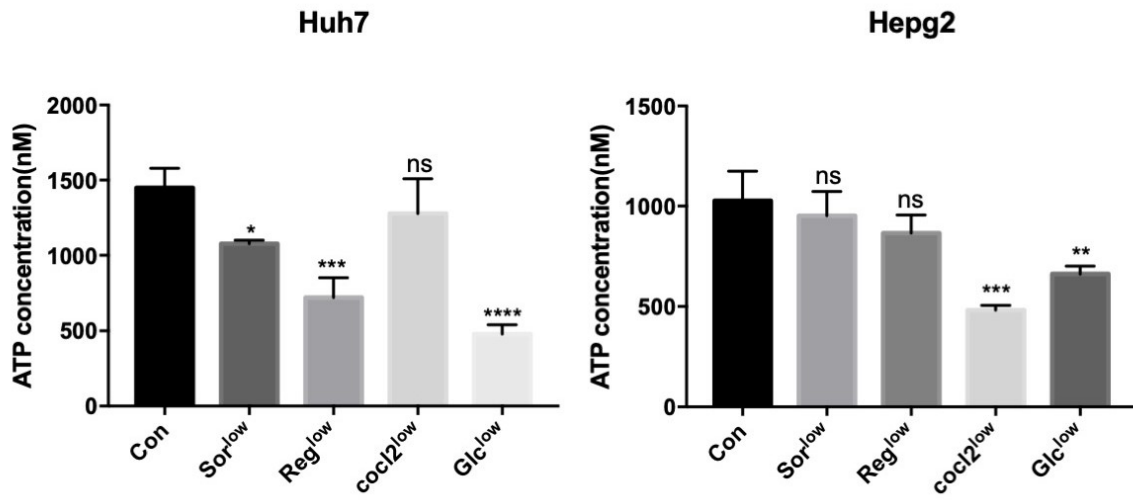
Moreover, to study the regulation of the target proteins of the eIF4F complex and 4EBP1, the proteins PERK, ATF4, ASNS and SLC1A5 as well as related regulators were evaluated in tumor and corresponding non-tumor tissues from patients diagnosed with HCC (Figure 4D). As shown in Figure 4E-4G, the expression ratio of most proteins in tumor compared with non-tumor tissue were associated with the degree of tumor stage. In stage 3, the expression of ASNS was the fourth highest expression after c-Myc, eIF4E and eIF4G, followed also by mTOR as fifth and SLC1A5 as sixth. These biomarkers expressed higher in stage 3 than stage 1 and 2, which implicated the increased protein synthesis and vigorous metabolism in advanced tumor. In additional correlation analysis, a significant and positive correlation was confirmed between eIF4E and c-Myc, eIF4E and 4EBP1, ATF4/ASNS/mTOR cascades and 4EBP1 (score >0.5). Therefore, up-regulated expression of ASNS has a prognostic implication for HCC patients and suggested that asparagine biosynthesis is required for tumor differentiation and growth.

To define that ASNS activity is responsive to cellular stress, gene analysis of ASNS and related factors ATF4, mTOR, 4EBP1, eIF4F complex, SCL1A5 and Myc were evaluated based on public online gene databases from human hepatocellular carcinoma that ASNS expressed up in tumor tissues comparing with normal liver tissues (Figure 4H). In addition, by using dataset of Expression Profiles of HepG2 cells treated with 22 compounds vs solvent controls, or combined dataset of Cysteine and leucine deprivation in liver cell lines (Figure 4I), the conditions that significantly affected the expression of genes were identified. Comparing with others, highly elevated ASNS protein expression as observed in the current trial was previously associated with therapies or amino acids deprivation. This was coincident
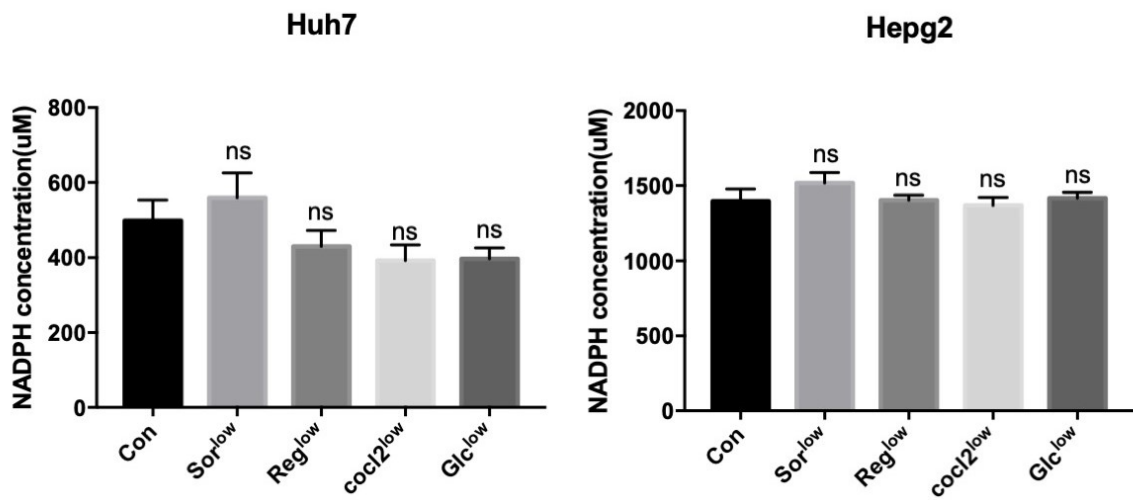
with the results of our study. Thus, it is verified that ASNS expression levels may also be directly correlated with the response to endogenous and exogenous stress in cancer to drive asparagine biosynthesis.

To address the importance of asparagine relative to other NEAA, cells were cultured with asparagine or NEAA in presence or absence of glutamine and cellular viability was evaluated. Total NEAA added into medium without glutamine retained the cellular proliferation ability (Figure 4J). Substitution with Alanine (A), Aspartic acid (D), Glutamic acid (E), or Proline (P) (which were present in DMEM, high glucose, NEAA, no glutamine medium in contrast to DMEM, high glucose, no glutamine medium) failed to reverse glutamine deprivation induced cell growth arrest. Except that, only single asparagine (N) mostly was able to maintain cancer cell growth and shown no significance in comparing with the promoted proliferative effects of total NEAA medium. The exogenous asparagine promoted cell growth in the presence of glutamine (Q). Consistently, the protein synthesis was regained and enhanced by adding exogenous asparagine into the medium in absence as well as presence of glutamine (Figure 4K). To assess the regulation of glutamine and asparagine on the cell cycle, flow cytometry was used. As shown in Figure 4L, glutamine deprivation inhibited the cell proliferation by arresting cell growth in the G1 phase and shortens the S phase significantly. In contrast, supplementation of exogenous asparagine led to recovery of cells which entered from G1 induced arrest into S phase. These results identified that glutamine independence confers exogenous asparagine dependence for cell proliferation in cancer cells.
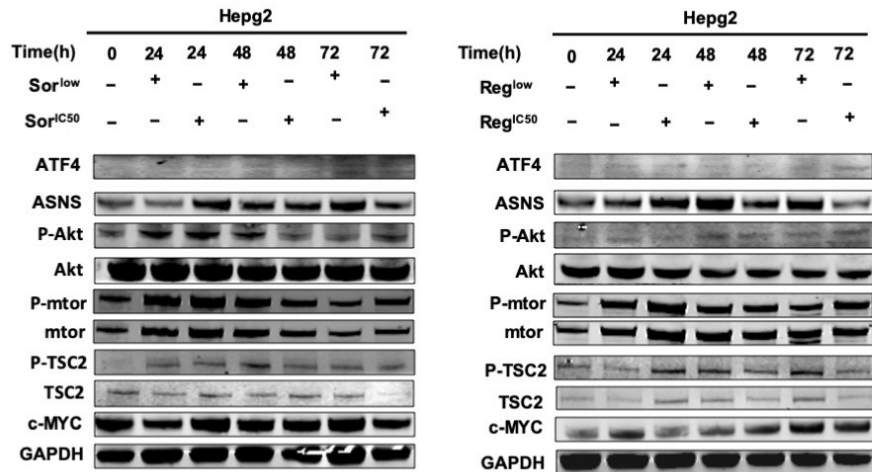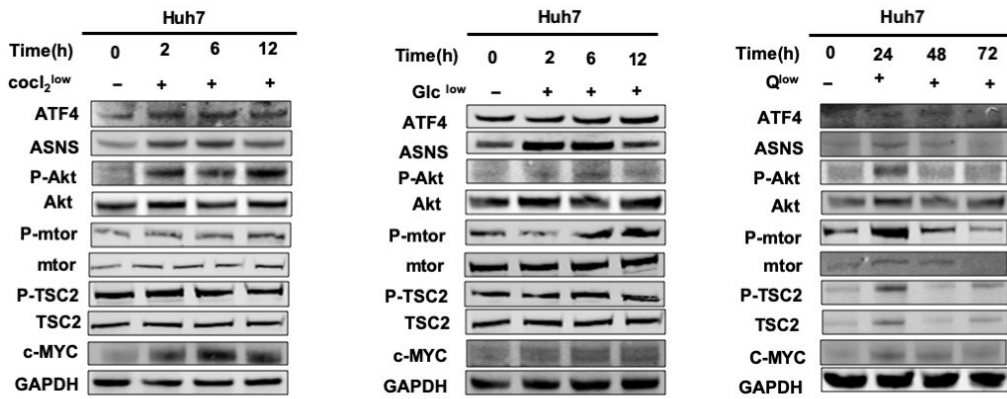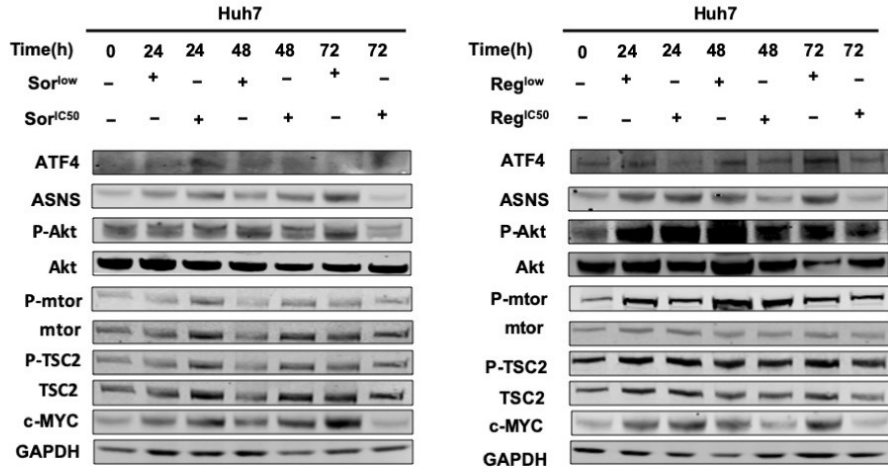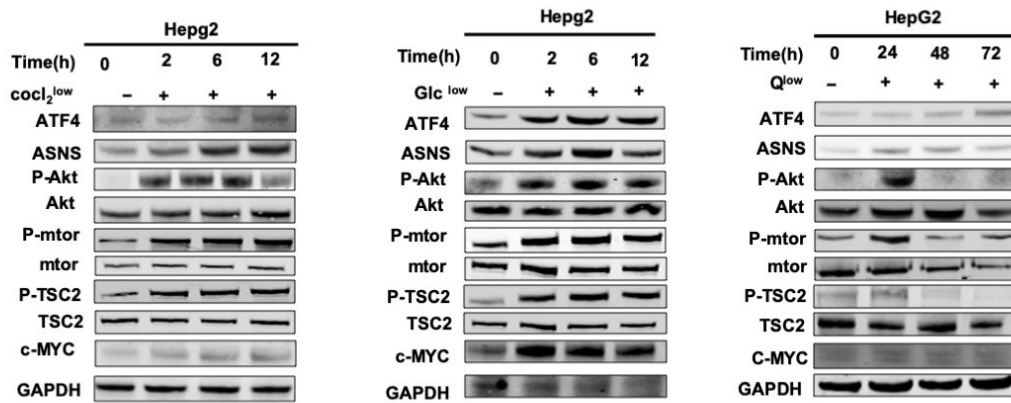
A

Huh7

Hepg2

B

Huh7

Hepg2

C

C

D

E

F

G

H

EIF4A1 · EIF4A2 · EIF4E · EIF4G1 · EIF4EBP1
ASNS · ATF4 · SLC1A5 · MYC · MTOR

Level of expression

LOW	MEDIUM (=IQR)	HIGH

Homo sapiens (2)

	8	9	10	11	12	13	14	15	16	samples	avg. expr.
liver										21	11.71
liver, hepatocellular carcinoma, NOS										22	10.75

8 9 10 11 12 13 14 15 16

I

Log2-ratio
-2.5 -2.0 -1.5 -1.0 -0.5 0.0 0.5 1.0 1.5 2.0 2.5
Down-regulated / Up-regulated

24 of 24 perturbations fulfilled the filter criteria

Filter values for selected measure(s)

Homo sapiens (24)	EIF4A1	EIF4A2	EIF4E	EIF4G1	EIF4EBP1	ASNS	ATF4	SLC1A5	MYC	MTOR	Pi-score	Log2-ra... ▽	no filter Fold-Change	no filter p-value
HS-01057 diclofenac study 6 (55uM) / vehicle (PBS) treated HepG2 sample											14.40	3.60	11.66	<0.001
HS-01057 ethinylestradiol study 3 (90uM) / vehicle (DMSO) treated HepG2 sa...											13.31	3.33	7.99	<0.001
HS-01057 paracetamol (acetaminophen) study 7 (10000uM) / vehicle (DMSO)...											13.10	3.28	7.76	<0.001
HS-01057 ciclosporin study 6 (20uM) / vehicle (DMSO) treated HepG2 sample											12.20	3.05	6.60	<0.001
HS-01057 tetracycline study 7 (2000uM) / vehicle (DMSO) treated HepG2 sa...											12.04	3.01	6.42	<0.001
HS-01057 nifedipine study 8 (106.25uM) / vehicle (DMSO) treated HepG2 sa...											10.19	2.55	4.71	<0.001
HS-01057 ciclosporin study 6 (3uM) / vehicle (DMSO) treated HepG2 sample											9.46	2.37	4.34	<0.001
HS-01057 tolbutamide study 7 (2000uM) / vehicle (DMSO) treated HepG2 sa...											6.40	1.96	3.17	<0.001
HS-01057 chlorpromazine study 11 (20uM) / vehicle (DMSO) treated HepG2 ...											2.67	1.35	2.09	0.011
HS-01057 amiodarone study 7 (15uM) / vehicle (DMSO) treated HepG2 sample											1.83	1.24	2.41	0.033
HS-01057 azathioprine study 7 (250uM) / vehicle (DMSO) treated HepG2 sa...											1.57	1.14	2.13	0.042
HS-01057 phenobarbital study 4 (1000uM) / vehicle (DMSO) treated HepG2 ...											1.31	1.00	1.63	0.050
HS-01057 estradiol study 24 (30uM) / vehicle (DMSO) treated HepG2 sample											0.18	0.43	1.10	0.388
HS-01057 valproic acid study 26 (2000uM) / vehicle (PBS) treated HepG2 sa...											0.37	0.43	1.29	0.136
HS-01057 D-mannitol study 1 (250uM) / vehicle (PBS) treated HepG2 sample											0.34	0.41	1.28	0.151
HS-01057 cyclophosphamide study 4 (2000uM) / vehicle (PBS) treated HepG...											0.09	0.24	1.25	0.426
HS-01057 mitomycin study 1 (0.2uM) / vehicle (DMSO) treated HepG2 sample											0.02	0.17	-1.12	0.726
HS-01057 clonidine study 4 (500uM) / vehicle (DMSO) treated HepG2 sample											0.02	0.17	-1.10	0.732
HS-01057 paraquat study 1 (120uM) / vehicle (PBS) treated HepG2 sample											0.04	0.16	1.08	0.557
HS-01057 D-mannitol study 1 (2000uM) / vehicle (PBS) treated HepG2 sample											0.01	-0.09	-1.11	0.741
HS-01057 isoniazid study 7 (2000uM) / vehicle (DMSO) treated HepG2 sample											0.02	-0.14	-1.38	0.768
HS-01057 lithium carbonate study 1 (2000uM) / vehicle (PBS) treated HepG2 ...											0.10	-0.24	-1.22	0.394
HS-01057 adefovir study 1 (50uM) / vehicle (DMSO) treated HepG2 sample											0.14	-0.39	-1.64	0.428
HS-01057 cisplatin study 4 (20uM) / vehicle (PBS) treated HepG2 sample											2.99	-1.13	-2.18	0.002

Log2-ratio
-2.5 -2.0 -1.5 -1.0 -0.5 0.0 0.5 1.0 1.5 2.0 2.5
Down-regulated / Up-regulated

4 of 4 perturbations fulfilled the filter criteria

Filter values for selected measure(s)

Homo sapiens (4)	EIF4A1	EIF4A2	EIF4E	EIF4G1	EIF4EBP1	ASNS	ATF4	SLC1A5	MYC	MTOR	Pi-score	Log2-ra... ▽	no filter Fold-Change	no filter p-value
HS-00510 leucine deprivation study 1 / non-deprivated HepG2/C3A cell sam...											7.69	1.92	3.79	<0.001
HS-00385 cysteine deprivation study 2 / non-deprivated C3A/HepG2 cell sa...											5.40	1.35	2.55	<0.001
HS-00385 cysteine deprivation study 1 (long) / non-deprivated C3A/HepG2 c...											2.78	0.70	1.62	<0.001
HS-00385 cysteine deprivation study 1 (short) / non-deprivated C3A/HepG2 ...											0.26	0.15	1.11	0.020

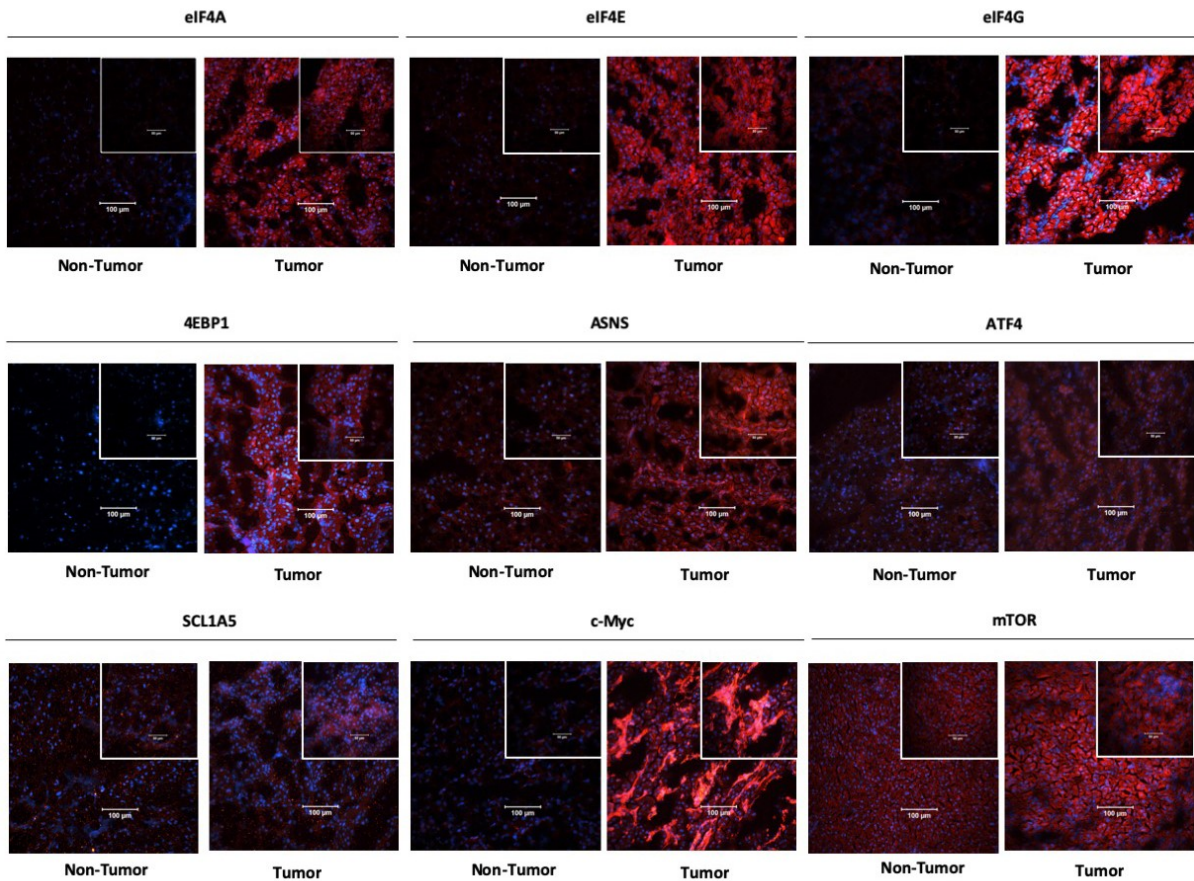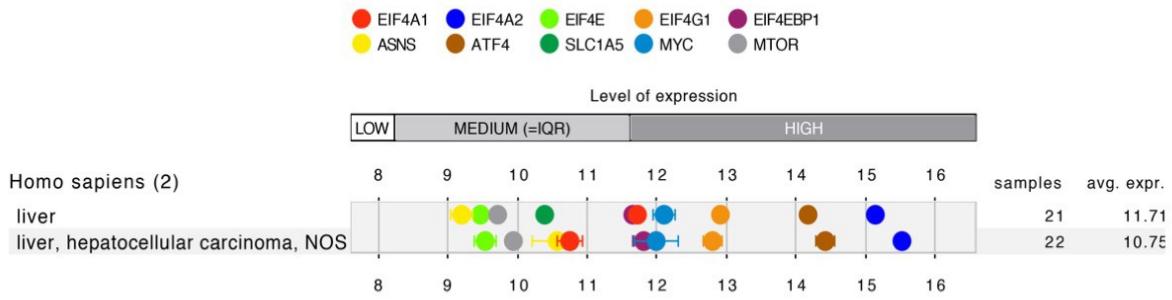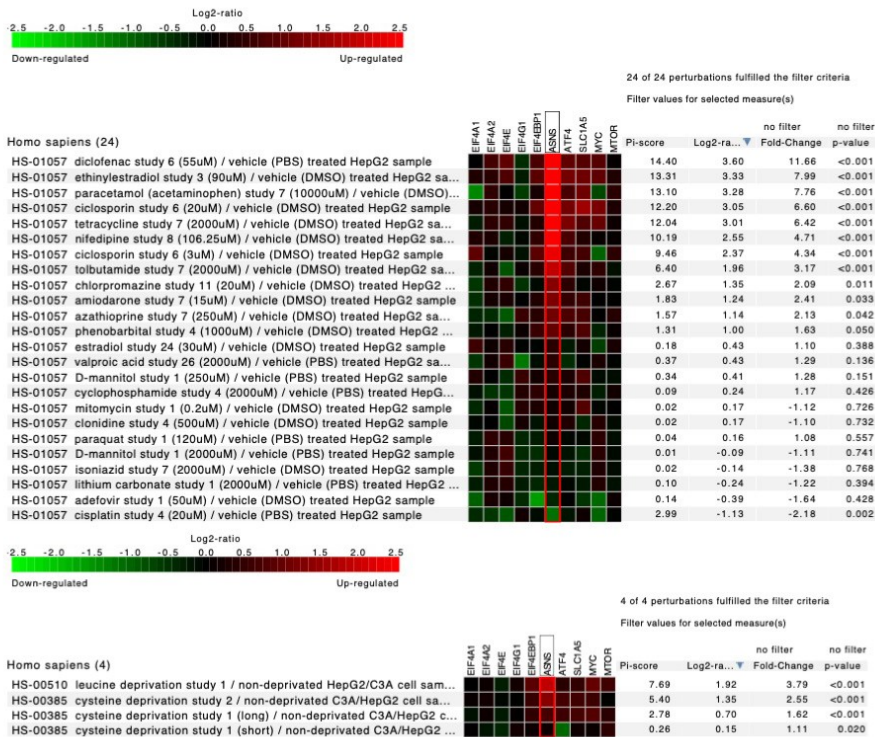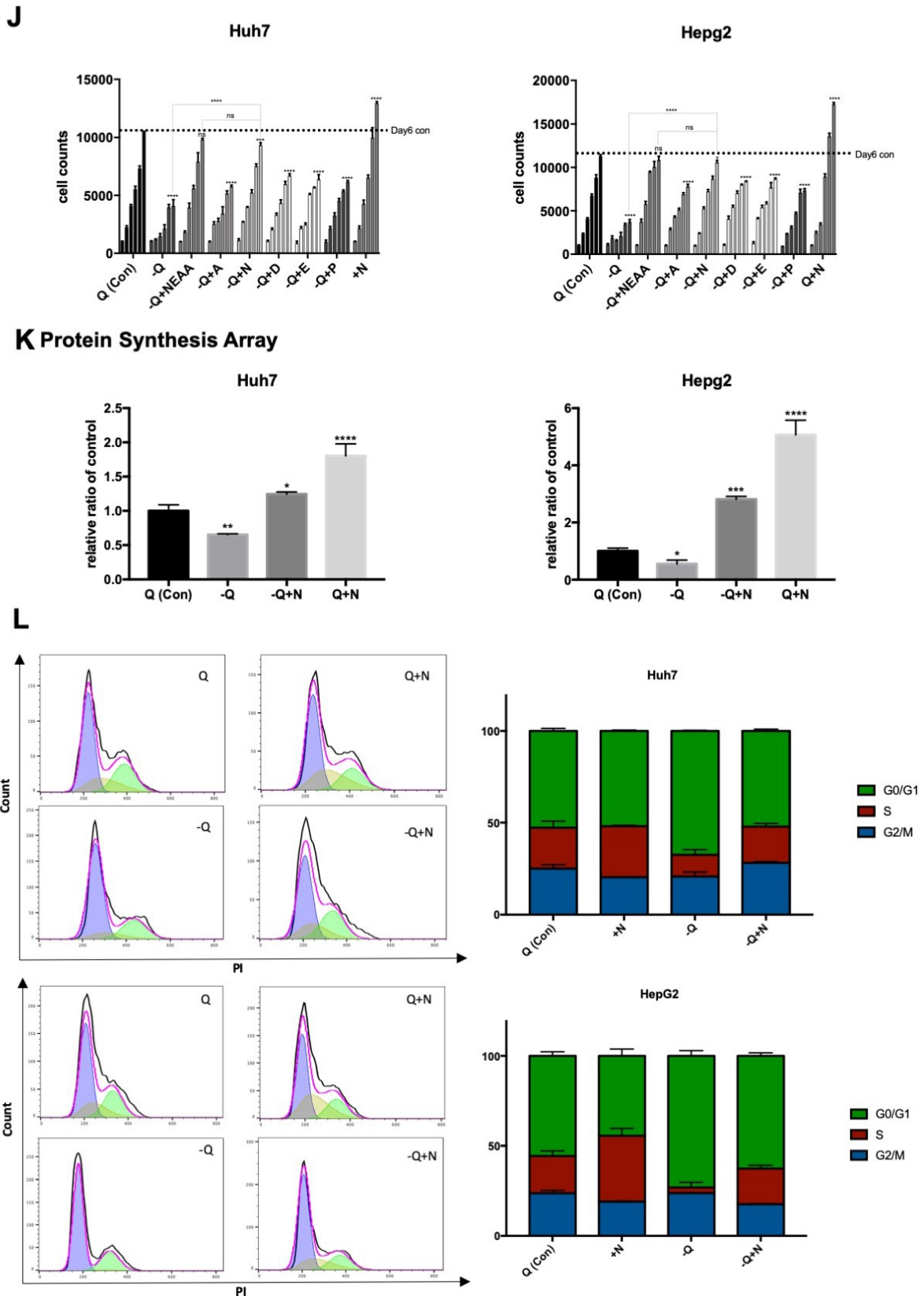**Figure 4. Synergic de novo biosynthesis of Asparagine in cancer cells experiencing ER stress response and its high expression in tumor tissue.** (A) Quantitative determination of

ATP in Huh7 and HepG2 treated by low concentration of Sorafenib (Sor), Regorafenib (Reg), glucose (Glc) and glutamine (Q) for 48 hours and Cocl2 for 12 hours. (B) Quantitative determination of NADPH in Huh7 and HepG2 treated by low concentration of Sorafenib (Sor), Regorafenib (Reg), glucose (Glc) and glutamine (Q) for 48 hours and Cocl2 for 12 hours. (C) Western blots of cells expressing ATF4, ASNS and the downstream mTOR pathway of ASNS and its phosphorylation in Huh7 and HepG2 treated by Sorafenib^{IC50}, Sorafenib^{low}, Regorafenib ^{IC50}, Regorafenib^{low}, glucose^{low} and glutamine^{low} at time-point: 24, 48 and 72 hours; and Cocl2^{low} at time-point: 2, 6 and 12 hours. (D) The eIF4F complex comprising eIF4E, eIF4G, and eIF4A is regulated by the MAPK pathway, the Pi3K/AKT/mTOR pathway, and transcription factors located downstream of receptor tyrosine kinases(Malka-Mahieu *et al.*, 2017). (Own Created Image) (E) Heatmap of expression ratio of eIF4F complex regulators in tumor tissue comparing with corresponding non-tumor tissue from 26 HCC patients after resection, and average expression ratio of each regulator in different TNM stages. (F) Correlation matrix of associations between variables from patients' tissues. (G) Immunofluorescence cytochemistry analysis of the expression of eIF4F complex, 4EBP1, ASNS, ATF4, SCL1A5, c-MYC, and m-TOR in tumor tissue in contrast to corresponding non-tumor tissues from HCC patients. Fluorescence was detected by a Leica microscope at a magnification of 200x and 400x. (H) Expression of genes eIF4F complex, 4EBP1, ASNS, ATF4, SCL1A5, c-MYC, and m-TOR in tumor tissue in contrast to corresponding non-tumor tissues from public HCC patients database (GSM363434) by using gene analysis tool: Genevestigator (Hruz *et al.*, 2008). (I) Gene perturbations analysis of eIF4F complex, 4EBP1, ASNS, ATF4, SCL1A5, c-MYC, and m-TOR in HCC cell lines HepG2 treated by 22 compounds and solvent controls from public database (GSM1255715), or by amino acids deprivation from public database (GSM241156 and GSM329159) by using gene analysis tool: Genevestigator (Hruz *et al.*, 2008). (J) Cell proliferation of Huh7 and
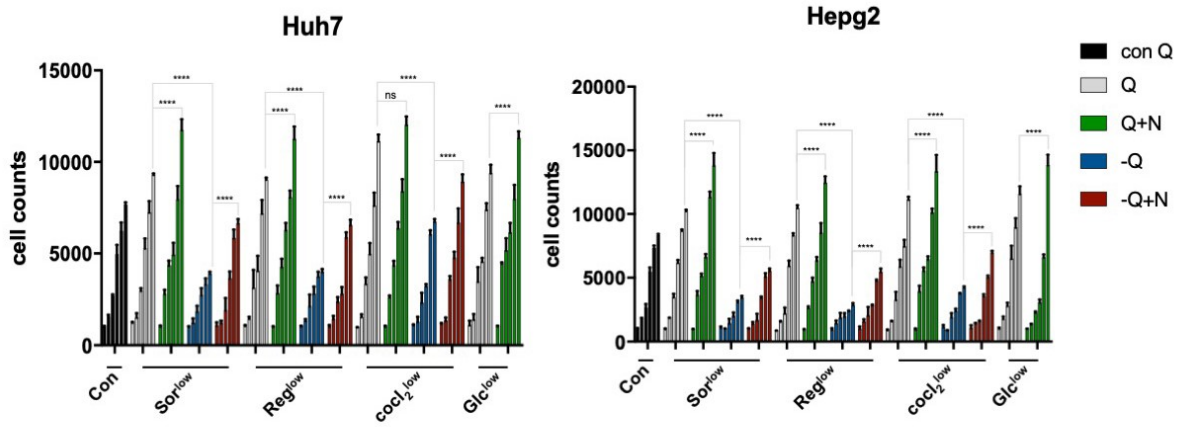
HepG2 cultured with normal DMEM high glucose medium with abundant glutamine (Q, con); normal medium added exogenous asparagine (+N); no glutamine high glucose medium (-Q); no glutamine high glucose and NEAA medium (-Q+NEAA); no glutamine high glucose medium (-Q) with alanine (A), aspartic acid (D), glutamic acid (E), or proline (P) separately for 6 days. (K) The quantitative determination of protein synthesis in Huh7 and HepG2 cultured with normal medium (Q); no glutamine medium (-Q); no glutamine medium added exogenous asparagine (-Q+N); normal medium added exogenous asparagine (Q+N) for 24 hours. (L) Flow cytometry analysis of cell cycle of Huh7 and HepG2 stained with Propidium iodide (PI) after being cultured with normal medium (Q); no glutamine medium (-Q); no glutamine medium added exogenous asparagine (-Q+N); normal medium added exogenous asparagine (Q+N) for 48 hours. P values were calculated by the Student's t-test: *$P \leq 0.05$; **$P \leq 0.01$; ***$P \leq 0.001$; ****$P \leq 0.0001$; ns=not significant.

3.4 Glutamine independence confers exogenous asparagine dependence involved in resistance to ER stress induced apoptosis

The results above suggest that up-regulation of asparagine de novo biosynthesis happened simultaneously with the increasing transport and metabolism of extracellular glutamine in cancer cells responding to ER stress. Exogenous asparagine was sufficient to support survival during long-term glutamine starvation. To address the hypothesis that synthetic asparagine might be used for resistance to ER stress induced apoptosis in cancer cells; cell proliferation and apoptosis were tested when glutamine was withdrawn, and exogenous asparagine was supplemented (Figure 5A). Significantly, the culture medium without glutamine didn't sufficiently support cell growth. However, the pro-survival effect of exogenous asparagine was confirmed to promote cell proliferation under low cellular stress conditions no matter whether glutamine was present. Consistently, the cellular ability to protein synthesis was rescued by adding asparagine in the absence of glutamine (Figure 5B). Glutamine depletion-

induced apoptosis has been shown to be suppressed by exogenous asparagine previously (Zhang *et al.*, 2014). Therefore, to investigate further anti-apoptotic ability of asparagine in resistance to cellular stress, the Annexin V/PI apoptosis assay was used (Figure 5C). HCC cells were treated by Sorafenib or Regorafenib at IC50 concentration after 48 hours. Here, Sorafenib and Regorafenib at IC50 concentration were used for cancer cells treatment based on the consideration of feasibility and availability of drugs IC50 value in clinic. Glutamine deprivation leaded more treated cells to apoptosis, which was blocked by adding exogenous asparagine. These results were even more dramatic in simultaneous presence of exogenous asparagine and glutamine. At protein levels (Figure 5D), removing glutamine from culture medium reduced the expression of ASNS in contrast to sustained expression of ATF4 and CHOP. Additionally, the phosphorylation of mTOR, 4EBP1 and eIF4e was inhibited, but was recovered by exogenous asparagine. The results above are in agreement with the hypothesis that glutamine-deprived cells lose the adaptability of ER stress and covert into apoptosis progress, which could be rescued by exogenous asparagine. Asparagine de novo synthesis is the benefit of cellular resistance to cellular stress provided by ASNS expression, rather than of another aspect of the ASNS reaction.

A

Huh7

Hepg2

con Q
Q
Q+N
-Q
-Q+N

cell counts

B Protein Synthesis Array

Huh7

Hepg2

Q
-Q
-Q+N
Q+N

relative ratio of control

C

Huh7

Q3
Q4
Q2
Q1
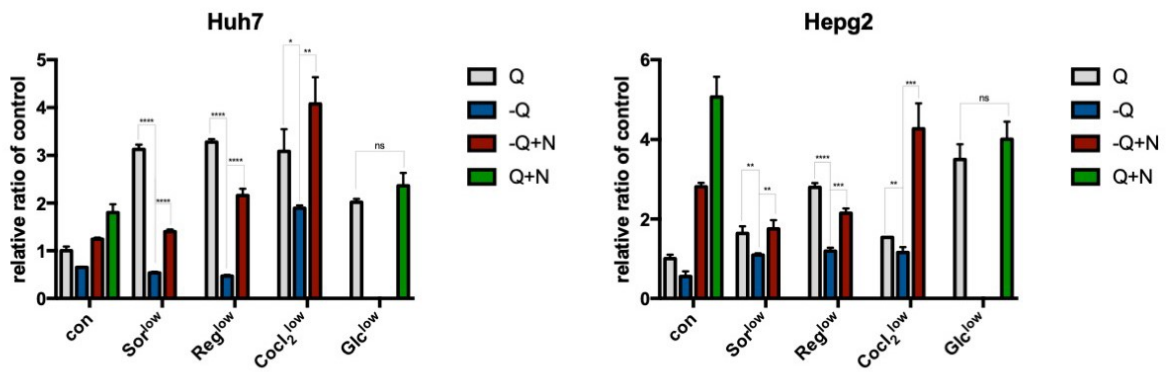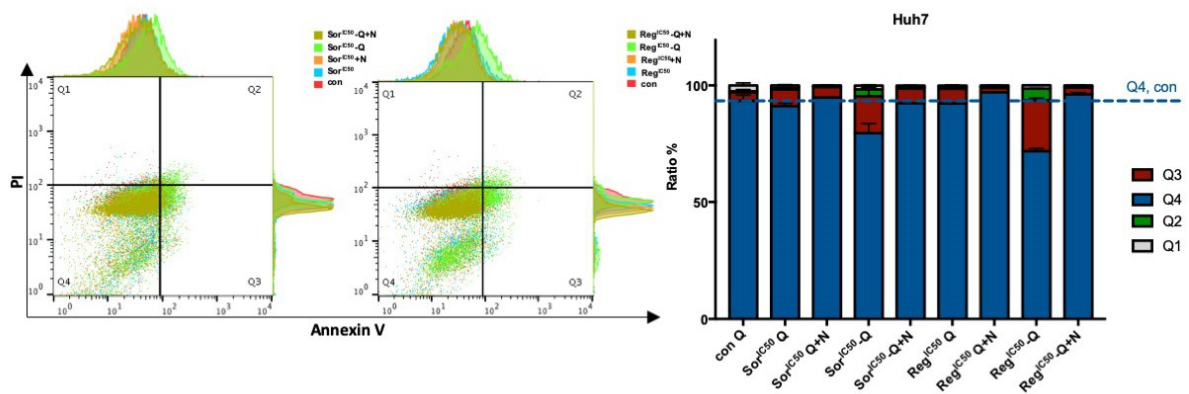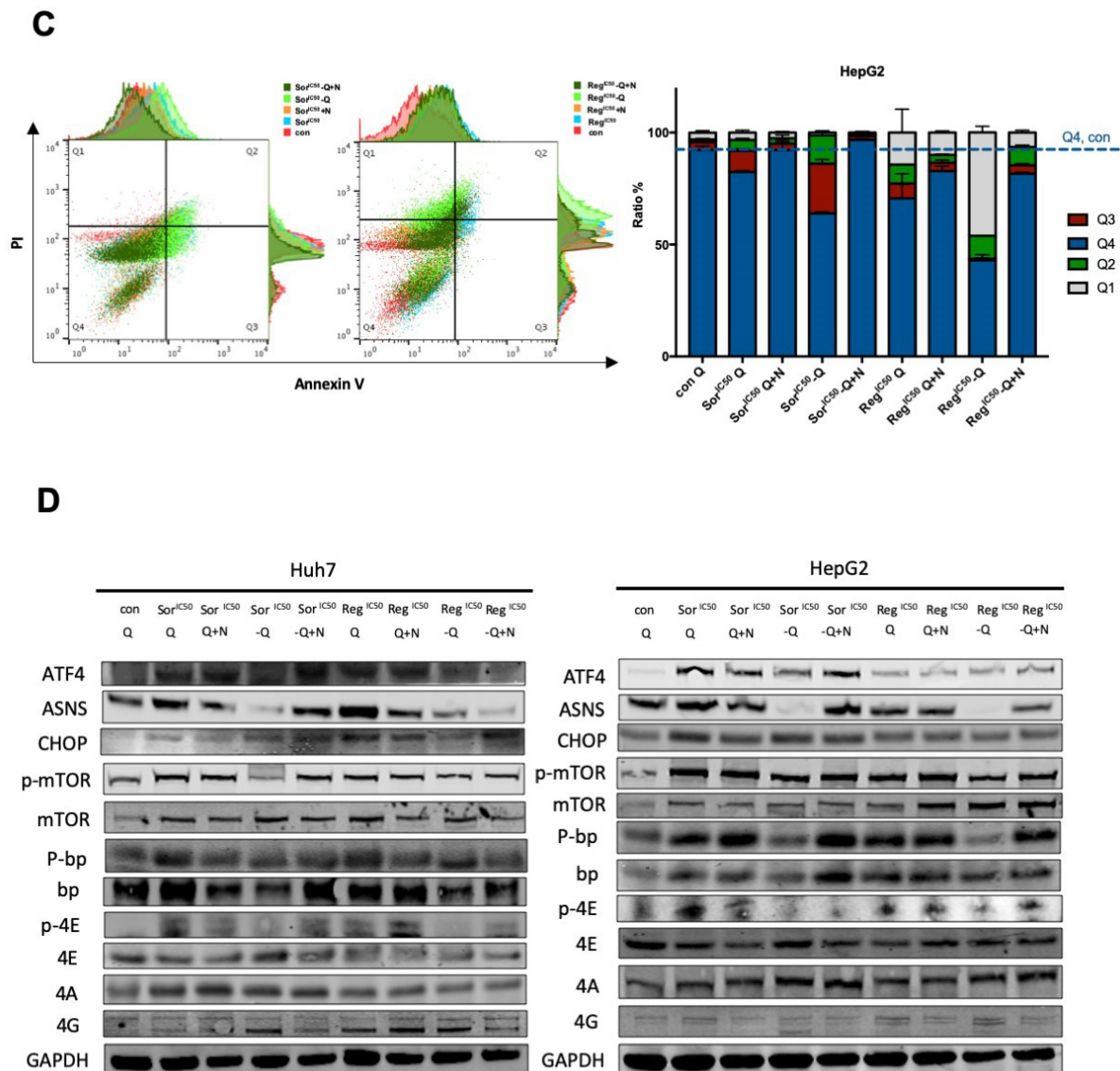
Figure 5. Glutamine independence confers asparagine dependence for adaptability of cancer cells to ER stress. (A) Proliferation curve of Huh7 and HepG2 treated by low concentration of Sorafenib (Sor), Regorafenib (Reg), Cocl2 and glucose (Glc) in contrast to untreated control group in four different culture mediums: normal medium (Q); no glutamine medium (-Q); no glutamine medium added exogenous asparagine (-Q+N); normal medium added exogenous asparagine (Q+N). (B) Quantities of protein synthesis in Huh7 and HepG2 cultured with normal medium (Q); no glutamine medium (-Q); no glutamine medium added

exogenous asparagine (-Q+N); normal medium added exogenous asparagine (Q+N) when exposed to low stress conditions for 24 hours. (C) Apoptosis events of Huh7 and HepG2 treated by Sorafenib (Sor) or Regorafenib (Reg) at IC50 concentration at 48 hours in different culture mediums: normal medium (Q); no glutamine medium (-Q); no glutamine medium added exogenous asparagine (-Q+N); cells were stained with Propidium iodide (PI) and Annexin V before being tested by Flow cytometry. (D) After 48 hours treatment of Sorafenib (Sor) or Regrafenib (Reg) in normal medium (Q); no glutamine medium (-Q); no glutamine medium added exogenous asparagine (-Q+N), the expression of ATF4, ASNS, CHOP, p-mTOR, mTOR, p-4EBP1, 4EBP1, p-eIF4E, eIF4E, p-eIF4A, eIF4A, p-eIF4G, and eIF4G of HCC cells was detected by using Western Blots. P values were calculated by the Student's t-test: *P≤0.05; **P≤0.01; ***P≤0.001; ****P≤0.0001; ns, not significant.

3.5 Nucleotides and protein synthesis, the final target of Asparagine and Glutamine, is used for cellular homeostasis

To study the effects of either glutamine deprivation or asparagine addition on cellular metabolism under ER stress response, human central metabolism PCR array was applied to detect the expression of metabolic genes from low concentration Sorafenib treated cells cultured in no glutamine medium, no glutamine plus asparagine medium, normal glutamine medium, and normal glutamine plus asparagine medium and compared to gene expression from cells cultured in normal medium without treatments as a control group. As shown in Figure 6A, 178 genes were detectable in the low Sorafenib, no glutamine treated group; 199 genes in the low Sorafenib, no glutamine added asparagine treated group; 295 genes in the low Sorafenib, normal glutamine treated group; and 98 genes in the low Sorafenib treated, normal glutamine added asparagine treated group. Of them, 92 genes were detected commonly. Glutamine depletion caused an up-regulated expression of metabolic genes,

which was reduced by adding exogenous asparagine. When glutamine existed in the medium and exogenous asparagine was added, the expression of a total of 92 genes was even lower than that in control group. Further, when subset of genes from different metabolic pathways were picked up for analysis (Figure 6B), glutamine deprivation induced a high expression of genes which were declined when exogenous asparagine was added. In low concentration Sorafenib treated cells cultured with medium including both, glutamine and asparagine, metabolic pathways were all down regulated to the lowest. These data suggested that cells mobilize compensatory metabolic pathways to sustain itself in absence of glutamine. Potentially this could be mitigated by exogenous asparagine. Notably, 23 of 92 genes were enriched in nucleotides metabolism pathway, which is the maximal genes enrichment subset. The participant of Asparagine in nucleotides was demonstrated in a previous study (Lu *et al.*, 2010). It was also confirmed in the current study that exogenous asparagine reversed up-regulated expression of related genes when glutamine was removed. In the ATP determination analysis (Figure 6C) exogenous asparagine promoted ATP synthesis rapidly in untreated cells cultured with medium containing normal glutamine. However, asparagine inhibited ATP synthesis in stressed cells either when glutamine was deprived or not. This implicated that under ER stress response, energy fuels is not the mechanism of asparagine sustain cellular homeostasis from apoptosis. Similarly, in NAPDH determination analysis (Figure 6D), no significant changes of NAPDH levels were found. Neither exogenous nor endogenous Asparagine therefore didn't supply glutathione synthesis for redox balance in cancer cell facing cellular stress.

Asparagine was shown to coordinate protein synthesis. To define that protein synthesis might be the one of mechanisms, by which asparagine promote cancer cell resistance to ER stress induced apoptosis, subunits of eIF4F complex (eIF4A, eIF4E, eIf4G and 4EBP1) were silenced using stable expression of short hairpin RNA (shRNA), to inhibit the initiation of

protein synthesis. As shown in Figure 6E-F, the binding of the eIF4F complex was reduced via knocking down any subunits in PLA assay, followed by the inhibition of protein synthesis (Figure 6H). The cell proliferation was reduced after eIF4F complex or 4EBP1 knockdown compared with untreated cells (Figure 6G). However, cells treated with low concentration stress, and additionally added supplementation of asparagine didn't recover its adaptability to ER stress. Transfected cells were observed to show more apoptosis after 48 hours treatment with Sorafenib or Regorafenib at IC50 concentration (Figure 6I). Therefore, the activity of the eIF4F complex by asparagine contributes to drive protein synthesis in cells resistance to ER stress induced apoptosis.
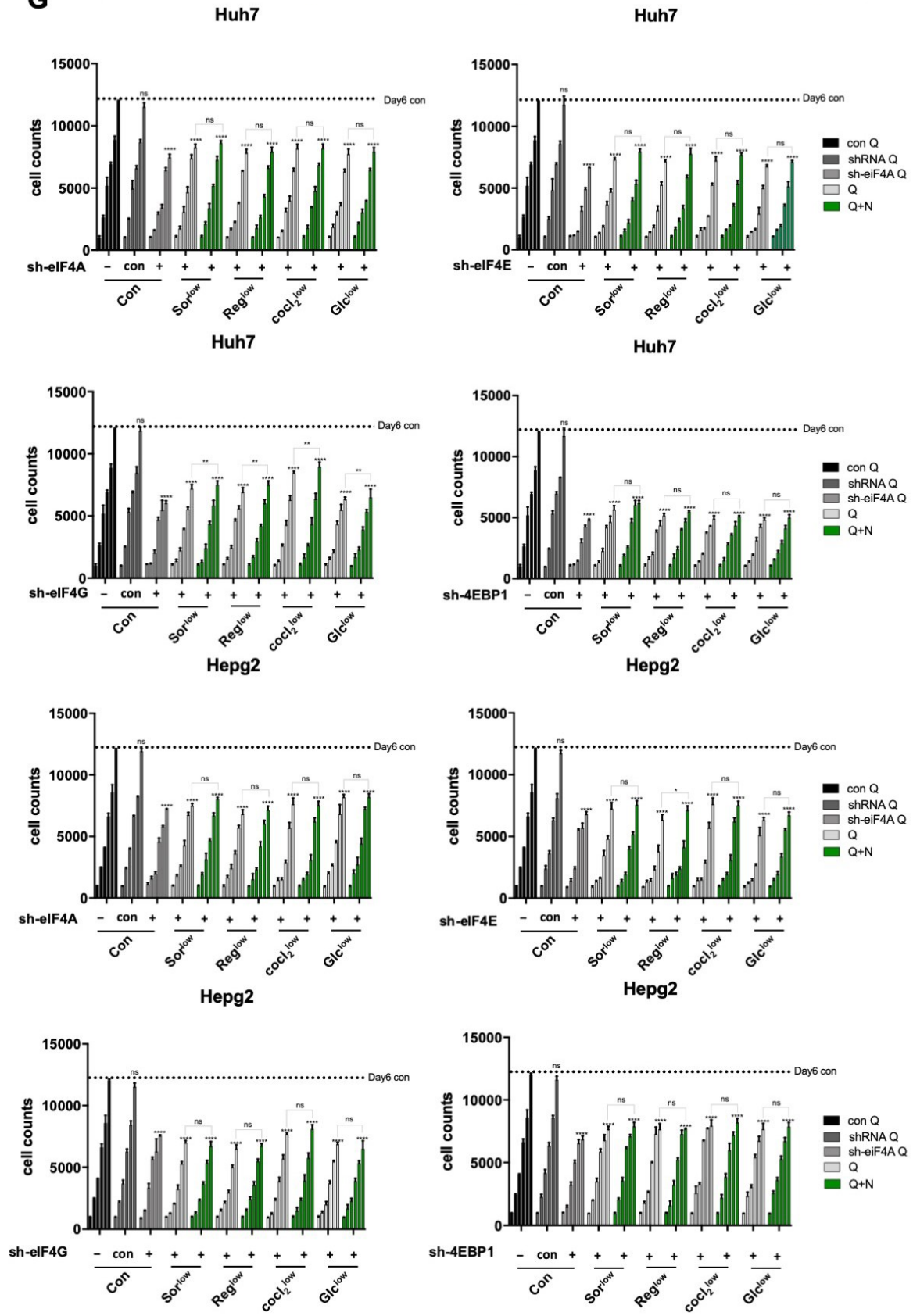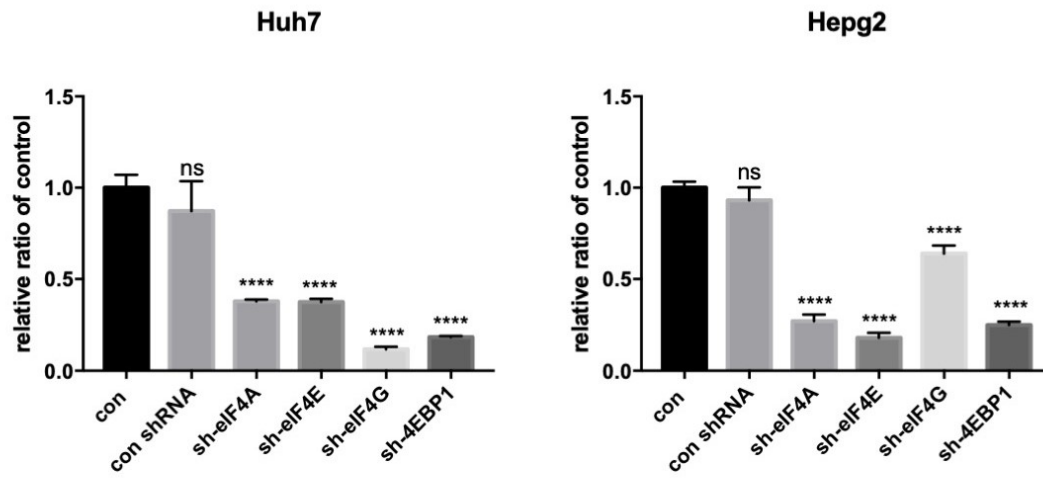
C

Huh7

HepG2

D

Huh7

Hepg2

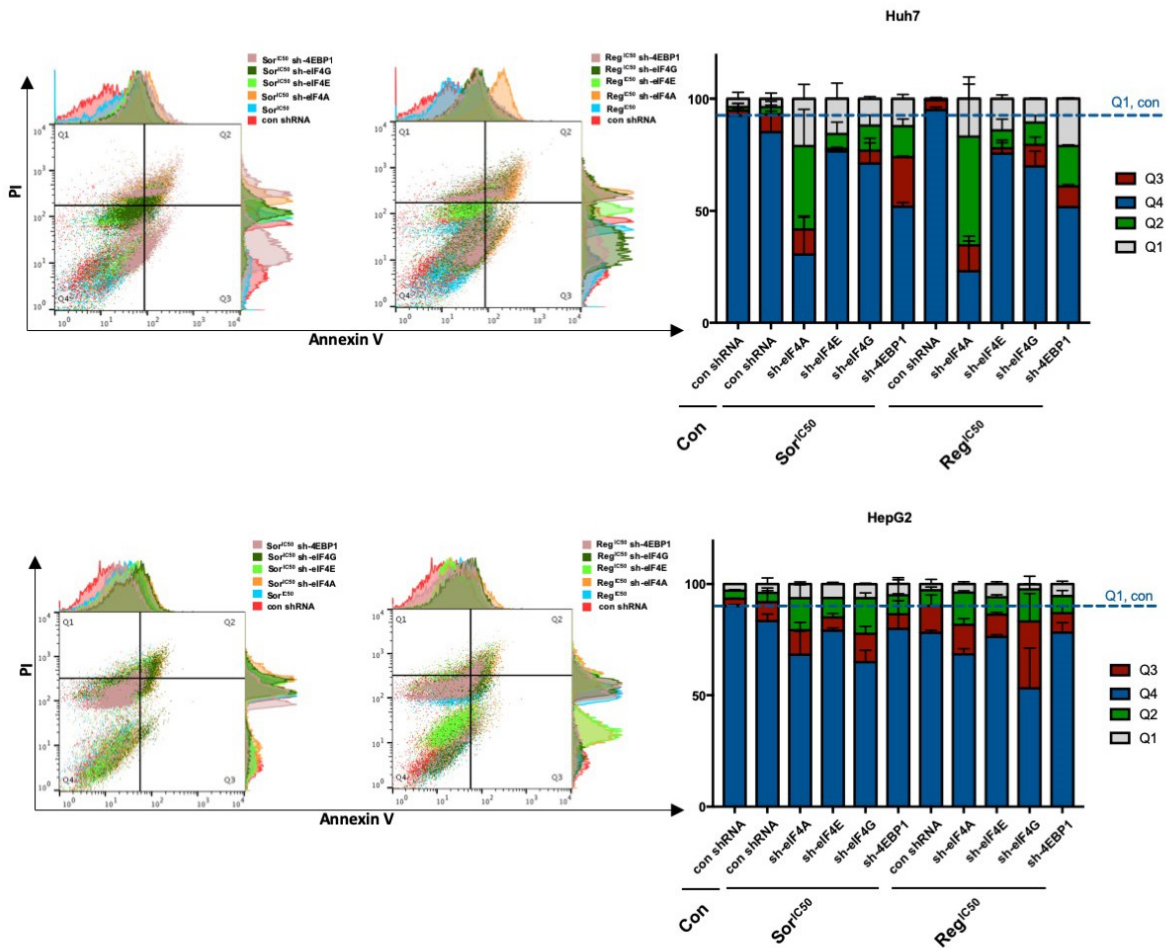**E**
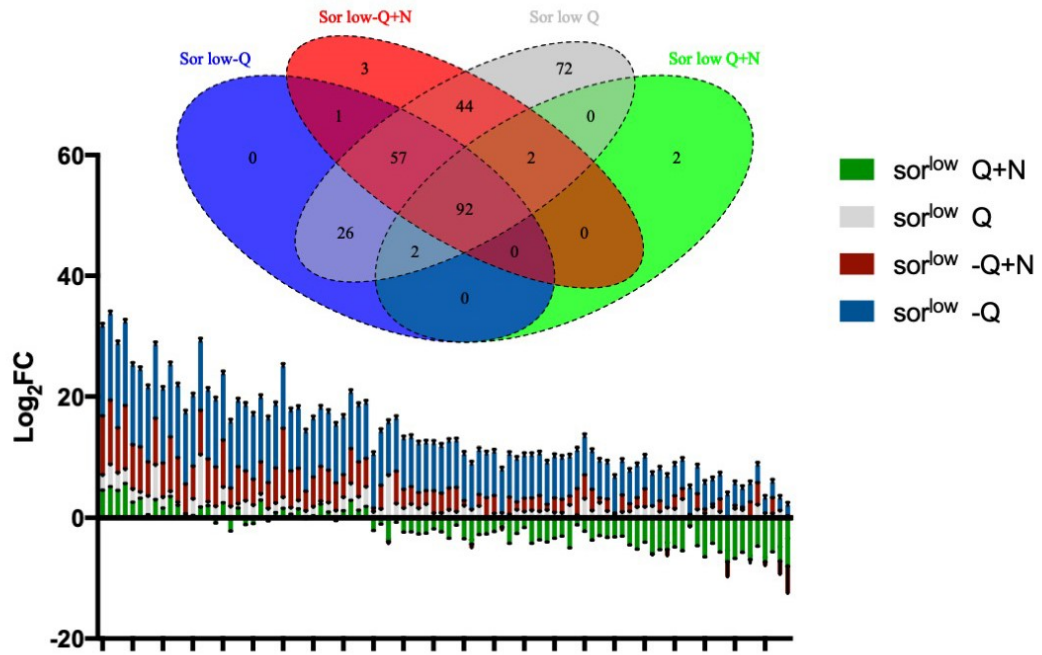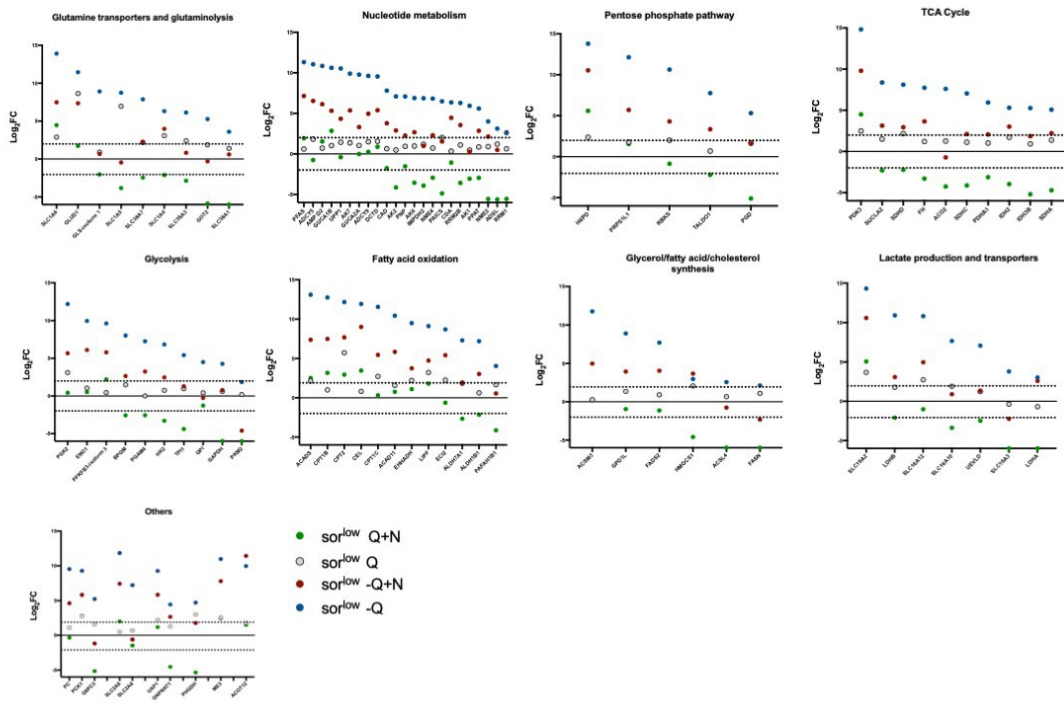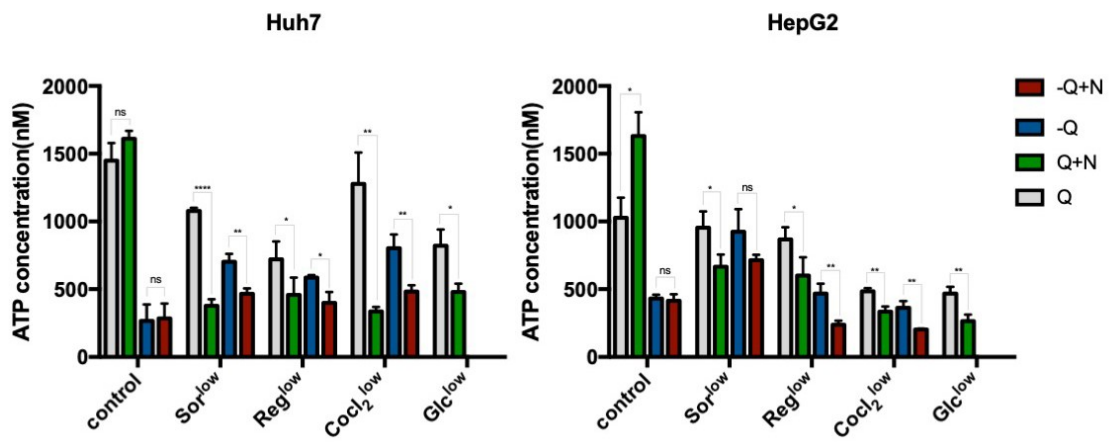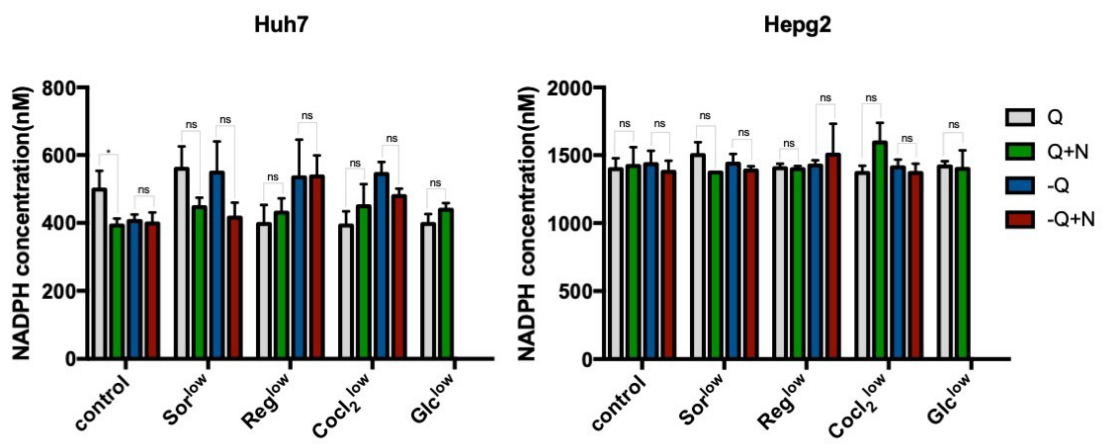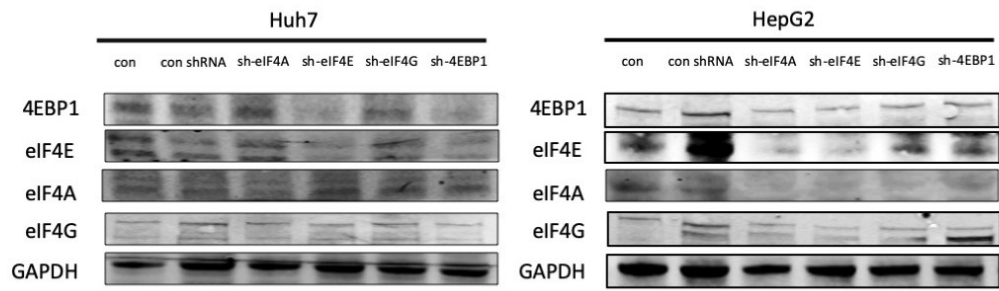
F **PLA array**
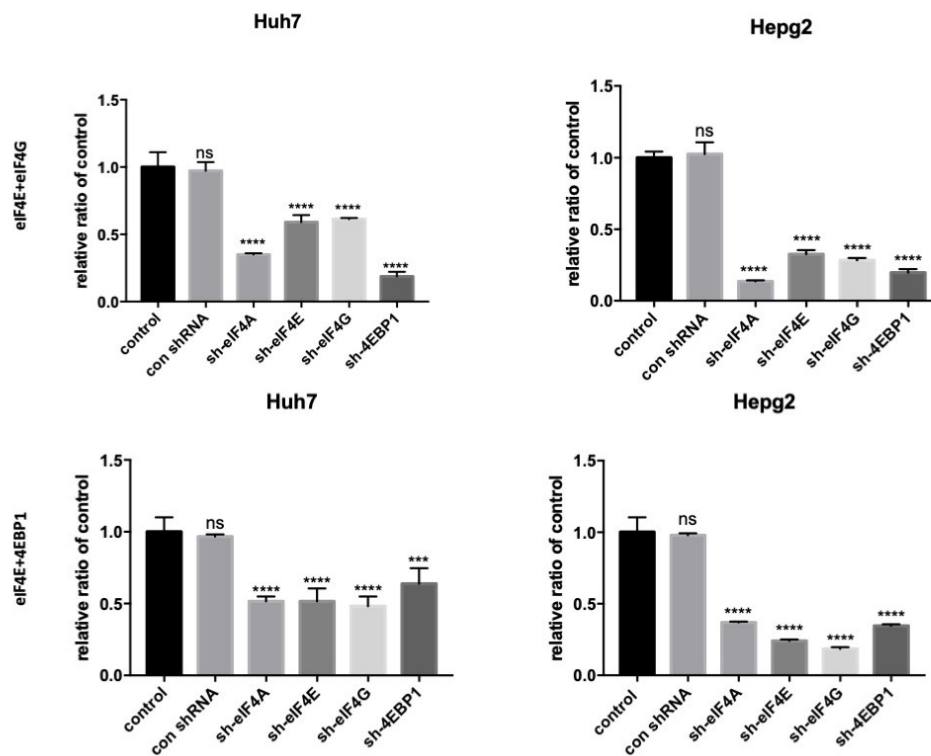
Figure G

Figure 6. Deactivated eIF4F complex converts cell response from adaptation to apoptosis under ER stress response. (A) Venn diagram of 92 overlap genes from four Huh7
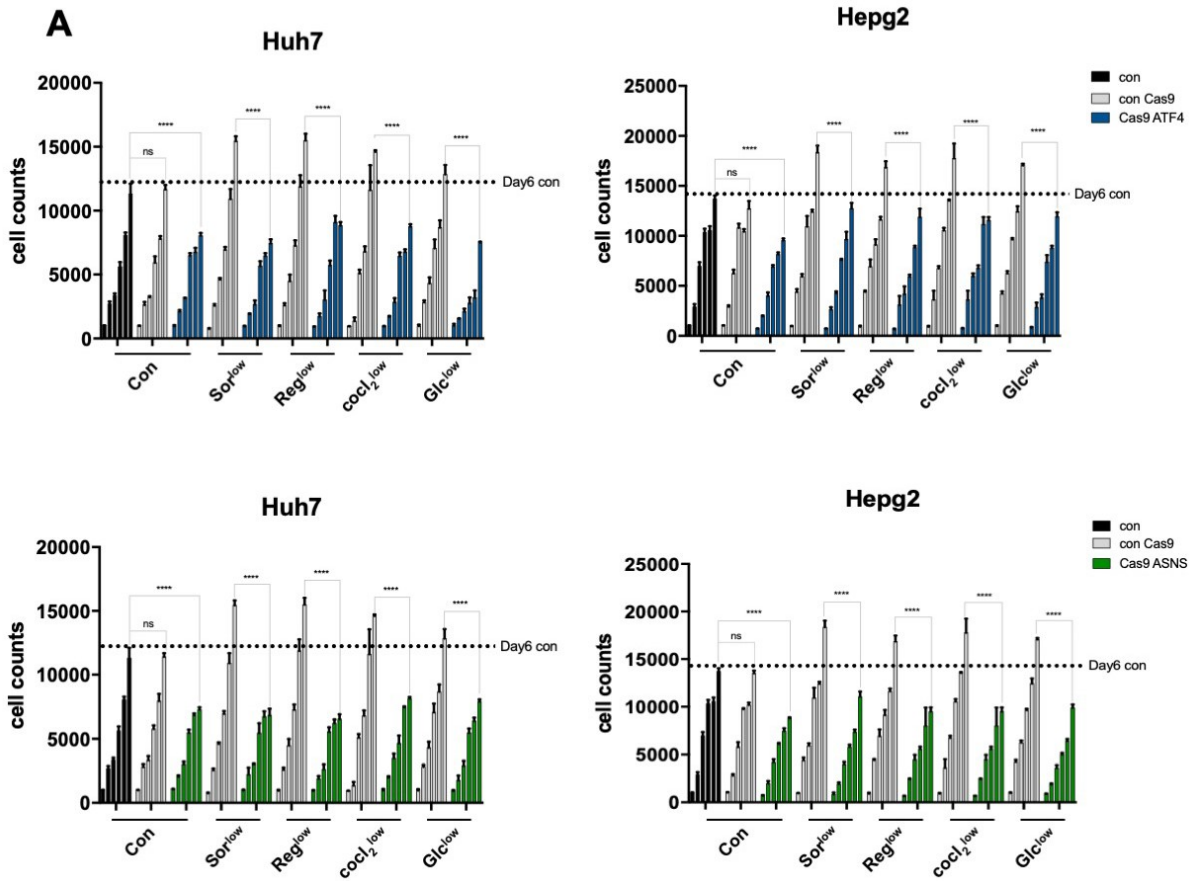
treated groups: Sorafenib^{low} in normal medium with abundant glutamine; Sorafenib^{low} in abundant glutamine medium added by exogenous asparagine; Sorafenib^{low} in no glutamine medium; and Sorafenib^{low} in no glutamine medium added by exogenous asparagine. The exposure time in all four treatments was 48 hours. Bar graph of log$_2$FC value of 92 genes. (B) log$_2$FC value of 92 genes in different gene enrichment subsets located in corresponding metabolic pathways. (C) ATP level of Huh7 and HepG2 treated by stress conditions at low concentration in four different mediums for 48 hours: with normal medium (Q); no glutamine medium (-Q); no glutamine medium added exogenous asparagine (-Q+N); normal medium added exogenous asparagine (Q+N). (D) NAPDH level of Huh7 and HepG2 cells treated by stress conditions at low concentration in four different mediums for 48 hours: with normal medium (Q); no glutamine medium (-Q); no glutamine medium added exogenous asparagine (-Q+N); normal medium added exogenous asparagine (Q+N). (E) Western Blots of expression of the stable knockdown of 4EBP1, eIF4A, eIF4E and eIF4G by shRNA in Huh7 and HepG2. (F) Binding ability of eIF4E+eIF4G and eIF4E+4EBP1 in Huh7 and HepG2 after 48 hours transfection of silencing- 4EBP1, eIF4A, eIF4E and eIF4G separately. (G) Cellular proliferation of transferred Huh7 and HepG2 treated by low concentration of Sorafenib, Regorafenib, Cocl2 and glucose in glutamine contained medium with/without exogenous asparagine for 6 days. (H) Protein synthesis of in Huh7 and HepG2 after 48 hours transfection of silencing- 4EBP1, eIF4A, eIF4E and eIF4G separately. (I) Detection of apoptosis in shRNA- 4EBP1, eIF4A, eIF4E and eIF4G transferred Huh7 and HepG2 treated by Sorafenib and Regorafenib at IC50 concentration for 48 hours. Annexin V and PI double stained cells to represent early and later phase of apoptosis. P values were calculated by the Student's t-test: *P≤0.05; **P≤0.01; ***P≤0.001; ****P≤0.0001; ns, not significant.

3.6 ATF4 targets ASNS contributes to cellular adaptability to ER stress in cancer
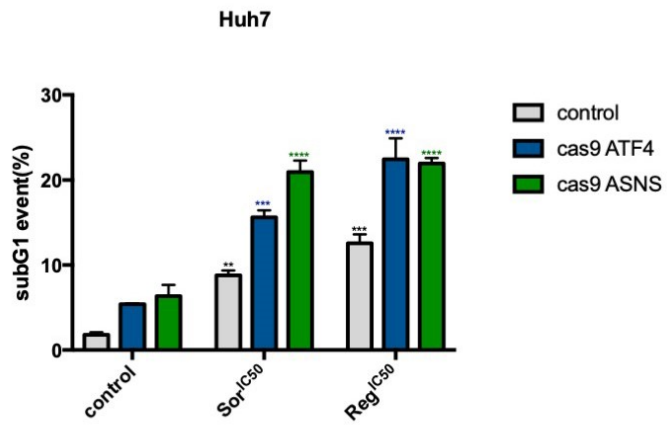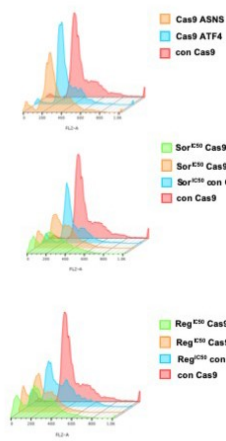
To study that ASNS regulated asparagine de novo synthesis is the downstream target of ATF4 in response to ER stress, CRISPR-Cas9-mediated knock out of ATF4 and ASNS were applied in in vitro study. In all cell lines, ATF4 knockout or ASNS knockout decreased cellular viability under low concentration cellular stress and glutamine-abundant conditions (Figure 7A). Likewise, the rate of subG1 events, representing apoptotic cells in flow cytometry, was dramatically up in ATF4 knockout or ASNS knockout cell lines treated by Sorafenib or Regorafenib at IC50 concentration after 48 hours (Figure 7B). When ATF4 was suppressed, CHOP, ASNS, mTOR, 4EBP1 and eIF4E protein levels were down-regulated under ER stress (Figure 7C). Also suppressed ASNS caused the inhibition of downstream proteins mTOR, 4EBP1 and eIF4E. These results demonstrated that ATF4 targeted ASNS contributes to cellular adaptability to ER stress via downstream mTOR/eIF4F complex regulated protein synthesis. The suppression effect of ASNS knockout on the expression of ATF4 was observed notably, which suggested a feedback effect of ASNS on ATF4.

Previous work has suggested both pro- and anti-oncogenic roles for ATF4. In supporting the anti-oncogenic role, ATF4 targets downstream gene CHOP to promote apoptosis (Hetz, 2012). However, CHOP induced autophagy was reported as a pro-survival mechanism in response to ER stress conditions (Senft and Ronai, 2015). To define the role of CHOP in cells responding to ER stress, silenced CHOP in HCC cell lines by transfected targeting CHOP siRNA was be studied. Cell proliferation was augmented in untreated cells, and in cellular stress treated cells cultured with glutamine-included and-excluded medium, when CHOP gene was knocked down (Figure 7D). Reduced cellular apoptosis was observed in cells, which were transfected by targeting CHOP siRNA und treated by Sorafenib or Regorafenib with IC50 concentration at 48 hours (Figure 7E).
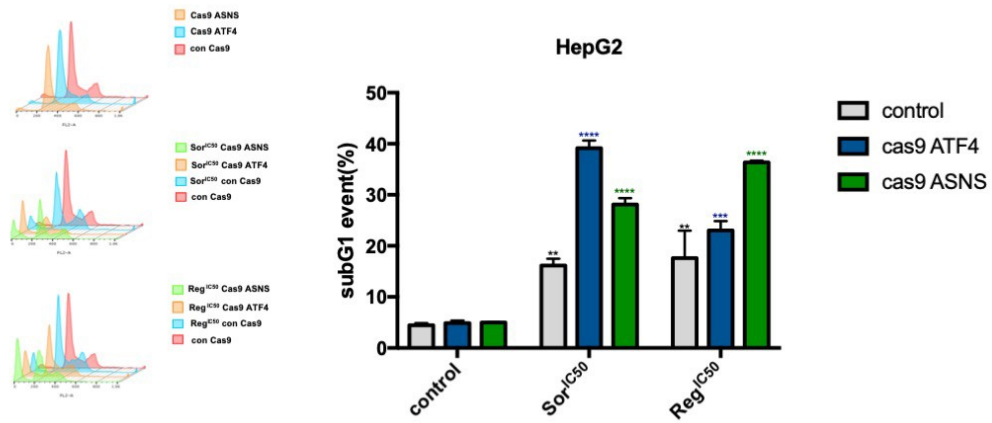
There was no effect of CHOP knockdown on the expression of the ATF4/ASNS/eIF4F-complex axis at protein level (Figure 7F). This indicated that the benefit of CHOP knockdown on cell proliferation is due to the inhibition of CHOP induced apoptosis alone, which was also observed in untreated cells (Figure 7D, 7E), rather than other aspects of CHOP. Furthermore ASNS, but not CHOP, is the main target regulated by ATF4 as a critical pro-survival mechanism for ER stress resistance in cancer cells.
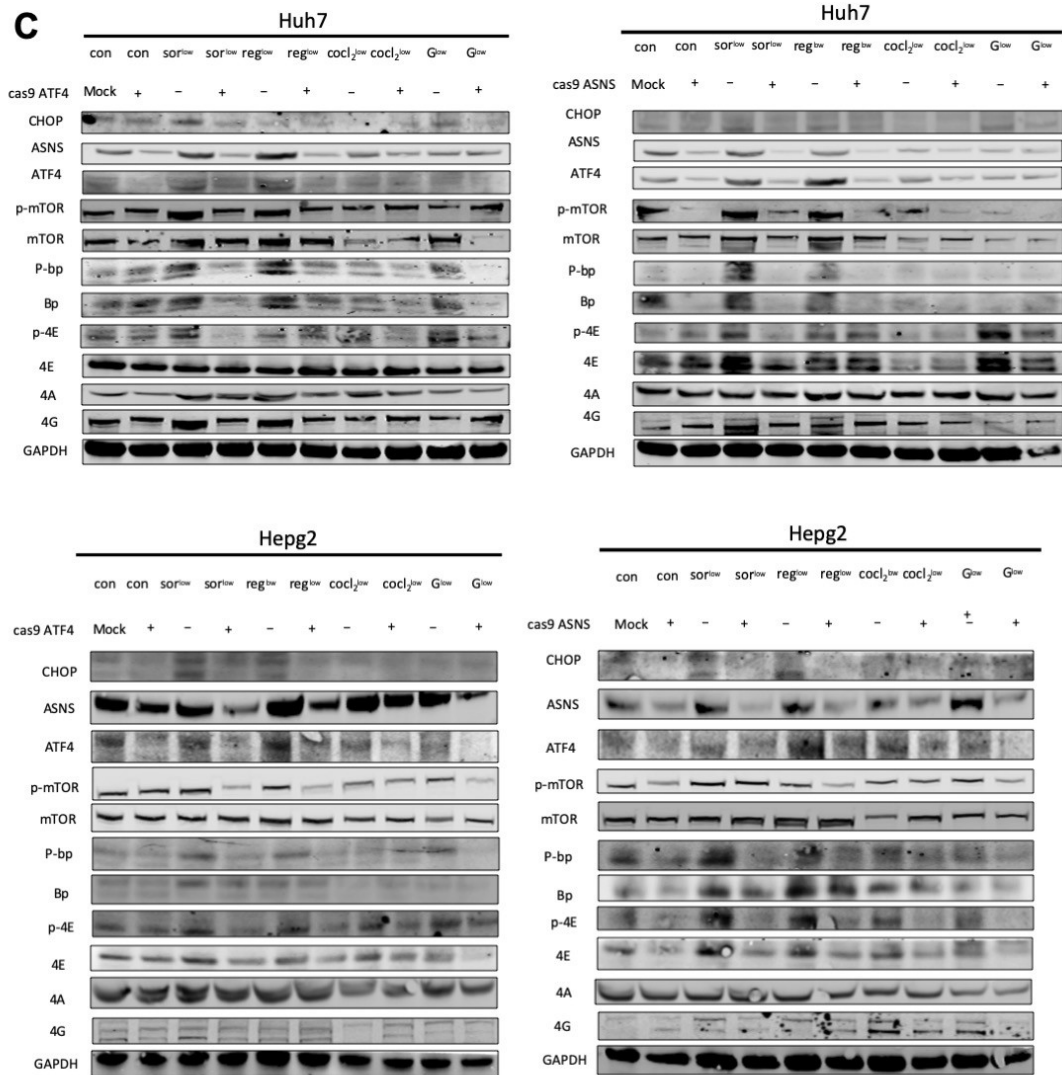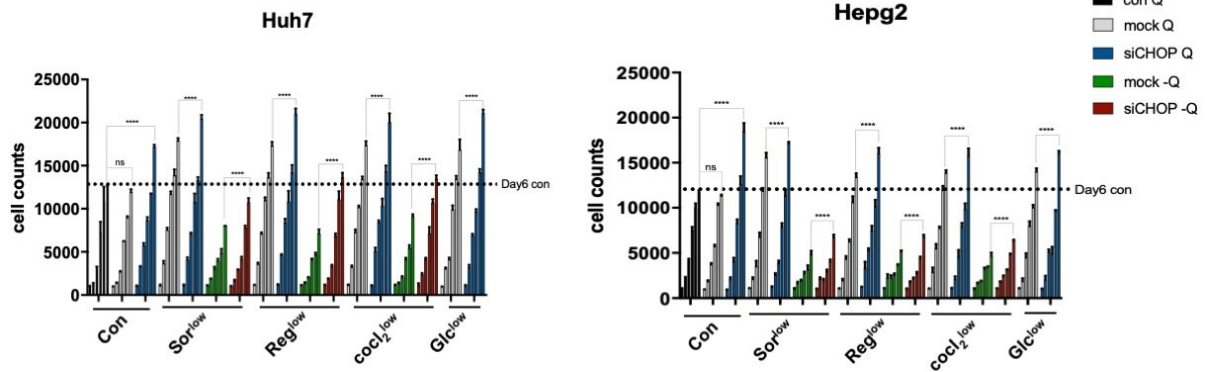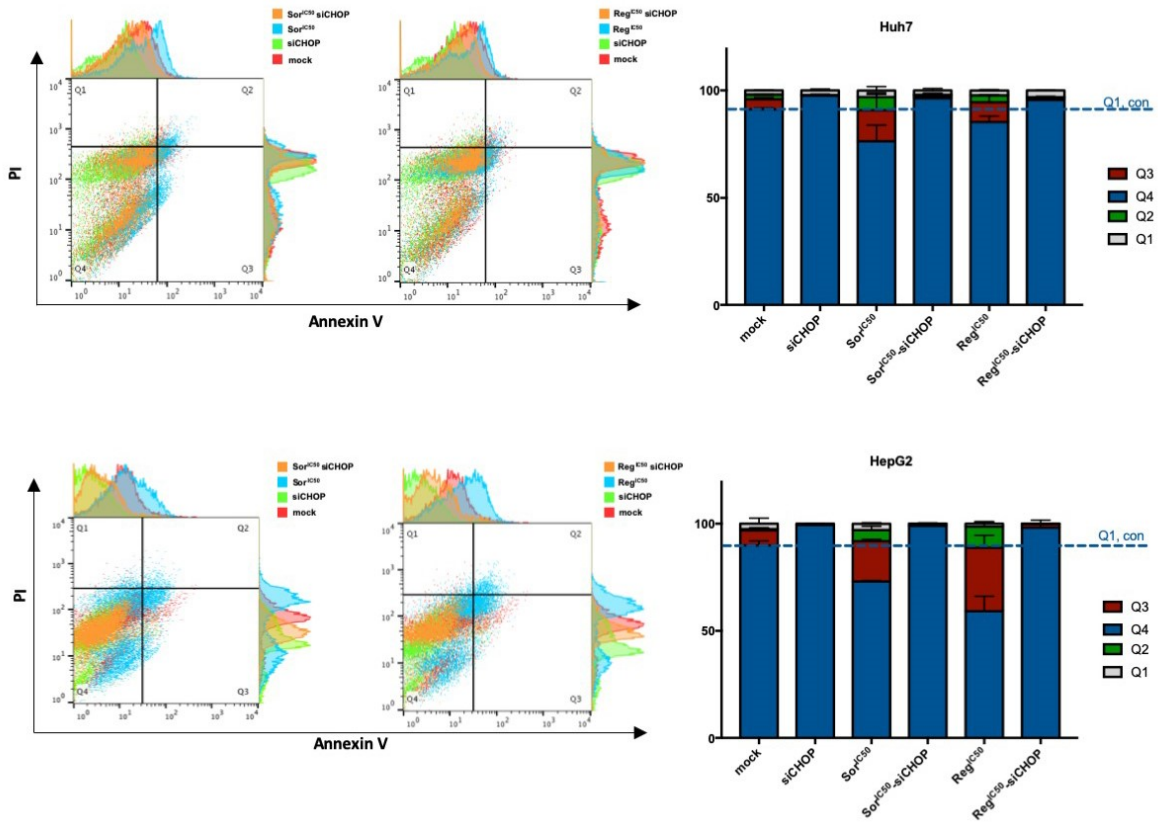
B

HepG2

control
cas9 ATF4
cas9 ASNS

C

Huh7

Huh7

Hepg2

Hepg2

D

Huh7

Hepg2

con Q
mock Q
siCHOP Q
mock -Q
siCHOP -Q
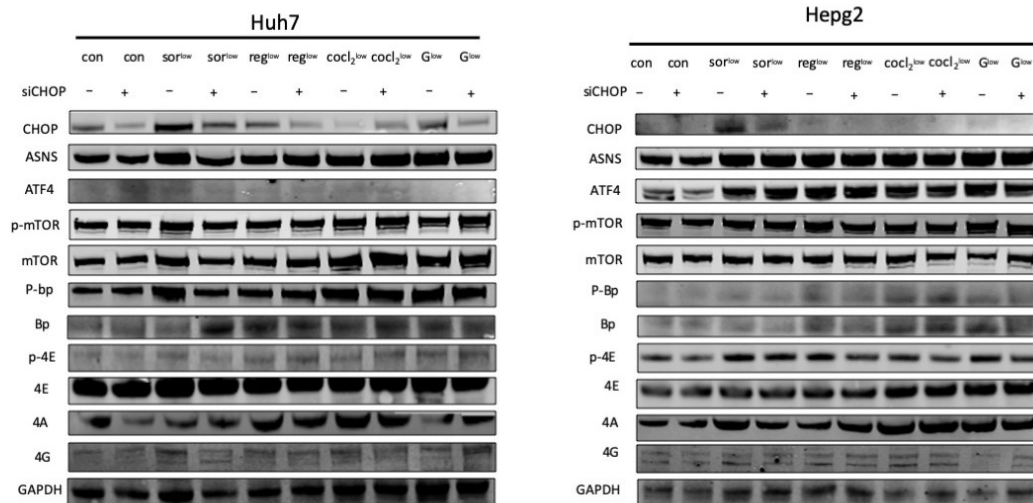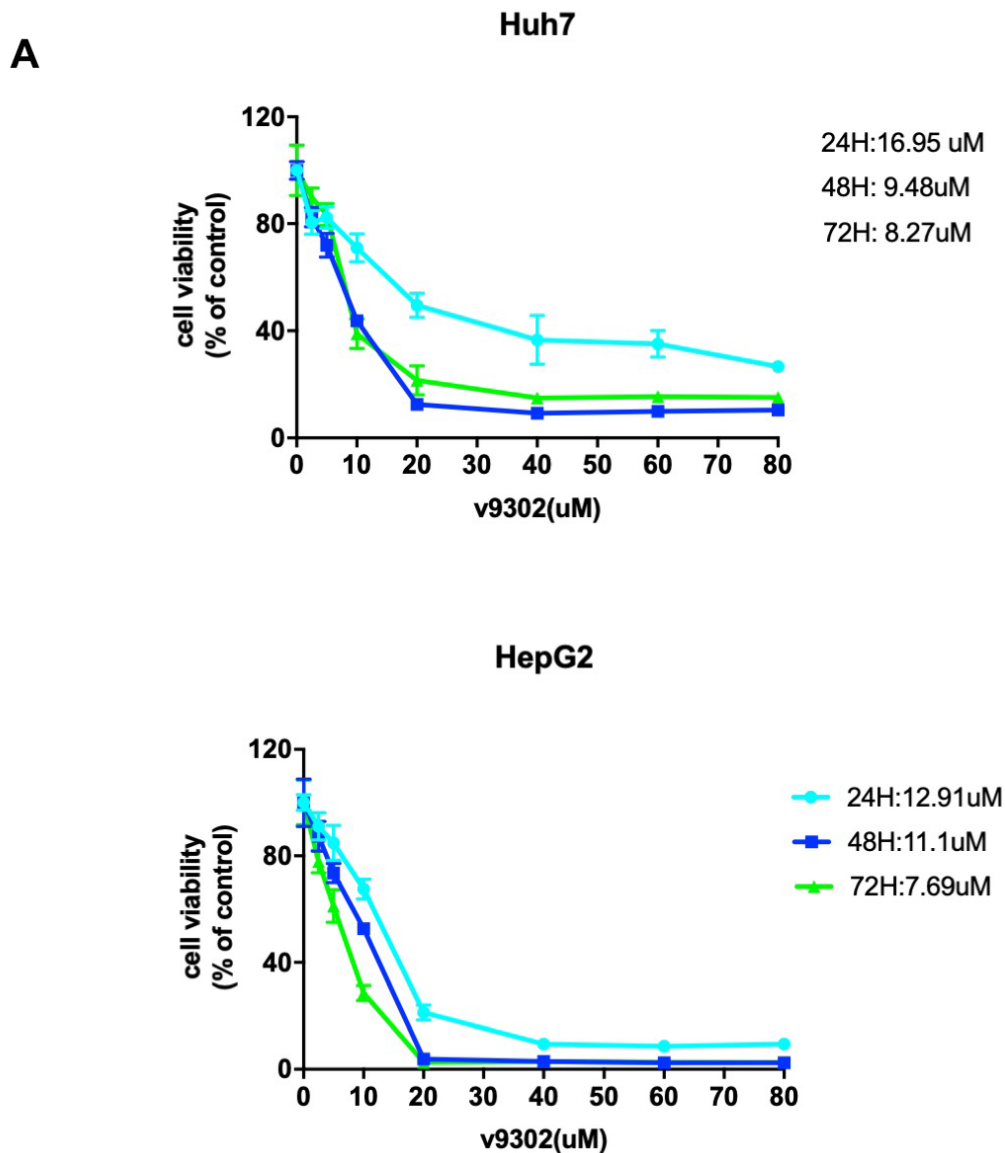
E

Huh7

HepG2

Q3
Q4
Q2
Q1

F

Figure 7. Cellular homeostasis in response to stress dependent on the regulation of axis ATF4/ASNS/eIF4F. (A) Six days proliferation curve of Huh7 and HepG2 cells after knockout of AFT4 or ASNS by crispr cas9 treated by Sorafenib, Regorafenib, Cocl2 and glucose at low concentration. (B) Detection of subG1 apoptosis events of knockout-ATF4 or ASNS HCC cell lines Huh7 and HepG2 stained with PI after 48 hours treatment of Sorafenib or Regorafenib at IC50 concentration. (C) Western Blots of expression of CHOP, ATF4, ASNS and downstream of ASNS: mTOR/4EBP1, subunits of eIF4F complex in knockout-ATF4 or ASNS cells Huh7 and HepG2 after 48 hours treatment of Sorafenib, Regorafenib, Cocl2, or glucose at low concentration. (D) Sixdays proliferation curve of Sorafenib, Regorafenib, Cocl2 and glucose at low concentration treated Huh7 and HepG2 after knockdown CHOP by siRNA. (E) Detection of apoptosis in siRNA-CHOP transferred Huh7 and HepG2 treated by Sorafenib and Regorafenib at IC50 concentration for 48 hours. Annexin V and PI double stained cells to represent early and later phase of apoptosis. (F) Western Blots of expression of CHOP, ATF4, ASNS and downstream of ASNS: mTOR/4EBP1, subunits of eIF4F complex in Huh7 and HepG2 with CHOP Knockdown after 48 hours treatment of Sorafenib, Regorafenib, Cocl2, or glucose at low concentration. P

values were calculated by the Student's t-test: *P≤0.05; **P≤0.01; ***P≤0.001; ****P≤0.0001; ns, not significant.
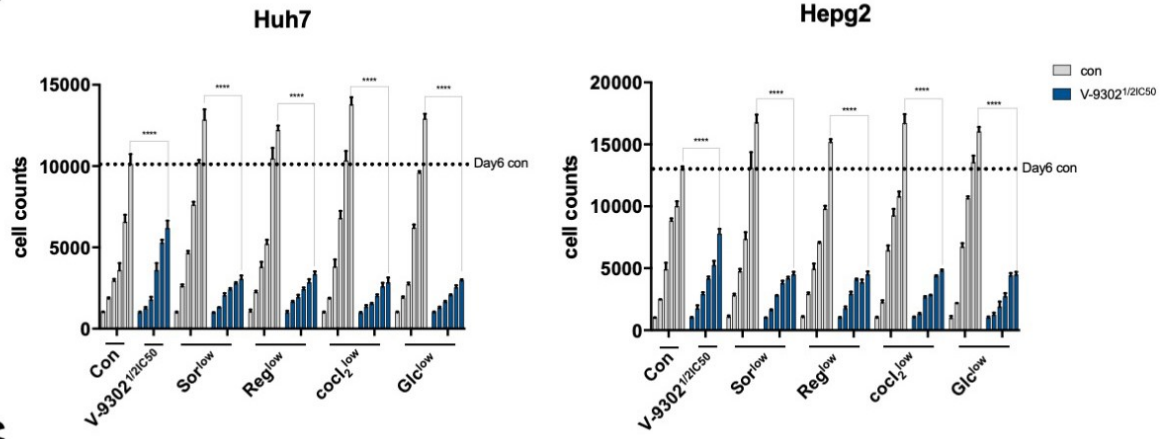
3.7 Glutamine transport blocked with V-9302, or Asparagine depletion with L-asparaginase is an effect combination therapy

Glutamine uptake by cells for protein synthesis, is a nitrogen donor and amino acid precursor, a carbon donor, a supporter of NADPH production in redox balance, and a substrate of chromatin organization (Zhang *et al.*, 2017). Under ER stress conditions, glutamine was found to be used for asparagine de novo synthesis regulated by ASNS, which is important for protection against apoptosis, activation of protein biosynthesis and induction of mTORC1 signaling (Gwinn *et al.*, 2018). This indicated the availability of targeting glutamine and asparagine for tumor treatment. It was hypothesized that antagonization of cell-surface glutamine transport either by blocking the classic transport SCL1A5 with an antagonist: V-9302, which could potentially be capable of abrogating multiple facets of glutamine metabolism, or directly limiting asparagine synthesis with one of L-asparaginase: Spectrila, may represent a more efficacious supplementary approach to Sorafenib and Regorafenib. IC50value of V-9302 and Spectrila was confirmed by MTT assay in all cell lines (Figure 8A). The anti-tumor efficacy of combined therapies were tested at half IC50 value concentration based on the consideration of higher toxicity induced by combined treatments (Felson *et al.*, 1994). As shown in Figure 8B-C, inhibition of cellular glutamine uptake by V-9302 resulted in attenuated cancer cell growth and proliferation, increased cell death, which converted cells from resistance to apoptosis in response to ER stress and contributed to anti-tumor effect of Sorafenib and Regorafenib. At protein level (Figure 8D), V-9302 at IC50 concentration effectively inhibited the expression of transport SCL1A5 and promoted pro-apoptotic proteins FADD and cleaved caspase 8 high expression by combining with Sorafenib or

90

Regorafenib treatment. Consistently, when asparagine is depleted by Spectrila, it was observed that cells were altered to sensitivity to ER stress induced apoptosis and the treatments of Sorafenib and Regorafenib (Figure 8F-G). This was also in confirmed Western Blot analysis (Figure 8H). These results above suggest that a combination treatment with V-9302, or Spectrila could be a therapeutic supplementation for Sorafenib and Regorafenib in HCC. The utility of targeting glutamine and asparagine metabolism in oncology represents a new promising class of targeted therapy.

A

Huh7

24H:16.95 uM
48H: 9.48uM
72H: 8.27uM

HepG2

24H:12.91uM
48H:11.1uM
72H:7.69uM

Huh7

- 24H:91.71Unit/ml
- 48H:59.8Unit/ml
- 72H:25.16Unit/ml

HepG2

- 24H:49.25Unit/ml
- 48H:41.7Unit/ml
- 72H:3.51Unit/ml
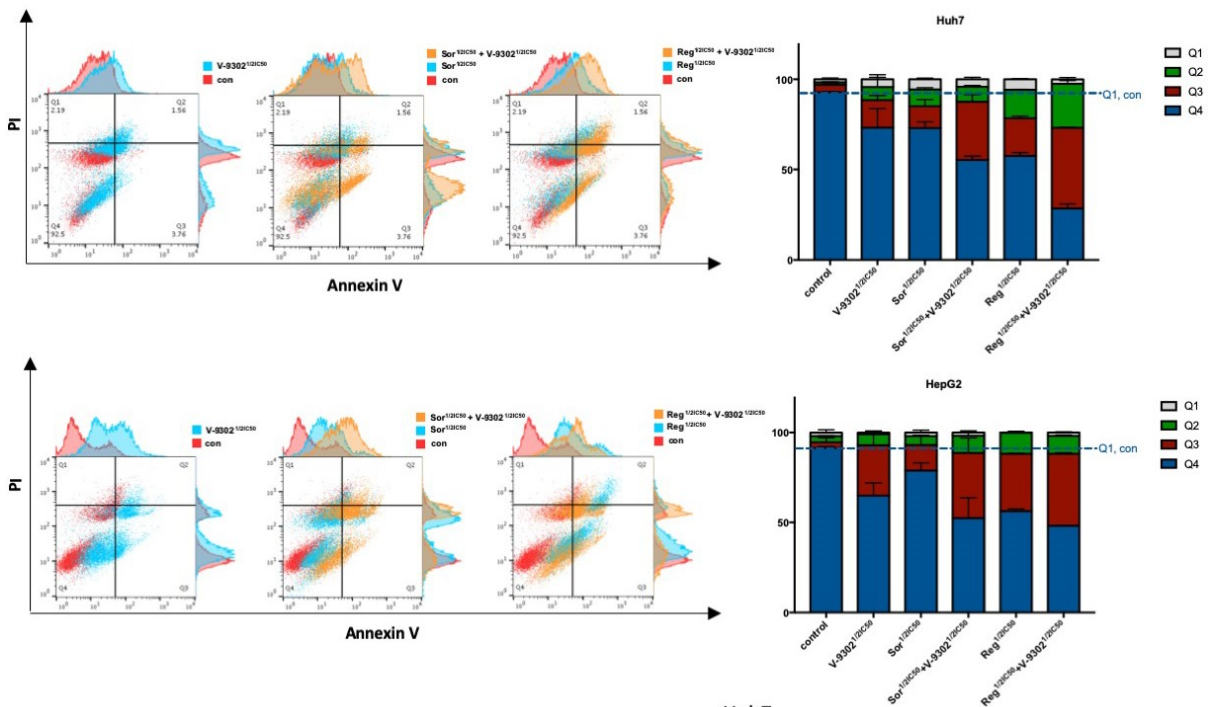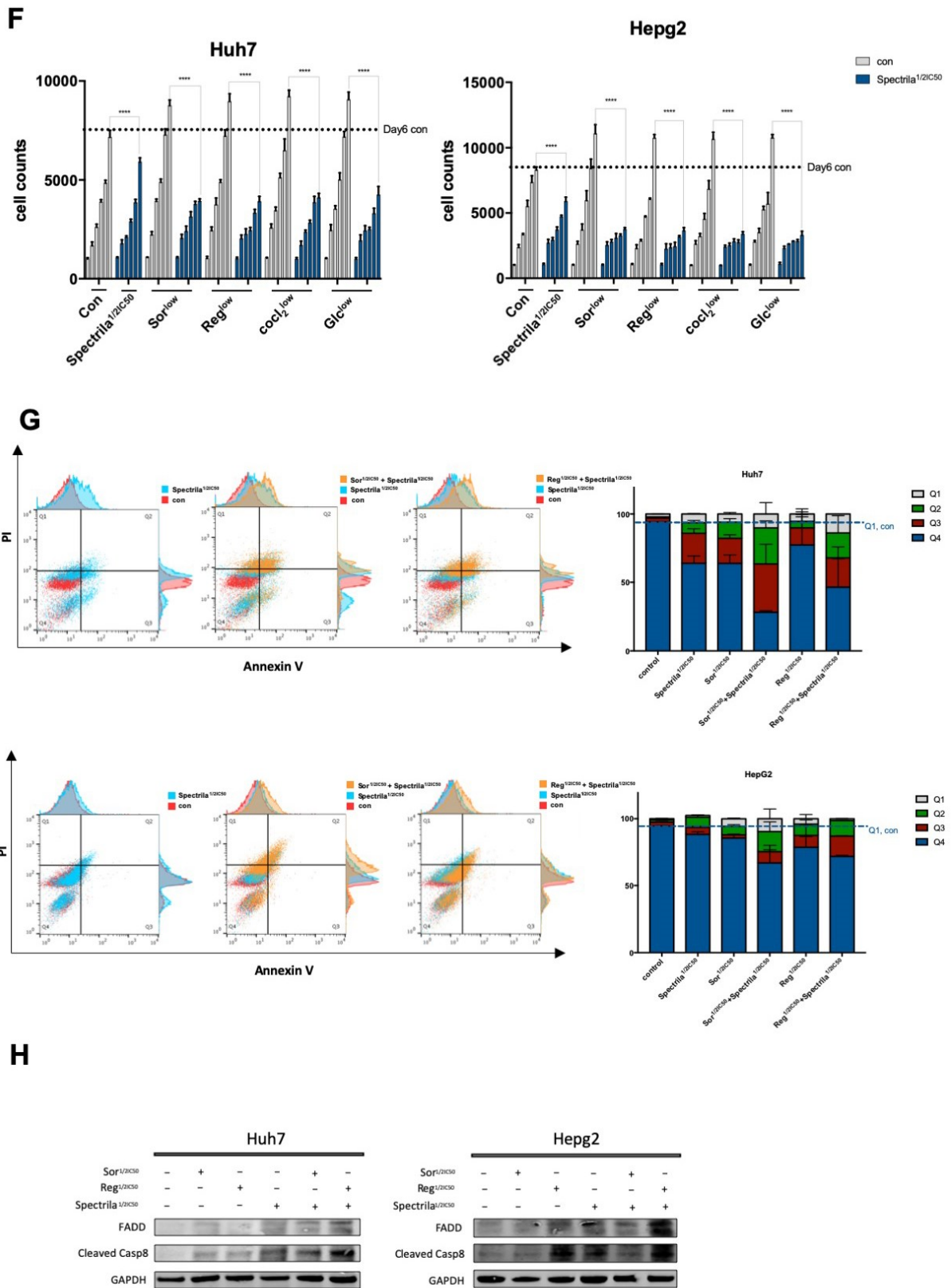
Figure 8. The synergistic effect of V-9302 and Spectrila to inhibit cellular proliferation and to induce apoptosis by combining with Sorafenib or Regorafenib. (A) IC50 value of

V-9302 on HCC cell lines Huh7 and HepG2 for 24, 48 and 72 hours. (B) Six days cell proliferation in Huh7 and HepG2 treated by Sorafenib, Regorafenib at low concentration added with/without V-9302 at half IC50 concentration. (C) Apopt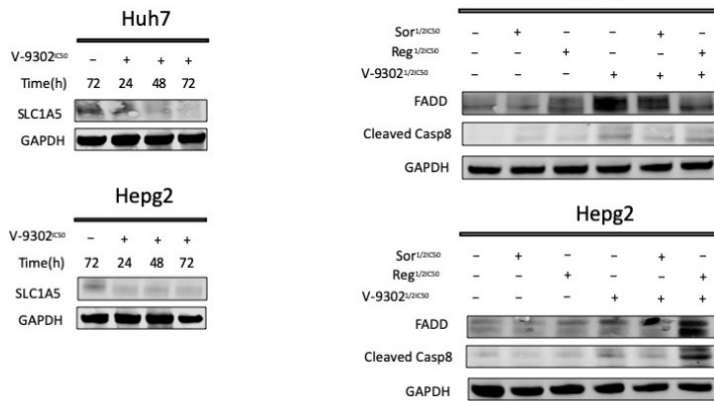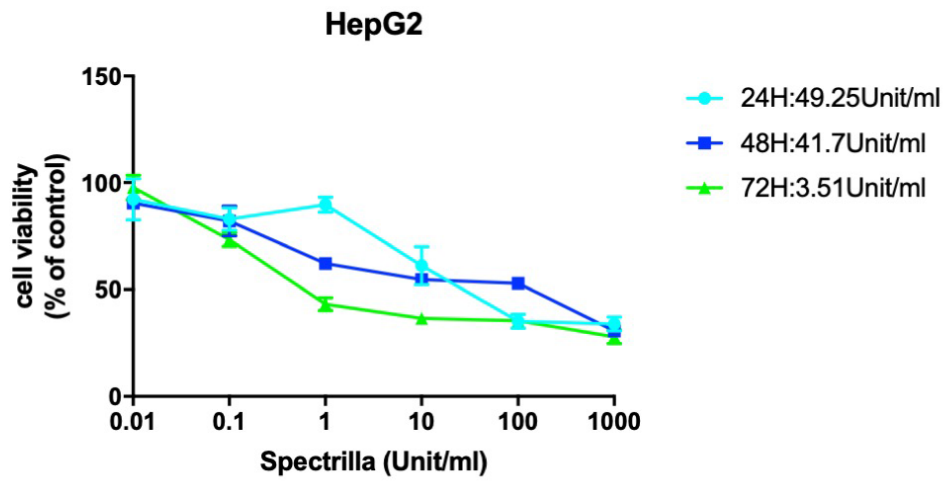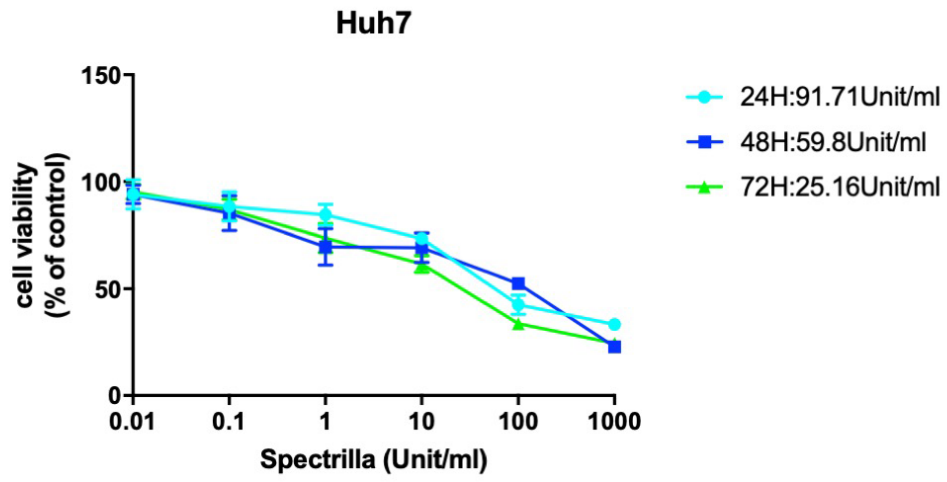osis analysis of Huh7 and HepG2 by Flow cytometry after 48 hours treatment of Sorafenib, Regorafenib with/without V-9302 at half IC50 concentration. (D) Expression of SCL1A5 in protein level in Huh7 and HepG2 treated by V-9302 at IC50 concentration for 24, 48, 72 hours. Western Blots of the expression of FADD and Cleaved Caspase 8 in Huh7 and HepG2 treated by Sorafenib, Regorafenib, V-9302 alone, and the combine treatments of Sorafenib+V-9302 and Regorafenib+V-9302. (E) IC50 value of Spectrila on HCC cell lines Huh7 and HepG2 for 24,48 and 72 hours. (F) Six days cell proliferation in Huh7 and HepG2 treated by Sorafenib, Regorafenib at low concentration added with/without Spectrila at half IC50 concentration. (G) Apoptosis analysis of Huh7 and HepG2 by Flow cytometry after 48 hours treatment of Sorafenib, Regorafenib with/without Spectrila at half IC50 concentration. (H) Western Blots of FADD and Cleaved Caspase 8 expression in Huh7 and HepG2 cells treated by Sorafenib, Regorafenib, Spectrila alone, and the combined treatments of Sorafenib with Spectrila and Regorafenib with Spectrila.

4. DISCUSSION

Tumor cells face endogenous and exogenous challenges when proliferating rapidly while maintaining metabolic homeostasis required for growth. The simultaneous tumorigenic and pro-apoptotic effects of ER stress in cancer were widely studied (Cubillos-Ruiz *et al.*, 2017; Hetz, 2012). This risky balancing act also endows cancer cells with selective vulnerabilities that could be harnessed to therapeutic advantage. Here, it was shown that extracellular glutamine uptake is the key response of cells in resistance to intrinsic and extrinsic stresses. Furthermore, asparagine was identified as a glutamine derived key metabolite which is regulated by ASNS to support cellular homeostasis. Asparagine was discussed previously to be a critical alternative substrate for tumor progression when glutamine is deprived (Gwinn *et al.*, 2018; Krall *et al.*, 2016; Pavlova *et al.*, 2018; Zhang *et al.*, 2014). However, its role in helping tumor cells to meet other challenges, like nutrient deprivation, hypoxia and external therapies, is not clear. The current study shows that glutamine-dependent de novo synthetic Asparagine promotes cellular adaptability to ER stress, for which the activation of ATF4 and its down target ASNS is required. Furthermore, protein- and nucleotides-synthesis are the crucial mechanism, by which glutamine and asparagine maintain cellular resistance to ER stress induced apoptosis. Lastly, it is indicated that depletion of glutamine or asparagine sensitizes cells to external cancer treatments, potentially providing a new paradigm for targeting amino acids metabolism within a combination therapy in HCC.

4.1 Identification of the interaction between ER stress, glutamine transport and metabolism

In response to ER stress activated glutamine uptake via SCL1A5 glutamine transport was observed in the current study in HCC cells. The underlying mechanism is not clear yet. It is broadly reported that short-term glutamine restriction triggers an ER stress response (Gwinn

et al., 2018; Shanware *et al.*, 2014). However, in turn, it is barely studied that cells expressing extrinsic and intrinsic stress increase the extracellular glutamine transport into cells and enhance their glutamine metabolism. In endocrine treatment resistant breast cancer, tumor cells overexpressed MYC and UPR to increase glutamine uptake and maintain cell survival in adapt to glucose deprivation (Shajahan-Haq *et al.*, 2014). Here it has been demonstrated that high glutamine uptake occurs not only in cancer cells as an adaptive response to ER stress, but also in the apoptosis phase when cells were exposed to high dose treatments of Sorafenib or Regorafenib.

Glutamine plays a crucial role in cancer cells to attenuate apoptosis. Glutamine metabolism fuels the TCA cycle, nucleotide and fatty acid biosynthesis, other NEAAs biosynthesis, and influences the redox balance in cancer cells (Zhang *et al.*, 2017). The increased glutamine uptake and glutaminolysis replenishs the intermediates in the TCA cycle by supplying with the glutamate α-ketoacid form, α-ketoglutarate (Wise *et al.*, 2008; Yuneva *et al.*, 2007). This is redirected to biosynthetic reactions. Glutamine activates the mTOR signaling, suppresses ER stress and promotes the eIF4F complex modified protein synthesis (Altman *et al.*, 2016c). Here it could be shown that, Asparagine de novo synthesis derives from extracellular absorbed glutamine and is used together with glutamine for keeping homeostasis under cellular stress. Glutamine depletion restricts the rate-limited enzyme ASNS to synthesize asparagine. This emphasizes that the presence of glutamine is the prerequisite that ASNS regulates asparagine biosynthesis in cancer.

4.2 Identification of the interaction between ER stress and asparagine biosynthesis and metabolism

Previous studies have indicated that extracellular asparagine is an important contributor to suppress cancer cell apoptosis and promote cellular adaptation to depletion of glutamine (Krall *et al.*, 2016; Pavlova *et al.*, 2018; Zhang *et al.*, 2014). However, most solid tumors

express glutamine-dependent ASNS and synthesize asparagine de novo (Balasubramanian *et al.*, 2013). ASNS is a transcriptional target of ATF4 in response to amino acid starvation through the GCN2/eIF2a axis (Zhang *et al.*, 2014). In vivo, GCN2- or ATF4-deficient cells failed to enhance tumor growth (Horiguchi *et al.*, 2012). The activated PERK/ATF4 axis, one of three classic arms of UPR, inhibits the suppressive functions of eIF2a in protein synthesis and up-regulates the expression of ASNS in cancer cells facing intrinsic-or extrinsic-stress (Hetz, 2012; Ron and Walter, 2007). This suggests that the asparagine biosynthesis induced in response to ER stress in cancer. Present data define that sustained levels of extracellular or intracellular asparagine promote cellular adaptation to ER stress induced apoptosis, while intracellular depletion of asparagine via ASNS knockout induces apoptosis even in the face of an abundant supply of glutamine. The impact of asparagine on cell fate suggests that the influence of glutamine on cellular homeostasis may be in part mediated by glutamine-dependent asparagine synthesis via ASNS.

It is reported that the main use of asparagine in mammalian cells is in protein synthesis (Krall *et al.*, 2016; Ubuka and Meister, 1971). Like glutamine, asparagine influences the protein synthesis through mTORC1 activation and downstream activation of translation initiation factors, such as eIF4E (Altman *et al.*, 2016a). Reduced intracellular protein synthesis via eIF4F complex knockdown lead to a conversion of the cellular resistance to apoptosis in response to ER stress. This was found even in glutamine abundant medium with or without the addition of extracellular asparagine. One could summarize that maintenance of asparagine production is critical for protein synthesis in tumor progression in an environment with endogenous and exogenous challenges.

4.3 ATF4/ASNS/eIF4F complex, but not ATF4/CHOP represents an important metabolism axis in tumor homeostasis

The consequence of ATF4 induction in tumor cell survival during metabolic stress is controversial (Ma and Hendershot, 2004). Previously it was discussed, that ATF4 activates the C/EBP- homologous protein (CHOP/GADD153) by inducing cell autophagy and death, as an integrated cellular stress response (Hetz, 2012). The current results demonstrate that CHOP knockdown has no effects on the expression of ATF4, ASNS and downstream targets no matter whether cancer cells are facing cellular stress. Inhibition of the pro-apoptotic function of CHOP via siRNA promoted cellular growth (Allagnat *et al.*, 2012; Nishitoh, 2012). CHOP knockdown has no effect on the expression of ATF4/ASNS/eIF4F complex axis.

The present data also demonstrate that activation of the key axis ATF4/ASNS/eIF4F n is required to keep cellular metabolism homeostasis in response to cellular stress. ATF4 knockout inhibits ASNS expression and asparagine synthesis followed by lower expression of downstream mTOR, 4EBP1 and eIF4e, as well as reduction of protein synthesis, leading to increased cell death even in presence of glutamine. In turn, ASNS knockout to suppress intrinsic asparagine biosynthesis results in the similar effects. Furthermore, ASNS knockout also down regulates the protein level of ATF4, which suggests that there might be a feedback regulation mechanism of ASNS on ATF4. The reduced intracellular asparagine levels via ATF4 or ASNS knockout even in the presence of abundant glutamine sensitizes cells to ER stress induced apoptosis. This demonstrates that the main role of the ATF4/ASNS/eIF4F axis might be regulation of asparagine biosynthesis and its functions in cancer cells during ER stress.

4.4 Potential therapeutic use of improved the anti-tumor efficacy after targeting of the glutamine transport or asparagine synthesis

The present results support the hypothesis that glutamine-dependent de novo synthetic asparagine has a key role in keeping cellular adaptability to extrinsic and intrinsic stress in cancer. They also suggest that inhibition of the glutamine transport via a SCL1A5 antagonist V-9302, or depletion of asparagine via L-asparaginase Spectrila may be additional treatments options in hepatocellular carcinoma.

Given a versatile usage of glutamine in proliferating cells, a number of glutamine-mimetic compounds have been evaluated in preclinical and clinical settings for their anti-tumor activities (Zhang *et al.*, 2017). However, it is proved that blocking cellular glutamine transport would impart a greater impact on glutamine metabolism in cancer cells than targeting downstream enzyme activity, such as GLS1, particularly given the extensive biological plasticity leveraged by cancer cells to maintain intracellular glutamate pools (Schulte *et al.*, 2018). V-9302 is designed to abrogate all facets of glutamine signaling and metabolism downstream of SCL1A5-mediated import (Schulte *et al.*, 2018). This includes asparagine biosynthesis, mTOR pathway regulated protein synthesis and nucleotides synthesis which play the important roles in cancer cell in resistance to ER stress as shown in the present data.

The depletion of asparagine using L-asparaginase has been used successfully as a chemotherapeutic treatment of acute lymphoblastic leukemia (Avramis, 2012). Previously, the efficacy of L-asparaginase has been correlated with ASNS levels (Zhang *et al.*, 2014). In contrast to lower organisms, most mammalian cells do not express cytosolic asparaginase that catabolizes asparagine to aspartate to maintain metabolic biosynthesis or TCA cycle (Su *et al.*, 2002; Uhlen *et al.*, 2015). This provides the possibility of L-asparaginase treatment in solid

tumors and newer formulations have recently shown promising results in some cancers (Knott *et al.*, 2018; Krall *et al.*, 2016; Zhang *et al.*, 2014).

Notably, since cancers evade asparaginase sensitivity by upregulating ASNS expression, presumably to recover intracellular asparagine pools via ASNS-catalysed synthesis from glutamine (Krall *et al.*, 2016). Combined treatment of asparaginase with targeted therapy on the glutamine metabolism, may improve the efficacy of asparaginase treatment. Altogether, it was demonstrated that introduction of V-9302 or L-asparaginase sensitizes HCC tumors to Sorafenib and Regorafenib therapies, which represents a potential treatment approach for therapy resistant HCC patients.

5. CONCLUSION

Here, it is demonstrated that the adaptation to endogenous and exogenous cellular stress leads to the requisition of extracellular glutamine uptake in HCC. As one of consequences, asparagine de novo biosynthesis is induced, which has in collaboration with glutamine a synergic role in coordinating protein and nucleotide synthesis in response to ER stress. For this, the activated axis ATF4/ASNS/eIF4F complex plays the key regulative role. Disrupting this axis, by inhibiting glutamine transportation, or depleting asparagine may overcome ER stress resistance and sensitize HCC cells to therapies. This opens new perspectives for the treatment of aggressive and resistant solid tumors (Figure 9).
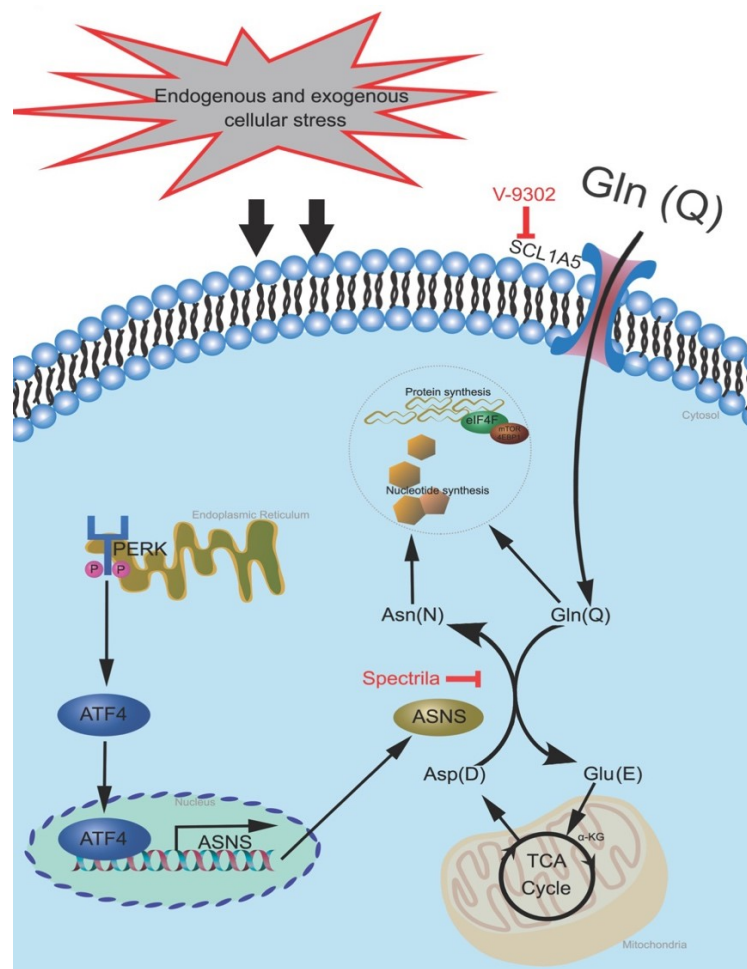

Figure 9. Mechanisms involved in regulating of glutamine and asparagine metabolism in ER stress response. (Own created image)

6. SUMMARY AND ZUSAMMENFASSUNG

Many stressful conditions on cells, including hypoxia, nutrition deprivation, inflammation, infections, and changes in cell microenvironment, challenge the folding capacity of the cell and promote endoplasmic reticulum (ER) stress. The unfolded protein response (UPR), a homeostatic signaling network, buffers and orchestrates the recovery of ER function, and when it fails, ER stress results in apoptosis. Tumor cells face endogenous and exogenous challenges when proliferating rapidly while maintaining metabolic homeostasis required for growth. The simultaneous tumorigenic and pro-apoptotic effects of ER stress in cancer were widely studied. This risky balancing act also endows cancer cells with selective vulnerabilities that could be harnessed to therapeutic advantage.

Here, it is observed that rapid cell proliferation and protein synthesis occur in response to endogenous and exogenous cellular stress at low concentration, such as Sorafenib, Regorafenib, hypoxia, glucose, but except low glutamine cell culture in HCC cancer. Furthermore, it is confirmed that cancer cells increase extracellular glutamine uptake via the activation of glutamine classic transporter, SLC1A5 in adaptation to ER stress. The absorbed glutamine is used for nucleotide and protein synthesis, but not for ATP and NAPDH production. Notably, it is defined that glutamine is also used for the supply of asparagine de novo synthesis by up-regulating glutamine-dependent asparagine synthetase, which plays the key role in coordinating nucleotide and protein synthesis in resistance to ER stress induced apoptosis.

Most solid tumors express glutamine-dependent ASNS and synthesize asparagine de novo. The current data demonstrate that ASNS, the transcriptional target of ATF4, is activated to synthesize intrinsic asparagine in response to ER stress. ATF4 knockout or ASNS knockout decreases the expression of the downstream targets mTOR, 4EBP1 and eIF4E at protein level. Therefore, it is defined that the key axis ATF4/ASNS/eIF4F complex activation is required to

keep cellular metabolism homeostasis in response to cellular stress. Present data also suggest that intracellular depletion of asparagine via ASNS knockout induces apoptosis even in the face of an abundant supply of glutamine. This confirms that the influence of glutamine on cellular homeostasis may be in part mediated by glutamine-dependent asparagine synthesis via ASNS. Like glutamine, asparagine is shown to up-regulate the protein synthesis via the eIF4F complex in resistance to cellular stress. The eIF4F complex knockdown inhibits the protein synthesis and converts cells from adaptability into apoptosis when facing ER stress, which cannot be rescued at presence of glutamine or by adding exogenous asparagine.

The present results support the hypothesis that glutamine-dependent de novo synthetic asparagine has a key role in keeping cellular adaptability to extrinsic and intrinsic stress in cancer, suggesting that targeting of amino acids has the possibility for additional treatments of tumors. Here, V-9302, an antagonist designed to abrogate all facets of glutamine signaling and metabolism downstream of SCL1A5-mediated import, is applied as an additional treatment and sensitizes HCC cells to ER stress and the treatments of Sorafenib and Regorafenib. Likewise, L- asparaginase—Spectrila is applied here to deplete asparagine and alert cells to sensitivity to ER stress and the treatments of Sorafenib and Regorafenib. Based on the findings above it can be suggested that combination treatment with V-9302, or Spectrila could be a therapeutic supplementation for Sorafenib and Regorafenib in HCC. Targeting of glutamine and asparagine metabolism may represent a new promising class of targeted oncological therapy.

Zusammenfassung

Exogene und endogene Stressstimulati wie z.B. Hypoxie, Nahrungsentzug, Infektionen und Veränderung der Zellmikroumgebung beeinflussen die Proteinfaltungskapazität des endoplasmatischen Retikulums (ER) signifikant. Die Unfolded Protein Response (UPR) stellt eine Stressreaktion des ER dar, bei der Ansammlungen von Proteinen mit fehlerhafter Faltung entstehen, welche jedoch im Normalfall keine Auswirkungen auf ER-Funktionen haben. Scheitert die Kompensation der ER-Stress-Reaktion jedoch führt dies zu Apoptose.

Insbesondere in Tumorzellen wirken eine Vielzahl Stressoren, wenn diese zum eine schnell proliferieren und gleichzeitig die erforderliche metabolische Homöostase aufrechterhalten müssen. Durch die gleichzeitig ablaufenden tumorigenen und pro-apoptotischen Prozesse im Rahmen von ER-Stress entsteht eine zelluläre Vulnerabilität die potentielle selektive Targets für neue therapeutische Optionen auch in hochresistenten Tumoren wie dem HCC bieten könnte.

In der vorliegenden Arbeit wurde gezeigt, dass HCC-Zellen auf endogenen Zellstress durch Hypoxie und Glucose und exogenen durch Sorafenib und Regorafenib Behandlung, mit einer schnelle Zellproliferation, vermehrter Proteinsynthese und Resistenz gegen die verwendeten Therapeutika reagieren. Interessanterweise traten diese Effekte jedoch nicht in einer Glutamin-armen Zellkultur auf. Es konnte gezeigt werden, dass unter Stress stehende Tumorzellen die extrazelluläre Glutamin Aufnahme durch Aktivierung des klassischen Glutamin Transporters SLC1A5 erhöhen, und sich an den ER-Stress anpassen. Hierbei wird Glutamin vermehrt für die Nukleotid- und Protein-Synthese verwendet, wobei Glutamin zusätzlich durch die Aktivierung der Glutamin-abhängigen Asparagin Synthetase (ASNS) für Asparagin-de-novo-Synthese sorgt. Daraus lies sich postulieren, dass der Einfluss von Glutamin auf die zelluläre Homöostase teilweise durch die Glutamin-abhängige Asparagin-

Synthese vermittelt werden kann. Dieser Prozess spielt eine Schlüsselrolle bei der Resistenz von Tumorzellen gegen stressinduzierte ER-Stress-Apoptose.

In dieser Studie wurde nachgewiesen, dass ASNS als Transkriptionsziel von ATF4 in HCC-Zellen aktiviert wird, um intrinsisches Asparagin zu synthetisieren und dadurch eine Resistenz gegen die zelluläre stressinduzierte Apoptose zu entwickeln. Die Aktivierung des ATF4 / ASNS / eIF4F-Komplexes ist erforderlich, um die Homöostase des Zellstoffwechsels aufrechtzuerhalten, wenn sich Tumorzellen auf zellulären Stress reagieren. ATF4-Knockout oder ASNS-Knockout verringern die Expression der Downstream-Targets mTOR, 4EBP1 und eIF4E und induzieren darüber ER-Stress-Apoptose. Die vorliegenden Daten konnten nachweisen, dass die intrazelluläre Reduktion von Asparagin mittels ASNS Knockout bei ausreichender Glutamin Versorgung ebenfalls Apoptose induziert. Analog zu Glutamin induzierte Asparagin die Proteinsynthese mittels eIF4FKomplex-Aktivierung. Knockdown des eIF4F-Komplexes hemmt die Proteinsynthese und induziert eine stärkere Apoptose als Reaktion auf ER-Stress, welche auch durch Zugabe von exogenem Asparagin oder Glutamin nicht reversibel war. Die vorliegenden Ergebnisse unterstützen daher die Hypothese, dass Glutamin-abhängiges synthetisches de novo-Asparagin eine Schlüsselrolle bei der zellulären Anpassungsfähigkeit an extrinsischen und intrinsischen Stress bei Tumoren spielt Die Blockade des SCL1A5-getriggerten Glutamin-Transportes mittels V-9302, sensibilisiert HCC-Zellen für ER-Stress und stellt die Sensitivität für Therapien mit Sorafenib und Regorafenib wiederher. Analog dazu induzierte eine Behandlung mit der L-Asparaginase Spectrila verstärkte antitumorale Effekte. Modulationen des Glutamin- und Asparagin-Stoffwechsel könnten basierend auf den hier präsentierten Erkenntnissen neue potentielle Targets in der onkologischen Therapie hochresistenter Tumore darstellen.

8. REFERENCES

Acosta-Alvear, D., Zhou, Y., Blais, A., Tsikitis, M., Lents, N. H., Arias, C., Lennon, C. J., Kluger, Y. and Dynlacht, B. D. (2007). **XBP1 controls diverse cell type- and condition-specific transcriptional regulatory networks**. Mol Cell *27*, 53-66, doi: 10.1016/j.molcel.2007.06.011.

Akcakanat, A., Hong, D. S. and Meric-Bernstam, F. (2014). **Targeting translation initiation in breast cancer**. Translation (Austin) *2*, e28968, doi: 10.4161/trla.28968.

Allagnat, F., Fukaya, M., Nogueira, T. C., Delaroche, D., Welsh, N., Marselli, L., Marchetti, P., Haefliger, J. A., Eizirik, D. L. and Cardozo, A. K. (2012). **C/EBP homologous protein contributes to cytokine-induced pro-inflammatory responses and apoptosis in beta-cells**. Cell Death Differ *19*, 1836-1846, doi: 10.1038/cdd.2012.67.

Altekruse, S. F., McGlynn, K. A., Dickie, L. A. and Kleiner, D. E. (2012). **Hepatocellular carcinoma confirmation, treatment, and survival in surveillance, epidemiology, and end results registries, 1992-2008**. Hepatology *55*, 476-482, doi: 10.1002/hep.24710.

Altman, B. J., Stine, Z. E. and Dang, C. V. (2016a). **From Krebs to clinic: glutamine metabolism to cancer therapy**. Nat Rev Cancer *16*, 773, doi: 10.1038/nrc.2016.131.

Altman, B. J., Stine, Z. E. and Dang, C. V. (2016b). **From Krebs to clinic: glutamine metabolism to cancer therapy**. Nat Rev Cancer *16*, 749, doi: 10.1038/nrc.2016.114.

Altman, B. J., Stine, Z. E. and Dang, C. V. (2016c). **From Krebs to clinic: glutamine metabolism to cancer therapy**. Nat Rev Cancer *16*, 619-634, doi: 10.1038/nrc.2016.71.

Ameri, K. and Harris, A. L. (2008). **Activating transcription factor 4**. Int J Biochem Cell Biol *40*, 14-21, doi: 10.1016/j.biocel.2007.01.020.

Avramis, V. I. (2012). **Asparaginases: biochemical pharmacology and modes of drug resistance**. Anticancer Res *32*, 2423-2437.

Balasubramanian, M. N., Butterworth, E. A. and Kilberg, M. S. (2013). **Asparagine synthetase: regulation by cell stress and involvement in tumor biology**. Am J Physiol Endocrinol Metab *304*, E789-799, doi: 10.1152/ajpendo.00015.2013.

Beard, R. E., Hanto, D. W., Gautam, S. and Miksad, R. A. (2013). **A comparison of surgical outcomes for noncirrhotic and cirrhotic hepatocellular carcinoma patients in a Western institution**. Surgery *154*, 545-555, doi: 10.1016/j.surg.2013.02.019.

Berasain, C. (2013). **Hepatocellular carcinoma and sorafenib: too many resistance mechanisms?** Gut *62*, 1674-1675, doi: 10.1136/gutjnl-2013-304564.

Bhat, M., Robichaud, N., Hulea, L., Sonenberg, N., Pelletier, J. and Topisirovic, I. (2015). **Targeting the translation machinery in cancer**. Nat Rev Drug Discov *14*, 261-278, doi: 10.1038/nrd4505.

Bhoori, S., Schiavo, M., Russo, A. and Mazzaferro, V. (2007). **First-line treatment for hepatocellular carcinoma: resection or transplantation?** Transplant Proc *39*, 2271-2273, doi: 10.1016/j.transproceed.2007.06.015.

Birsoy, K., Possemato, R., Lorbeer, F. K., Bayraktar, E. C., Thiru, P., Yucel, B., Wang, T., Chen, W. W., Clish, C. B. and Sabatini, D. M. (2014). **Metabolic determinants of cancer cell sensitivity to glucose limitation and biguanides**. Nature *508*, 108-112, doi: 10.1038/nature13110.

Bonomo, G., Pedicini, V., Monfardini, L., Della Vigna, P., Poretti, D., Orgera, G. and Orsi, F. (2010). **Bland embolization in patients with unresectable hepatocellular carcinoma using precise, tightly size-calibrated, anti-inflammatory microparticles: first clinical experience and one-year follow-up**. Cardiovasc Intervent Radiol *33*, 552-559, doi: 10.1007/s00270-009-9752-y.

Bourguignon, L. Y., Spevak, C. C., Wong, G., Xia, W. and Gilad, E. (2009). **Hyaluronan-CD44 interaction with protein kinase C(epsilon) promotes oncogenic signaling by the stem cell marker Nanog and the Production of microRNA-21, leading to down-regulation of the tumor suppressor protein PDCD4, anti-apoptosis, and chemotherapy resistance in breast tumor cells**. J Biol Chem *284*, 26533-26546, doi: 10.1074/jbc.M109.027466.

Boussemart, L., Malka-Mahieu, H., Girault, I., Allard, D., Hemmingsson, O., Tomasic, G., Thomas, M., Basmadjian, C., Ribeiro, N., Thuaud, F., Mateus, C., Routier, E., Kamsu-Kom, N., Agoussi, S., Eggermont, A. M., Desaubry, L., Robert, C. and Vagner, S. (2014). **eIF4F is a nexus of resistance to anti-BRAF and anti-MEK cancer therapies**. Nature *513*, 105-109, doi: 10.1038/nature13572.

Broome, J. D. (1963). **Evidence that the L-asparaginase of guinea pig serum is responsible for its antilymphoma effects. I. Properties of the L-asparaginase of guinea pig serum in relation to those of the antilymphoma substance**. J Exp Med *118*, 99-120, doi: 10.1084/jem.118.1.99.

Bruix, J., Qin, S., Merle, P., Granito, A., Huang, Y. H., Bodoky, G., Pracht, M., Yokosuka, O., Rosmorduc, O., Breder, V., Gerolami, R., Masi, G., Ross, P. J., Song, T., Bronowicki, J. P., Ollivier-Hourmand, I., Kudo, M., Cheng, A. L., Llovet, J. M., Finn, R. S., LeBerre, M. A., Baumhauer, A., Meinhardt, G., Han, G. and Investigators, R. (2017). **Regorafenib for patients with hepatocellular carcinoma who progressed on sorafenib treatment (RESORCE): a randomised, double-blind, placebo-controlled, phase 3 trial**. Lancet *389*, 56-66, doi: 10.1016/S0140-6736(16)32453-9.

Bruix, J., Sherman, M. and American Association for the Study of Liver, D. (2011). **Management of hepatocellular carcinoma: an update**. Hepatology *53*, 1020-1022, doi: 10.1002/hep.24199.

Buxade, M., Parra-Palau, J. L. and Proud, C. G. (2008). **The Mnks: MAP kinase-interacting kinases (MAP kinase signal-integrating kinases)**. Front Biosci *13*, 5359-5373.

Calderaro, J., Rousseau, B., Amaddeo, G., Mercey, M., Charpy, C., Costentin, C., Luciani, A., Zafrani, E. S., Laurent, A., Azoulay, D., Lafdil, F. and Pawlotsky, J. M. (2016). **Programmed death ligand 1 expression in hepatocellular carcinoma: Relationship With clinical and pathological features**. Hepatology *64*, 2038-2046, doi: 10.1002/hep.28710.

Calfon, M., Zeng, H., Urano, F., Till, J. H., Hubbard, S. R., Harding, H. P., Clark, S. G. and Ron, D. (2002). **IRE1 couples endoplasmic reticulum load to secretory capacity by processing the XBP-1 mRNA**. Nature *415*, 92-96, doi: 10.1038/415092a.

Cantor, J. R. and Sabatini, D. M. (2012). **Cancer cell metabolism: one hallmark, many faces**. Cancer Discov *2*, 881-898, doi: 10.1158/2159-8290.CD-12-0345.

Cheng, A. L., Kang, Y. K., Chen, Z., Tsao, C. J., Qin, S., Kim, J. S., Luo, R., Feng, J., Ye, S., Yang, T. S., Xu, J., Sun, Y., Liang, H., Liu, J., Wang, J., Tak, W. Y., Pan, H., Burock, K., Zou, J., Voliotis, D. and Guan, Z. (2009). **Efficacy and safety of sorafenib in patients in the Asia-Pacific region with advanced hepatocellular carcinoma: a phase III randomised, double-blind, placebo-controlled trial**. Lancet Oncol *10*, 25-34, doi: 10.1016/S1470-2045(08)70285-7.

Choi, Y. K. and Park, K. G. (2018). **Targeting Glutamine Metabolism for Cancer Treatment**. Biomol Ther (Seoul) *26*, 19-28, doi: 10.4062/biomolther.2017.178.

Clavell, L. A., Gelber, R. D., Cohen, H. J., Hitchcock-Bryan, S., Cassady, J. R., Tarbell, N. J., Blattner, S. R., Tantravahi, R., Leavitt, P. and Sallan, S. E. (1986). **Four-agent induction and intensive asparaginase therapy for treatment of childhood acute lymphoblastic leukemia**. N Engl J Med *315*, 657-663, doi: 10.1056/NEJM198609113151101.

Cubillos-Ruiz, J. R., Bettigole, S. E. and Glimcher, L. H. (2017). **Tumorigenic and Immunosuppressive Effects of Endoplasmic Reticulum Stress in Cancer**. Cell *168*, 692-706, doi: 10.1016/j.cell.2016.12.004.

Cucchetti, A., Piscaglia, F., Caturelli, E., Benvegnu, L., Vivarelli, M., Ercolani, G., Cescon, M., Ravaioli, M., Grazi, G. L., Bolondi, L. and Pinna, A. D. (2009). **Comparison of recurrence of hepatocellular carcinoma after resection in patients with cirrhosis to its occurrence in a surveilled cirrhotic population**. Ann Surg Oncol *16*, 413-422, doi: 10.1245/s10434-008-0232-4.

DeBerardinis, R. J., Mancuso, A., Daikhin, E., Nissim, I., Yudkoff, M., Wehrli, S. and Thompson, C. B. (2007). **Beyond aerobic glycolysis: transformed cells can engage in glutamine metabolism that exceeds the requirement for protein and nucleotide synthesis**. Proc Natl Acad Sci U S A *104*, 19345-19350, doi: 10.1073/pnas.0709747104.

DeNicola, G. M., Chen, P. H., Mullarky, E., Sudderth, J. A., Hu, Z., Wu, D., Tang, H., Xie, Y., Asara, J. M., Huffman, K. E., Wistuba, II, Minna, J. D., DeBerardinis, R. J. and Cantley, L. C. (2015). **NRF2 regulates serine biosynthesis in non-small cell lung cancer**. Nat Genet *47*, 1475-1481, doi: 10.1038/ng.3421.

Dever, T. E. (2002). **Gene-specific regulation by general translation factors**. Cell *108*, 545-556.

Dey, S., Sayers, C. M., Verginadis, II, Lehman, S. L., Cheng, Y., Cerniglia, G. J., Tuttle, S. W., Feldman, M. D., Zhang, P. J., Fuchs, S. Y., Diehl, J. A. and Koumenis, C. (2015). **ATF4-dependent induction of heme oxygenase 1 prevents anoikis and promotes metastasis**. J Clin Invest *125*, 2592-2608, doi: 10.1172/JCI78031.

Eagle, H. (1955). **Nutrition needs of mammalian cells in tissue culture**. Science *122*, 501-514.

Ebos, J. M., Lee, C. R., Cruz-Munoz, W., Bjarnason, G. A., Christensen, J. G. and Kerbel, R. S. (2009). **Accelerated metastasis after short-term treatment with a potent inhibitor of tumor angiogenesis**. Cancer Cell *15*, 232-239, doi: 10.1016/j.ccr.2009.01.021.

El-Khoueiry, A. B., Sangro, B., Yau, T., Crocenzi, T. S., Kudo, M., Hsu, C., Kim, T. Y., Choo, S. P., Trojan, J., Welling, T. H. R., Meyer, T., Kang, Y. K., Yeo, W., Chopra, A., Anderson, J., Dela Cruz, C., Lang, L., Neely, J., Tang, H., Dastani, H. B. and Melero, I. (2017). **Nivolumab in patients with advanced hepatocellular carcinoma (CheckMate 040): an open-label, non-comparative, phase 1/2 dose escalation and expansion trial**. Lancet *389*, 2492-2502, doi: 10.1016/S0140-6736(17)31046-2.

European Association For The Study Of The, L., European Organisation For, R. and Treatment Of, C. (2012). **EASL-EORTC clinical practice guidelines: management of hepatocellular carcinoma**. J Hepatol *56*, 908-943, doi: 10.1016/j.jhep.2011.12.001.

Felson, D. T., Anderson, J. J. and Meenan, R. F. (1994). **The efficacy and toxicity of combination therapy in rheumatoid arthritis. A meta-analysis**. Arthritis Rheum *37*, 1487-1491.

Forner, A., Llovet, J. M. and Bruix, J. (2012). **Chemoembolization for intermediate HCC: is there proof of survival benefit?** J Hepatol *56*, 984-986, doi: 10.1016/j.jhep.2011.08.017.

Gingras, A. C., Raught, B. and Sonenberg, N. (1999). **eIF4 initiation factors: effectors of mRNA recruitment to ribosomes and regulators of translation**. Annu Rev Biochem *68*, 913-963, doi: 10.1146/annurev.biochem.68.1.913.

Gwinn, D. M., Lee, A. G., Briones-Martin-Del-Campo, M., Conn, C. S., Simpson, D. R., Scott, A. I., Le, A., Cowan, T. M., Ruggero, D. and Sweet-Cordero, E. A. (2018). **Oncogenic KRAS Regulates Amino Acid Homeostasis and Asparagine Biosynthesis via ATF4 and Alters Sensitivity to L-Asparaginase**. Cancer Cell *33*, 91-107 e106, doi: 10.1016/j.ccell.2017.12.003.

Han, J., Back, S. H., Hur, J., Lin, Y. H., Gildersleeve, R., Shan, J., Yuan, C. L., Krokowski, D., Wang, S., Hatzoglou, M., Kilberg, M. S., Sartor, M. A. and Kaufman, R. J. (2013). **ER-stress-induced transcriptional regulation increases protein synthesis leading to cell death**. Nat Cell Biol *15*, 481-490, doi: 10.1038/ncb2738.

Hanahan, D. and Weinberg, R. A. (2011). **Hallmarks of cancer: the next generation**. Cell *144*, 646-674, doi: 10.1016/j.cell.2011.02.013.

Harding, H. P., Zhang, Y., Scheuner, D., Chen, J. J., Kaufman, R. J. and Ron, D. (2009). **Ppp1r15 gene knockout reveals an essential role for translation initiation factor 2 alpha (eIF2alpha) dephosphorylation in mammalian development**. Proc Natl Acad Sci U S A *106*, 1832-1837, doi: 10.1073/pnas.0809632106.

Harding, H. P., Zhang, Y., Zeng, H., Novoa, I., Lu, P. D., Calfon, M., Sadri, N., Yun, C., Popko, B., Paules, R., Stojdl, D. F., Bell, J. C., Hettmann, T., Leiden, J. M. and Ron, D. (2003). **An integrated stress response regulates amino acid metabolism and resistance to oxidative stress**. Mol Cell *11*, 619-633.

Hassanein, M., Qian, J., Hoeksema, M. D., Wang, J., Jacobovitz, M., Ji, X., Harris, F. T., Harris, B. K., Boyd, K. L., Chen, H., Eisenberg, R. and Massion, P. P. (2015). **Targeting SLC1a5-mediated glutamine dependence in non-small cell lung cancer**. Int J Cancer *137*, 1587-1597, doi: 10.1002/ijc.29535.

Haze, K., Yoshida, H., Yanagi, H., Yura, T. and Mori, K. (1999). **Mammalian transcription factor ATF6 is synthesized as a transmembrane protein and activated by proteolysis in response to endoplasmic reticulum stress**. Mol Biol Cell *10*, 3787-3799, doi: 10.1091/mbc.10.11.3787.

Heimbach, J. K., Kulik, L. M., Finn, R. S., Sirlin, C. B., Abecassis, M. M., Roberts, L. R., Zhu, A. X., Murad, M. H. and Marrero, J. A. (2018). **AASLD guidelines for the treatment of hepatocellular carcinoma**. Hepatology *67*, 358-380, doi: 10.1002/hep.29086.

Hensley, C. T., Wasti, A. T. and DeBerardinis, R. J. (2013). **Glutamine and cancer: cell biology, physiology, and clinical opportunities**. J Clin Invest *123*, 3678-3684, doi: 10.1172/JCI69600.

Hetz, C. (2012). **The unfolded protein response: controlling cell fate decisions under ER stress and beyond**. Nat Rev Mol Cell Biol *13*, 89-102, doi: 10.1038/nrm3270.

Hetz, C., Chevet, E. and Oakes, S. A. (2015). **Proteostasis control by the unfolded protein response**. Nat Cell Biol *17*, 829-838, doi: 10.1038/ncb3184.

Hollien, J. and Weissman, J. S. (2006). **Decay of endoplasmic reticulum-localized mRNAs during the unfolded protein response**. Science *313*, 104-107, doi: 10.1126/science.1129631.

Holohan, C., Van Schaeybroeck, S., Longley, D. B. and Johnston, P. G. (2013). **Cancer drug resistance: an evolving paradigm**. Nat Rev Cancer *13*, 714-726, doi: 10.1038/nrc3599.

Horiguchi, M., Koyanagi, S., Okamoto, A., Suzuki, S. O., Matsunaga, N. and Ohdo, S. (2012). **Stress-regulated transcription factor ATF4 promotes neoplastic**

transformation by suppressing expression of the INK4a/ARF cell senescence factors**. Cancer Res *72*, 395-401, doi: 10.1158/0008-5472.CAN-11-1891.

Hruz, T., Laule, O., Szabo, G., Wessendorp, F., Bleuler, S., Oertle, L., Widmayer, P., Gruissem, W. and Zimmermann, P. (2008). **Genevestigator v3: a reference expression database for the meta-analysis of transcriptomes**. Adv Bioinformatics *2008*, 420747, doi: 10.1155/2008/420747.

Hsieh, A. C., Costa, M., Zollo, O., Davis, C., Feldman, M. E., Testa, J. R., Meyuhas, O., Shokat, K. M. and Ruggero, D. (2010). **Genetic dissection of the oncogenic mTOR pathway reveals druggable addiction to translational control via 4EBP-eIF4E**. Cancer Cell *17*, 249-261, doi: 10.1016/j.ccr.2010.01.021.

Hsieh, A. C., Liu, Y., Edlind, M. P., Ingolia, N. T., Janes, M. R., Sher, A., Shi, E. Y., Stumpf, C. R., Christensen, C., Bonham, M. J., Wang, S., Ren, P., Martin, M., Jessen, K., Feldman, M. E., Weissman, J. S., Shokat, K. M., Rommel, C. and Ruggero, D. (2012). **The translational landscape of mTOR signalling steers cancer initiation and metastasis**. Nature *485*, 55-61, doi: 10.1038/nature10912.

Huang, K. and Fingar, D. C. (2014). **Growing knowledge of the mTOR signaling network**. Semin Cell Dev Biol *36*, 79-90, doi: 10.1016/j.semcdb.2014.09.011.

Ilic, N., Utermark, T., Widlund, H. R. and Roberts, T. M. (2011). **PI3K-targeted therapy can be evaded by gene amplification along the MYC-eukaryotic translation initiation factor 4E (eIF4E) axis**. Proc Natl Acad Sci U S A *108*, E699-708, doi: 10.1073/pnas.1108237108.

Jeon, Y. J., Khelifa, S., Ratnikov, B., Scott, D. A., Feng, Y., Parisi, F., Ruller, C., Lau, E., Kim, H., Brill, L. M., Jiang, T., Rimm, D. L., Cardiff, R. D., Mills, G. B., Smith, J. W., Osterman, A. L., Kluger, Y. and Ronai, Z. A. (2015). **Regulation of glutamine carrier proteins by RNF5 determines breast cancer response to ER stress-inducing chemotherapies**. Cancer Cell *27*, 354-369, doi: 10.1016/j.ccell.2015.02.006.

Jewell, J. L., Russell, R. C. and Guan, K. L. (2013). **Amino acid signalling upstream of mTOR**. Nat Rev Mol Cell Biol *14*, 133-139, doi: 10.1038/nrm3522.

Kafri, M., Metzl-Raz, E., Jona, G. and Barkai, N. (2016). **The Cost of Protein Production**. Cell Rep *14*, 22-31, doi: 10.1016/j.celrep.2015.12.015.

Kim, H. K., Choi, I. J., Kim, C. G., Kim, H. S., Oshima, A., Michalowski, A. and Green, J. E. (2011). **A gene expression signature of acquired chemoresistance to cisplatin and fluorouracil combination chemotherapy in gastric cancer patients**. PLoS One *6*, e16694, doi: 10.1371/journal.pone.0016694.

Knott, S. R. V., Wagenblast, E., Khan, S., Kim, S. Y., Soto, M., Wagner, M., Turgeon, M. O., Fish, L., Erard, N., Gable, A. L., Maceli, A. R., Dickopf, S., Papachristou, E. K., D'Santos, C. S., Carey, L. A., Wilkinson, J. E., Harrell, J. C., Perou, C. M., Goodarzi, H., Poulogiannis, G. and Hannon, G. J. (2018). **Asparagine bioavailability governs metastasis in a model of breast cancer**. Nature *554*, 378-381, doi: 10.1038/nature25465.

Koyama, S., Akbay, E. A., Li, Y. Y., Herter-Sprie, G. S., Buczkowski, K. A., Richards, W. G., Gandhi, L., Redig, A. J., Rodig, S. J., Asahina, H., Jones, R. E., Kulkarni, M. M., Kuraguchi, M., Palakurthi, S., Fecci, P. E., Johnson, B. E., Janne, P. A., Engelman, J. A., Gangadharan, S. P., Costa, D. B., Freeman, G. J., Bueno, R., Hodi, F. S., Dranoff, G., Wong, K. K. and Hammerman, P. S. (2016). **Adaptive resistance to therapeutic PD-1 blockade is associated with upregulation of alternative immune checkpoints**. Nat Commun *7*, 10501, doi: 10.1038/ncomms10501.

Krall, A. S., Xu, S., Graeber, T. G., Braas, D. and Christofk, H. R. (2016). **Asparagine promotes cancer cell proliferation through use as an amino acid exchange factor**. Nat Commun *7*, 11457, doi: 10.1038/ncomms11457.

Lanza, E., Donadon, M., Poretti, D., Pedicini, V., Tramarin, M., Roncalli, M., Rhee, H., Park, Y. N. and Torzilli, G. (2016). **Transarterial Therapies for Hepatocellular Carcinoma**. Liver Cancer *6*, 27-33, doi: 10.1159/000449347.

Laplante, M. and Sabatini, D. M. (2012). **mTOR signaling in growth control and disease**. Cell *149*, 274-293, doi: 10.1016/j.cell.2012.03.017.

Le, A., Ng, A., Kwan, T., Cusmano-Ozog, K. and Cowan, T. M. (2014). **A rapid, sensitive method for quantitative analysis of underivatized amino acids by liquid chromatography-tandem mass spectrometry (LC-MS/MS)**. J Chromatogr B Analyt Technol Biomed Life Sci *944*, 166-174, doi: 10.1016/j.jchromb.2013.11.017.

Lee, K., Tirasophon, W., Shen, X., Michalak, M., Prywes, R., Okada, T., Yoshida, H., Mori, K. and Kaufman, R. J. (2002). **IRE1-mediated unconventional mRNA splicing and S2P-mediated ATF6 cleavage merge to regulate XBP1 in signaling the unfolded protein response**. Genes Dev *16*, 452-466, doi: 10.1101/gad.964702.

Liang, S., Zhou, Y., Chen, Y., Ke, G., Wen, H. and Wu, X. (2014). **Decreased expression of EIF4A1 after preoperative brachytherapy predicts better tumor-specific survival in cervical cancer**. Int J Gynecol Cancer *24*, 908-915, doi: 10.1097/IGC.0000000000000152.

Livraghi, T., Meloni, F., Di Stasi, M., Rolle, E., Solbiati, L., Tinelli, C. and Rossi, S. (2008). **Sustained complete response and complications rates after radiofrequency ablation of very early hepatocellular carcinoma in cirrhosis: Is resection still the treatment of choice?** Hepatology *47*, 82-89, doi: 10.1002/hep.21933.

Llovet, J. M., Ricci, S., Mazzaferro, V., Hilgard, P., Gane, E., Blanc, J. F., de Oliveira, A. C., Santoro, A., Raoul, J. L., Forner, A., Schwartz, M., Porta, C., Zeuzem, S., Bolondi, L., Greten, T. F., Galle, P. R., Seitz, J. F., Borbath, I., Haussinger, D., Giannaris, T., Shan, M., Moscovici, M., Voliotis, D., Bruix, J. and Group, S. I. S. (2008). **Sorafenib in advanced hepatocellular carcinoma**. N Engl J Med *359*, 378-390, doi: 10.1056/NEJMoa0708857.

Lopez-Lastra, M., Rivas, A. and Barria, M. I. (2005). **Protein synthesis in eukaryotes: the growing biological relevance of cap-independent translation initiation**. Biol Res *38*, 121-146.

Lorenzi, P. L., Llamas, J., Gunsior, M., Ozbun, L., Reinhold, W. C., Varma, S., Ji, H., Kim, H., Hutchinson, A. A., Kohn, E. C., Goldsmith, P. K., Birrer, M. J. and Weinstein, J. N. (2008). **Asparagine synthetase is a predictive biomarker of L-asparaginase activity in ovarian cancer cell lines**. Mol Cancer Ther *7*, 3123-3128, doi: 10.1158/1535-7163.MCT-08-0589.

Lu, W., Pelicano, H. and Huang, P. (2010). **Cancer metabolism: is glutamine sweeter than glucose?** Cancer Cell *18*, 199-200, doi: 10.1016/j.ccr.2010.08.017.

Ma, Y. and Hendershot, L. M. (2004). **The role of the unfolded protein response in tumour development: friend or foe?** Nat Rev Cancer *4*, 966-977, doi: 10.1038/nrc1505.

Makarova-Rusher, O. V., Medina-Echeverz, J., Duffy, A. G. and Greten, T. F. (2015). **The yin and yang of evasion and immune activation in HCC**. J Hepatol *62*, 1420-1429, doi: 10.1016/j.jhep.2015.02.038.

Malka-Mahieu, H., Newman, M., Desaubry, L., Robert, C. and Vagner, S. (2017). **Molecular Pathways: The eIF4F Translation Initiation Complex-New Opportunities for Cancer Treatment**. Clin Cancer Res *23*, 21-25, doi: 10.1158/1078-0432.CCR-14-2362.

Malys, N. and McCarthy, J. E. (2011). **Translation initiation: variations in the mechanism can be anticipated**. Cell Mol Life Sci *68*, 991-1003, doi: 10.1007/s00018-010-0588-z.

Marciniak, S. J., Yun, C. Y., Oyadomari, S., Novoa, I., Zhang, Y., Jungreis, R., Nagata, K., Harding, H. P. and Ron, D. (2004). **CHOP induces death by promoting protein synthesis and oxidation in the stressed endoplasmic reticulum**. Genes Dev *18*, 3066-3077, doi: 10.1101/gad.1250704.

Martinez, A., Sese, M., Losa, J. H., Robichaud, N., Sonenberg, N., Aasen, T. and Ramon, Y. C. S. (2015). **Phosphorylation of eIF4E Confers Resistance to Cellular Stress and DNA-Damaging Agents through an Interaction with 4E-T: A Rationale for Novel Therapeutic Approaches**. PLoS One *10*, e0123352, doi: 10.1371/journal.pone.0123352.

Mazzaferro, V., Regalia, E., Doci, R., Andreola, S., Pulvirenti, A., Bozzetti, F., Montalto, F., Ammatuna, M., Morabito, A. and Gennari, L. (1996). **Liver transplantation for the treatment of small hepatocellular carcinomas in patients with cirrhosis**. N Engl J Med *334*, 693-699, doi: 10.1056/NEJM199603143341104.

Mazzaferro, V., Romito, R., Schiavo, M., Mariani, L., Camerini, T., Bhoori, S., Capussotti, L., Calise, F., Pellicci, R., Belli, G., Tagger, A., Colombo, M., Bonino, F., Majno, P., Llovet, J. M. and Force, H. C. C. I. T. (2006). **Prevention of hepatocellular carcinoma recurrence with alpha-interferon after liver resection in HCV cirrhosis**. Hepatology *44*, 1543-1554, doi: 10.1002/hep.21415.

Mazzaferro, V., Sposito, C., Bhoori, S., Romito, R., Chiesa, C., Morosi, C., Maccauro, M., Marchiano, A., Bongini, M., Lanocita, R., Civelli, E., Bombardieri, E., Camerini, T.

and Spreafico, C. (2013). **Yttrium-90 radioembolization for intermediate-advanced hepatocellular carcinoma: a phase 2 study**. Hepatology *57*, 1826-1837, doi: 10.1002/hep.26014.

Milman, H. A. and Cooney, D. A. (1979). **Partial purification and properties of L-asparagine synthetase from mouse pancreas**. Biochem J *181*, 51-59, doi: 10.1042/bj1810051.

Mishra, R., Watanabe, T., Kimura, M. T., Koshikawa, N., Ikeda, M., Uekusa, S., Kawashima, H., Wang, X., Igarashi, J., Choudhury, D., Grandori, C., Kemp, C. J., Ohira, M., Verma, N. K., Kobayashi, Y., Takeuchi, J., Koshinaga, T., Nemoto, N., Fukuda, N., Soma, M., Kusafuka, T., Fujiwara, K. and Nagase, H. (2015). **Identification of a novel E-box binding pyrrole-imidazole polyamide inhibiting MYC-driven cell proliferation**. Cancer Sci *106*, 421-429, doi: 10.1111/cas.12610.

Mori, K. (2009). **Signalling pathways in the unfolded protein response: development from yeast to mammals**. J Biochem *146*, 743-750, doi: 10.1093/jb/mvp166.

Nicklin, P., Bergman, P., Zhang, B., Triantafellow, E., Wang, H., Nyfeler, B., Yang, H., Hild, M., Kung, C., Wilson, C., Myer, V. E., MacKeigan, J. P., Porter, J. A., Wang, Y. K., Cantley, L. C., Finan, P. M. and Murphy, L. O. (2009). **Bidirectional transport of amino acids regulates mTOR and autophagy**. Cell *136*, 521-534, doi: 10.1016/j.cell.2008.11.044.

Nishitoh, H. (2012). **CHOP is a multifunctional transcription factor in the ER stress response**. J Biochem *151*, 217-219, doi: 10.1093/jb/mvr143.

Notte, A., Rebucci, M., Fransolet, M., Roegiers, E., Genin, M., Tellier, C., Watillon, K., Fattaccioli, A., Arnould, T. and Michiels, C. (2015). **Taxol-induced unfolded protein response activation in breast cancer cells exposed to hypoxia: ATF4 activation regulates autophagy and inhibits apoptosis**. Int J Biochem Cell Biol *62*, 1-14, doi: 10.1016/j.biocel.2015.02.010.

Oblinger, J. L., Burns, S. S., Akhmametyeva, E. M., Huang, J., Pan, L., Ren, Y., Shen, R., Miles-Markley, B., Moberly, A. C., Kinghorn, A. D., Welling, D. B. and Chang, L. S. (2016). **Components of the eIF4F complex are potential therapeutic targets for malignant peripheral nerve sheath tumors and vestibular schwannomas**. Neuro Oncol *18*, 1265-1277, doi: 10.1093/neuonc/now032.

Oh, W. J. and Jacinto, E. (2011). **mTOR complex 2 signaling and functions**. Cell Cycle *10*, 2305-2316, doi: 10.4161/cc.10.14.16586.

Paez-Ribes, M., Allen, E., Hudock, J., Takeda, T., Okuyama, H., Vinals, F., Inoue, M., Bergers, G., Hanahan, D. and Casanovas, O. (2009). **Antiangiogenic therapy elicits malignant progression of tumors to increased local invasion and distant metastasis**. Cancer Cell *15*, 220-231, doi: 10.1016/j.ccr.2009.01.027.

Pavlova, N. N., Hui, S., Ghergurovich, J. M., Fan, J., Intlekofer, A. M., White, R. M., Rabinowitz, J. D., Thompson, C. B. and Zhang, J. (2018). **As Extracellular**

Glutamine Levels Decline, Asparagine Becomes an Essential Amino Acid. Cell Metab *27*, 428-438 e425, doi: 10.1016/j.cmet.2017.12.006.

Pelletier, J., Graff, J., Ruggero, D. and Sonenberg, N. (2015). **Targeting the eIF4F translation initiation complex: a critical nexus for cancer development**. Cancer Res *75*, 250-263, doi: 10.1158/0008-5472.CAN-14-2789.

Pi, L., Li, X., Song, Q., Shen, Y., Lu, X. and Di, B. (2014). **Knockdown of glucose-regulated protein 78 abrogates chemoresistance of hypopharyngeal carcinoma cells to cisplatin induced by unfolded protein in response to severe hypoxia**. Oncol Lett *7*, 685-692, doi: 10.3892/ol.2013.1753.

Plaitakis, A., Kalef-Ezra, E., Kotzamani, D., Zaganas, I. and Spanaki, C. (2017). **The Glutamate Dehydrogenase Pathway and Its Roles in Cell and Tissue Biology in Health and Disease**. Biology (Basel) *6*, doi: 10.3390/biology6010011.

Pochini, L., Scalise, M., Galluccio, M. and Indiveri, C. (2014). **Membrane transporters for the special amino acid glutamine: structure/function relationships and relevance to human health**. Front Chem *2*, 61, doi: 10.3389/fchem.2014.00061.

Qing, G., Li, B., Vu, A., Skuli, N., Walton, Z. E., Liu, X., Mayes, P. A., Wise, D. R., Thompson, C. B., Maris, J. M., Hogarty, M. D. and Simon, M. C. (2012). **ATF4 regulates MYC-mediated neuroblastoma cell death upon glutamine deprivation**. Cancer Cell *22*, 631-644, doi: 10.1016/j.ccr.2012.09.021.

Raza, A. and Sood, G. K. (2014). **Hepatocellular carcinoma review: current treatment, and evidence-based medicine**. World J Gastroenterol *20*, 4115-4127, doi: 10.3748/wjg.v20.i15.4115.

Robichaud, N., del Rincon, S. V., Huor, B., Alain, T., Petruccelli, L. A., Hearnden, J., Goncalves, C., Grotegut, S., Spruck, C. H., Furic, L., Larsson, O., Muller, W. J., Miller, W. H. and Sonenberg, N. (2015). **Phosphorylation of eIF4E promotes EMT and metastasis via translational control of SNAIL and MMP-3**. Oncogene *34*, 2032-2042, doi: 10.1038/onc.2014.146.

Ron, D. and Walter, P. (2007). **Signal integration in the endoplasmic reticulum unfolded protein response**. Nat Rev Mol Cell Biol *8*, 519-529, doi: 10.1038/nrm2199.

Safer, B., Smith, C. M. and Williamson, J. R. (1971). **Control of the transport of reducing equivalents across the mitochondrial membrane in perfused rat heart**. J Mol Cell Cardiol *2*, 111-124.

Salaroglio, I. C., Panada, E., Moiso, E., Buondonno, I., Provero, P., Rubinstein, M., Kopecka, J. and Riganti, C. (2017). **PERK induces resistance to cell death elicited by endoplasmic reticulum stress and chemotherapy**. Mol Cancer *16*, 91, doi: 10.1186/s12943-017-0657-0.

Salem, R., Lewandowski, R. J., Kulik, L., Wang, E., Riaz, A., Ryu, R. K., Sato, K. T., Gupta, R., Nikolaidis, P., Miller, F. H., Yaghmai, V., Ibrahim, S. M., Senthilnathan, S., Baker, T., Gates, V. L., Atassi, B., Newman, S., Memon, K., Chen, R., Vogelzang, R.

L., Nemcek, A. A., Resnick, S. A., Chrisman, H. B., Carr, J., Omary, R. A., Abecassis, M., Benson, A. B., 3rd and Mulcahy, M. F. (2011). **Radioembolization results in longer time-to-progression and reduced toxicity compared with chemoembolization in patients with hepatocellular carcinoma**. Gastroenterology *140*, 497-507 e492, doi: 10.1053/j.gastro.2010.10.049.

Sangro, B., Carpanese, L., Cianni, R., Golfieri, R., Gasparini, D., Ezziddin, S., Paprottka, P. M., Fiore, F., Van Buskirk, M., Bilbao, J. I., Ettorre, G. M., Salvatori, R., Giampalma, E., Geatti, O., Wilhelm, K., Hoffmann, R. T., Izzo, F., Inarrairaegui, M., Maini, C. L., Urigo, C., Cappelli, A., Vit, A., Ahmadzadehfar, H., Jakobs, T. F., Lastoria, S. and European Network on Radioembolization with Yttrium-90 Resin, M. (2011). **Survival after yttrium-90 resin microsphere radioembolization of hepatocellular carcinoma across Barcelona clinic liver cancer stages: a European evaluation**. Hepatology *54*, 868-878, doi: 10.1002/hep.24451.

Sangro, B., Inarrairaegui, M. and Bilbao, J. I. (2012). **Radioembolization for hepatocellular carcinoma**. J Hepatol *56*, 464-473, doi: 10.1016/j.jhep.2011.07.012.

Sapisochin, G. and Bruix, J. (2017). **Liver transplantation for hepatocellular carcinoma: outcomes and novel surgical approaches**. Nat Rev Gastroenterol Hepatol *14*, 203-217, doi: 10.1038/nrgastro.2016.193.

Schroder, M. and Kaufman, R. J. (2005). **The mammalian unfolded protein response**. Annu Rev Biochem *74*, 739-789, doi: 10.1146/annurev.biochem.73.011303.074134.

Schulte, M. L., Fu, A., Zhao, P., Li, J., Geng, L., Smith, S. T., Kondo, J., Coffey, R. J., Johnson, M. O., Rathmell, J. C., Sharick, J. T., Skala, M. C., Smith, J. A., Berlin, J., Washington, M. K., Nickels, M. L. and Manning, H. C. (2018). **Pharmacological blockade of ASCT2-dependent glutamine transport leads to antitumor efficacy in preclinical models**. Nat Med *24*, 194-202, doi: 10.1038/nm.4464.

Senft, D. and Ronai, Z. A. (2015). **UPR, autophagy, and mitochondria crosstalk underlies the ER stress response**. Trends Biochem Sci *40*, 141-148, doi: 10.1016/j.tibs.2015.01.002.

Shah, R. P., Brown, K. T. and Sofocleous, C. T. (2011). **Arterially directed therapies for hepatocellular carcinoma**. AJR Am J Roentgenol *197*, W590-602, doi: 10.2214/AJR.11.7554.

Shajahan-Haq, A. N., Cook, K. L., Schwartz-Roberts, J. L., Eltayeb, A. E., Demas, D. M., Warri, A. M., Facey, C. O., Hilakivi-Clarke, L. A. and Clarke, R. (2014). **MYC regulates the unfolded protein response and glucose and glutamine uptake in endocrine resistant breast cancer**. Mol Cancer *13*, 239, doi: 10.1186/1476-4598-13-239.

Shanware, N. P., Bray, K., Eng, C. H., Wang, F., Follettie, M., Myers, J., Fantin, V. R. and Abraham, R. T. (2014). **Glutamine deprivation stimulates mTOR-JNK-dependent chemokine secretion**. Nat Commun *5*, 4900, doi: 10.1038/ncomms5900.

Shen, J., Chen, X., Hendershot, L. and Prywes, R. (2002). **ER stress regulation of ATF6 localization by dissociation of BiP/GRP78 binding and unmasking of Golgi localization signals**. Dev Cell *3*, 99-111.

Siegel, A. B. and Zhu, A. X. (2009). **Metabolic syndrome and hepatocellular carcinoma: two growing epidemics with a potential link**. Cancer *115*, 5651-5661, doi: 10.1002/cncr.24687.

Sieghart, W., Hucke, F., Pinter, M., Graziadei, I., Vogel, W., Muller, C., Heinzl, H., Trauner, M. and Peck-Radosavljevic, M. (2013). **The ART of decision making: retreatment with transarterial chemoembolization in patients with hepatocellular carcinoma**. Hepatology *57*, 2261-2273, doi: 10.1002/hep.26256.

Soderberg, O., Gullberg, M., Jarvius, M., Ridderstrale, K., Leuchowius, K. J., Jarvius, J., Wester, K., Hydbring, P., Bahram, F., Larsson, L. G. and Landegren, U. (2006). **Direct observation of individual endogenous protein complexes in situ by proximity ligation**. Nat Methods *3*, 995-1000, doi: 10.1038/nmeth947.

Song, M. J., Chun, H. J., Song, D. S., Kim, H. Y., Yoo, S. H., Park, C. H., Bae, S. H., Choi, J. Y., Chang, U. I., Yang, J. M., Lee, H. G. and Yoon, S. K. (2012). **Comparative study between doxorubicin-eluting beads and conventional transarterial chemoembolization for treatment of hepatocellular carcinoma**. J Hepatol *57*, 1244-1250, doi: 10.1016/j.jhep.2012.07.017.

Su, A. I., Cooke, M. P., Ching, K. A., Hakak, Y., Walker, J. R., Wiltshire, T., Orth, A. P., Vega, R. G., Sapinoso, L. M., Moqrich, A., Patapoutian, A., Hampton, G. M., Schultz, P. G. and Hogenesch, J. B. (2002). **Large-scale analysis of the human and mouse transcriptomes**. Proc Natl Acad Sci U S A *99*, 4465-4470, doi: 10.1073/pnas.012025199.

Suzuki, C., Garces, R. G., Edmonds, K. A., Hiller, S., Hyberts, S. G., Marintchev, A. and Wagner, G. (2008). **PDCD4 inhibits translation initiation by binding to eIF4A using both its MA3 domains**. Proc Natl Acad Sci U S A *105*, 3274-3279, doi: 10.1073/pnas.0712235105.

Topisirovic, I., Ruiz-Gutierrez, M. and Borden, K. L. (2004). **Phosphorylation of the eukaryotic translation initiation factor eIF4E contributes to its transformation and mRNA transport activities**. Cancer Res *64*, 8639-8642, doi: 10.1158/0008-5472.CAN-04-2677.

Torre, L. A., Bray, F., Siegel, R. L., Ferlay, J., Lortet-Tieulent, J. and Jemal, A. (2015). **Global cancer statistics, 2012**. CA Cancer J Clin *65*, 87-108, doi: 10.3322/caac.21262.

Truitt, M. L., Conn, C. S., Shi, Z., Pang, X., Tokuyasu, T., Coady, A. M., Seo, Y., Barna, M. and Ruggero, D. (2015). **Differential Requirements for eIF4E Dose in Normal Development and Cancer**. Cell *162*, 59-71, doi: 10.1016/j.cell.2015.05.049.

Truong, P., Rahal, A. and Kallail, K. J. (2016). **Metastatic Hepatocellular Carcinoma Responsive to Pembrolizumab**. Cureus *8*, e631, doi: 10.7759/cureus.631.

Tsaytler, P., Harding, H. P., Ron, D. and Bertolotti, A. (2011). **Selective inhibition of a regulatory subunit of protein phosphatase 1 restores proteostasis**. Science *332*, 91-94, doi: 10.1126/science.1201396.

Tsun, Z. Y. and Possemato, R. (2015). **Amino acid management in cancer**. Semin Cell Dev Biol *43*, 22-32, doi: 10.1016/j.semcdb.2015.08.002.

Ubuka, T. and Meister, A. (1971). **Studies on the utilization of asparagine by mouse leukemia cells**. J Natl Cancer Inst *46*, 291-298.

Uhlen, M., Fagerberg, L., Hallstrom, B. M., Lindskog, C., Oksvold, P., Mardinoglu, A., Sivertsson, A., Kampf, C., Sjostedt, E., Asplund, A., Olsson, I., Edlund, K., Lundberg, E., Navani, S., Szigyarto, C. A., Odeberg, J., Djureinovic, D., Takanen, J. O., Hober, S., Alm, T., Edqvist, P. H., Berling, H., Tegel, H., Mulder, J., Rockberg, J., Nilsson, P., Schwenk, J. M., Hamsten, M., von Feilitzen, K., Forsberg, M., Persson, L., Johansson, F., Zwahlen, M., von Heijne, G., Nielsen, J. and Ponten, F. (2015). **Proteomics. Tissue-based map of the human proteome**. Science *347*, 1260419, doi: 10.1126/science.1260419.

Vincent, H. A., Ziehr, B. and Moorman, N. J. (2016). **Human Cytomegalovirus Strategies to Maintain and Promote mRNA Translation**. Viruses *8*, 97, doi: 10.3390/v8040097.

Visioli, F., Wang, Y., Alam, G. N., Ning, Y., Rados, P. V., Nor, J. E. and Polverini, P. J. (2014). **Glucose-regulated protein 78 (Grp78) confers chemoresistance to tumor endothelial cells under acidic stress**. PLoS One *9*, e101053, doi: 10.1371/journal.pone.0101053.

von der Haar, T., Gross, J. D., Wagner, G. and McCarthy, J. E. (2004). **The mRNA cap-binding protein eIF4E in post-transcriptional gene expression**. Nat Struct Mol Biol *11*, 503-511, doi: 10.1038/nsmb779.

Walter, P. and Ron, D. (2011). **The unfolded protein response: from stress pathway to homeostatic regulation**. Science *334*, 1081-1086, doi: 10.1126/science.1209038.

Walters, B. and Thompson, S. R. (2016). **Cap-Independent Translational Control of Carcinogenesis**. Front Oncol *6*, 128, doi: 10.3389/fonc.2016.00128.

Ward, P. S. and Thompson, C. B. (2012). **Metabolic reprogramming: a cancer hallmark even warburg did not anticipate**. Cancer Cell *21*, 297-308, doi: 10.1016/j.ccr.2012.02.014.

Wendel, H. G., Silva, R. L., Malina, A., Mills, J. R., Zhu, H., Ueda, T., Watanabe-Fukunaga, R., Fukunaga, R., Teruya-Feldstein, J., Pelletier, J. and Lowe, S. W. (2007). **Dissecting eIF4E action in tumorigenesis**. Genes Dev *21*, 3232-3237, doi: 10.1101/gad.1604407.

Wilhelm, S. M., Dumas, J., Adnane, L., Lynch, M., Carter, C. A., Schutz, G., Thierauch, K. H. and Zopf, D. (2011). **Regorafenib (BAY 73-4506): a new oral multikinase**

inhibitor of angiogenic, stromal and oncogenic receptor tyrosine kinases with potent preclinical antitumor activity. Int J Cancer *129*, 245-255, doi: 10.1002/ijc.25864.

Wise, D. R., DeBerardinis, R. J., Mancuso, A., Sayed, N., Zhang, X. Y., Pfeiffer, H. K., Nissim, I., Daikhin, E., Yudkoff, M., McMahon, S. B. and Thompson, C. B. (2008). **Myc regulates a transcriptional program that stimulates mitochondrial glutaminolysis and leads to glutamine addiction**. Proc Natl Acad Sci U S A *105*, 18782-18787, doi: 10.1073/pnas.0810199105.

Xia, Y., Qiu, Y., Li, J., Shi, L., Wang, K., Xi, T., Shen, F., Yan, Z. and Wu, M. (2010). **Adjuvant therapy with capecitabine postpones recurrence of hepatocellular carcinoma after curative resection: a randomized controlled trial**. Ann Surg Oncol *17*, 3137-3144, doi: 10.1245/s10434-010-1148-3.

Yamamoto, K., Sato, T., Matsui, T., Sato, M., Okada, T., Yoshida, H., Harada, A. and Mori, K. (2007). **Transcriptional induction of mammalian ER quality control proteins is mediated by single or combined action of ATF6alpha and XBP1**. Dev Cell *13*, 365-376, doi: 10.1016/j.devcel.2007.07.018.

Yang, C., Sudderth, J., Dang, T., Bachoo, R. M., McDonald, J. G. and DeBerardinis, R. J. (2009). **Glioblastoma cells require glutamate dehydrogenase to survive impairments of glucose metabolism or Akt signaling**. Cancer Res *69*, 7986-7993, doi: 10.1158/0008-5472.CAN-09-2266.

Ye, J., Kumanova, M., Hart, L. S., Sloane, K., Zhang, H., De Panis, D. N., Bobrovnikova-Marjon, E., Diehl, J. A., Ron, D. and Koumenis, C. (2010). **The GCN2-ATF4 pathway is critical for tumour cell survival and proliferation in response to nutrient deprivation**. EMBO J *29*, 2082-2096, doi: 10.1038/emboj.2010.81.

Ye, J., Mancuso, A., Tong, X., Ward, P. S., Fan, J., Rabinowitz, J. D. and Thompson, C. B. (2012). **Pyruvate kinase M2 promotes de novo serine synthesis to sustain mTORC1 activity and cell proliferation**. Proc Natl Acad Sci U S A *109*, 6904-6909, doi: 10.1073/pnas.1204176109.

Ye, J., Rawson, R. B., Komuro, R., Chen, X., Dave, U. P., Prywes, R., Brown, M. S. and Goldstein, J. L. (2000). **ER stress induces cleavage of membrane-bound ATF6 by the same proteases that process SREBPs**. Mol Cell *6*, 1355-1364.

Yi, T., Papadopoulos, E., Hagner, P. R. and Wagner, G. (2013). **Hypoxia-inducible factor-1alpha (HIF-1alpha) promotes cap-dependent translation of selective mRNAs through up-regulating initiation factor eIF4E1 in breast cancer cells under hypoxia conditions**. J Biol Chem *288*, 18732-18742, doi: 10.1074/jbc.M113.471466.

Yoshida, H., Matsui, T., Yamamoto, A., Okada, T. and Mori, K. (2001). **XBP1 mRNA is induced by ATF6 and spliced by IRE1 in response to ER stress to produce a highly active transcription factor**. Cell *107*, 881-891.

Yuneva, M., Zamboni, N., Oefner, P., Sachidanandam, R. and Lazebnik, Y. (2007). **Deficiency in glutamine but not glucose induces MYC-dependent apoptosis in human cells**. J Cell Biol *178*, 93-105, doi: 10.1083/jcb.200703099.

Zhai, B. and Sun, X. Y. (2013). **Mechanisms of resistance to sorafenib and the corresponding strategies in hepatocellular carcinoma**. World J Hepatol *5*, 345-352, doi: 10.4254/wjh.v5.i7.345.

Zhang, J., Fan, J., Venneti, S., Cross, J. R., Takagi, T., Bhinder, B., Djaballah, H., Kanai, M., Cheng, E. H., Judkins, A. R., Pawel, B., Baggs, J., Cherry, S., Rabinowitz, J. D. and Thompson, C. B. (2014). **Asparagine plays a critical role in regulating cellular adaptation to glutamine depletion**. Mol Cell *56*, 205-218, doi: 10.1016/j.molcel.2014.08.018.

Zhang, J., Pavlova, N. N. and Thompson, C. B. (2017). **Cancer cell metabolism: the essential role of the nonessential amino acid, glutamine**. EMBO J *36*, 1302-1315, doi: 10.15252/embj.201696151.

Zhang, K., Shen, X., Wu, J., Sakaki, K., Saunders, T., Rutkowski, D. T., Back, S. H. and Kaufman, R. J. (2006). **Endoplasmic reticulum stress activates cleavage of CREBH to induce a systemic inflammatory response**. Cell *124*, 587-599, doi: 10.1016/j.cell.2005.11.040.

Zhou, Y., Zhou, B., Pache, L., Chang, M., Khodabakhshi, A. H., Tanaseichuk, O., Benner, C. and Chanda, S. K. (2019). **Metascape provides a biologist-oriented resource for the analysis of systems-level datasets**. Nat Commun *10*, 1523, doi: 10.1038/s41467-019-09234-6.

Zindy, P., Berge, Y., Allal, B., Filleron, T., Pierredon, S., Cammas, A., Beck, S., Mhamdi, L., Fan, L., Favre, G., Delord, J. P., Roche, H., Dalenc, F., Lacroix-Triki, M. and Vagner, S. (2011). **Formation of the eIF4F translation-initiation complex determines sensitivity to anticancer drugs targeting the EGFR and HER2 receptors**. Cancer Res *71*, 4068-4073, doi: 10.1158/0008-5472.CAN-11-0420.

9. APPENDIX

Supplementary table 1. Gene annotation database from NuRNA™ Human Central

Metabolism PCR Array

Functions	Gene name
Glucose transporters	SLC2A1, SLC2A2, SLC2A3, SLC2A4, SLC2A5, SLC2A6, SLC2A7, SLC2A8, SLC2A9, SLC2A10, SLC2A11, SLC2A12, SLC2A14
Glycolysis	ADPGK, ALDOA, ALDOB, ALDOC, BPGM, ENO1, ENO2, ENO3, GAPDH, GAPDHS, GCK, GPI, HK1, HK2, HK3, HKDC1, PFKFB1, PFKFB2, PFKFB3-isoform 1, PFKFB3-isoform 2, PFKFB3-isoform 3, PFKFB3-isoform 4, PFKFB4, PFKL, PFKM, PFKP, PGAM1, PGAM2, PGAM4, PGK1, PGK2, PKL, PKM1, PKM2, PKR, TPI1
Lactate production and transporters	LDHA, LDHB, LDHC, LDHAL6A, LDHAL6B, UEVLD, SLC16A1, SLC16A2, SLC16A3, SLC16A4, SLC16A5, SLC16A6, SLC16A7, SLC16A8, SLC16A9, SLC16A10, SLC16A11, SLC16A12
Gluconeogenesis	BCAT1, BCAT2, FBP1, FBP2, G6PC, G6PC2, G6PC3, GPT, GPT2, LDHD, PC, PCK1, PCK2
Glycogen metabolism	GBE1, GYS1, GYS2, PGM1, PGM2, UGP2
Hexosamine metabolism	GFPT1, GFPT2, GNPNAT1, PGM3, UAP1, UAP1L1
Pentose phosphate pathway	G6PD, H6PD, PGD, PGLS, PRPS1, PRPS1L1, PRPS2, RBKS, RPE, RPEL1, RPIA, TALDO1, TKT, TKTL1, TKTL2
Glycerol/fatty acid/cholesterol synthesis	ACACA, ACACB, ACAT1, ACAT2, ACLY, ACSBG1, ACSBG2, ACSL1, ACSL3, ACSL4, ACSL5, ACSL6, ACSM1, ACSM2A, ACSM2B, ACSM3, ACSM4, ACSM5, FADS1, FADS2, FASN, GPD1,

	GPD1L, HMGCR, HMGCS1, HMGCS2, MLYCD, SCD, SCD5, SLC25A1, SLC27A2
Serine/ glycine/ one-carbon metabolism	AHCY, AHCYL1, AHCYL2, AMT, BHMT, DHFR, DHFRL1, DLD, DNMT1, DNMT3A, DNMT3B, DNMT3L, GCSH, GLDC, MAT1A, MAT2A, MAT2B, MTHFD1, MTHFD1L, MTHFD2, MTHFD2L, MTHFR, MTR, PHGDH, PSAT1, PSPH, SHMT1, SHMT2
TCA cycle	ACO1, ACO2, D2HGDH, DHTKD1, DLAT, DLD, DLST, FH, IDH1, IDH2, IDH3A, IDH3B, IDH3G, L2HGDH, MDH1, MDH1B, MDH2, OGDH, OGDHL, PDHA1, PDHA2, PDHB, PDHX, PDK1, PDK2, PDK3, PDK4, PDP1, PDP2, PDPR, SDHA, SDHAF1, SDHAF2, SDHAF3, SDHAF4, SDHB, SDHC, SDHD, SUCLA2, SUCLG1, SUCLG2, UEVLD
Glutamine transporters and glutaminolysis	GLS2, GLS-isoform 1, GLS-isoform 2, GLS-isoform 3, GLUD1, GLUD2, GOT1, GOT2, SLC1A1, SLC1A2, SLC1A3, SLC1A4, SLC1A5, SLC1A6, SLC38A1, SLC38A3, SLC38A5, SLC38A7
Redox balance	CBS, CTH, G6PD, GCLC, GCLM, GSR, GSS, IDH1, IDH2, ME1, ME2, ME3, MTHFD1, NNT, PGD, SLC7A11
GSH synthesis	CBS, CTH, GCLC, GCLM, GSR, GSS, SLC7A11
Fatty acid oxidation	AADAC, ABHD12, ABHD6, ACAA1, ACAA2, ACAD10, ACAD11, ACAD8, ACAD9, ACADL, ACADM, ACADS, ACADSB, ACADVL, ALDH1B1, ALDH2, ALDH3A2, ALDH7A1, ALDH9A1, CEL, CPT1A, CPT1B, CPT1C, CPT2, ECH1, ECHS1, ECI1, ECI2, EHHADH, ETFA, ETFB, HADH, HADHA, HADHB, HSD17B10, HSD17B4, LIPC, LIPE, LIPF, LIPG, MGLL, PAFAH1B1, PAFAH1B2, PAFAH1B3, PNLIP, PNLIPRP1, PNLIPRP2, PNLIPRP3, PNPLA2, PNPLA3, SCP2
Acetate metabolism	ACOT12, ACSS1, ACSS2, ACSS3

Nucleotide metabolism	ADA, ADCY1, ADCY10, ADCY2, ADCY3, ADCY4, ADCY5, ADCY6, ADCY7, ADCY9, ADSL, ADSS, ADSSL1, AK1, AK2, AK3, AK4, AK5, AK6, AK7, AK8, AK9, AMPD1, AMPD2, AMPD3, APRT, ATIC, CAD, CANT1, CDA, CECR1, CMPK1, CMPK2, CTPS1, DCK, DCTD, DHODH, DTYMK, DUT, GART, GDA, GMPS, GUCA1A, GUCA1B, GUCA1C, GUCA2A, GUCA2B, GUCD1, GUCY1A2, GUCY1A3, GUCY1B3, GUCY2C, GUCY2D, GUCY2F, GUK1, HPRT1, IMPDH1, IMPDH2, NME1, NME2, NME3, NME4, NME6, NME7, NT5C2, PAICS, PDE10A, PDE4D, PFAS, PNP, PPAT, RRM1, RRM2, RRM2B, TK1, TK2, TYMP, TYMS, UCKL1, UMPS, UPP1, UPP2, XDH

Supplementary table 2. The differentially expressed genes and its functions in low

Sorafenib and low glucose treated HCC cells groups

Gene	Functions	Fold Change	Sor^{low} P value
L2HGDH	TCA cycle	804.867458	<0.0001****
TKTL2	Pentose phosphate pathway	471.9883421	<0.0001****
GLUD1	Glutamine transporters and glutaminolysis	399.6539162	<0.0001****
SLC1A5	Glutamine transporters and glutaminolysis	124.7250481	<0.0001****
CPT2	Fatty acid oxidation	53.5423077	<0.0001****
PDHA2	TCA cycle	20.14859613	0.0001***
PNLIP	Fatty acid oxidation	19.73394402	0.0001***
SLC16A2	Lactate production and transporters	12.92961503	0.0002***
PFKFB2	Glycolysis	9.935602225	0.0003***
LIPF	Fatty acid oxidation	9.334724318	0.0004***
PGK2	Glycolysis	8.649444114	0.0004***
SLC1A4	Glutamine transporters and glutaminolysis	8.471441128	0.0004***
PCK2	Gluconeogenesis	7.634890236	0.0005***
SLC1A6	Glutamine transporters and glutaminolysis	7.374817846	0.0005***
SLC38A5	Glutamine transporters and glutaminolysis	6.928809137	0.0006***
PCK1	Gluconeogenesis	6.833418175	0.0006***
SLC16A12	Lactate production and transporters	6.692788462	0.0007***
CPT1C	Fatty acid oxidation	6.646557995	0.0007***
ME3	Redox balance	5.907744429	0.0009***
ACACB	Glycerol/fatty acid/cholesterol synthesis	5.667087257	0.0009***
PDK3	TCA cycle	5.667087257	0.0009***
MTHFD1	Serine/ glycine/ one-carbon metabolism, Redox balance	5.667087257	0.0009***
SLC38A3	Glutamine transporters and glutaminolysis	5.3243574	0.0011**
H6PD	Pentose phosphate pathway	5.214783709	0.0011**
ECI2	Fatty acid oxidation	4.765433359	0.0014**
EHHADH	Fatty acid oxidation	4.667362159	0.0015**
SLC25A1	Glycerol/fatty acid/cholesterol synthesis	4.571309235	0.0015**
SLC38A7	Glutamine transporters and glutaminolysis	4.508374669	0.0016**
SDHD	TCA cycle	4.508374669	0.0016**
DHFRL1	Serine/ glycine/ one-carbon metabolism	4.477233051	0.0016**
ACADS	Fatty acid oxidation	4.446306543	0.0017**
GUCY2C	Nucleotide metabolism	4.324722057	0.0018**
HK1	Glycolysis	4.206462305	0.0019**
GUCY1A2	Nucleotide metabolism	4.091436372	0.0021**
PAICS	Nucleotide metabolism	4.091436372	0.0021**
RBKS	Pentose phosphate pathway	4.035108358	0.0021**

Gene	Functions	Fold Change	Glc^low P value
L2HGDH	TCA cycle	1350.917741	0.0004***
SLC1A6	Glutamine transporters and glutaminolysis	1128.135085	0.0003***
TKTL2	Pentose phosphate pathway	910.0008698	0.0002***
GLUD1	Glutamine transporters and glutaminolysis	643.4677859	0.0001***
PDK3	TCA cycle	412.9216104	<0.0001****
PRPS1L1	Pentose phosphate pathway	315.1127052	<0.0001****
SLC16A2	Lactate production and transporters	274.321543	<0.0001****
PKR	Glycolysis	196.6824081	<0.0001****
ME3	Redox balance	179.7345702	<0.0001****
ACAT1	Glycerol/fatty acid/cholesterol synthesis	167.6982838	<0.0001****
LIPF	Fatty acid oxidation	160.8669465	<0.0001****
RBKS	Pentose phosphate pathway	149.0573922	<0.0001****
SLC16A12	Lactate production and transporters	145.9898354	<0.0001****
SLC1A5	Glutamine transporters and glutaminolysis	137.1607715	<0.0001****
CPT2	Fatty acid oxidation	113.7501087	<0.0001****
PRPS2	Pentose phosphate pathway	111.4091653	<0.0001****
UPP1	Nucleotide metabolism	97.66191174	<0.0001****
H6PD	Pentose phosphate pathway	68.58038575	<0.0001****
CPT1B	Fatty acid oxidation	68.58038575	<0.0001****
LDHB	Lactate production and transporters	57.66900053	<0.0001****
ADCY7	Nucleotide metabolism	57.27065165	<0.0001****
PNLIP	Fatty acid oxidation	53.06630212	<0.0001****
CPT1C	Fatty acid oxidation	51.97421341	<0.0001****
PGK2	Glycolysis	47.49567082	<0.0001****
ACOT12	Acetate metabolism	45.87779391	<0.0001****
PFAS	Nucleotide metabolism	44.00892157	<0.0001****
SLC2A6	Glucose transporters	40.49646614	<0.0001****
ACADS	Fatty acid oxidation	39.93893933	<0.0001****
ENO2	Glycolysis	37.78453895	<0.0001****
PDHA2	TCA cycle	33.81810966	<0.0001****
GUCY1A2	Nucleotide metabolism	33.12214302	<0.0001****
GLS-isoform 2	Glutamine transporters and glutaminolysis	32.66614069	<0.0001****
PFKFB2	Glycolysis	29.03506008	<0.0001****
ACSM2B	Glycerol/fatty acid/cholesterol synthesis	28.43752718	<0.0001****
PC	Gluconeogenesis	27.27909947	<0.0001****
HK1	Glycolysis	25.98710671	<0.0001****
ACAD11	Fatty acid oxidation	24.58530101	<0.0001****
MTHFD1	Serine/ glycine/ one-carbon metabolism, Redox balance	22.46682128	<0.0001****
MLYCD	Glycerol/fatty acid/cholesterol synthesis	19.0236756	<0.0001****
SDHD	TCA cycle	18.50347219	<0.0001****
AMP D2	Nucleotide metabolism	16.67626287	<0.0001****
SLC16A10	Lactate production and transporters	15.34529116	<0.0001****
PGAM4	Glycolysis	14.8225742	<0.0001****
ADCY5	Nucleotide metabolism	14.31766291	<0.0001****
MTHFD2L	Serine/ glycine/ one-carbon metabolism	13.1749366	<0.0001****
UEVLD	Lactate production and transporters, TCA cycle	12.81466726	<0.0001****
ADCY9	Nucleotide metabolism	12.55094523	<0.0001****

GLS-isoform 1	Glutamine transporters and glutaminolysis	11.71044597	<0.0001****
SLC1A4	Glutamine transporters and glutaminolysis	10.55404485	<0.0001****
PGAM2	Glycolysis	10.05418416	<0.0001****
SLC2A7	Glucose transporters	9.779251961	<0.0001****
BPGM	Glycolysis	9.779251961	<0.0001****
SUCLA2	TCA cycle	9.644618109	<0.0001****
PCK2	Gluconeogenesis	9.31608701	<0.0001****
XDH	Nucleotide metabolism	8.338131437	<0.0001****
PFKFB3-isoform 3	Glycolysis	7.99847031	<0.0001****
FH	TCA cycle	7.833864171	<0.0001****
PDK2	TCA cycle	7.514744815	<0.0001****
TALDO1	Pentose phosphate pathway	7.309253723	<0.0001****
PCK1	Gluconeogenesis	7.109381795	<0.0001****
SLC38A3	Glutamine transporters and glutaminolysis	6.867210152	<0.0001****
PDK1	TCA cycle	6.451900162	<0.0001****
SDHC	TCA cycle	6.407333632	<0.0001****
DCTD	Nucleotide metabolism	6.146325254	<0.0001****
ACO2	TCA cycle	5.61670532	<0.0001****
PFKM	Glycolysis	5.539378478	<0.0001****
SLC2A11	Glucose transporters	5.501115196	<0.0001****
GMPS	Nucleotide metabolism	5.387903882	<0.0001****
ECI2	Fatty acid oxidation	5.350686912	<0.0001****
SLC38A5	Glutamine transporters and glutaminolysis	4.923636019	<0.0001****
PDHA1	TCA cycle	4.88962598	<0.0001****
GNPNAT1	Hexosamine metabolism	4.755918901	<0.0001****
SLC25A1	Glycerol/fatty acid/cholesterol synthesis	4.69044276	<0.0001****
SLC38A7	Glutamine transporters and glutaminolysis	4.625868048	<0.0001****
IMPDH2	Nucleotide metabolism	4.227263707	<0.0001****
HK2	Glycolysis	4.198063864	<0.0001****

10. LIST OF PUBLICATIONS

1**. Kai Wei**, Mao Li, Margot Zöller, Meng Wang, Arianeb Mehrabi, Katrin Hoffmann (2019). Targeting c-MET by Tivantinib through synergistic activation of JNK/c-jun pathway in cholangiocarcinoma. Cell Death & Disease. 2019; 10:231. doi.org/10.1038/s41419-019-1460-1.

2. Liangtao Ye, Julia Mayerle, Andreas Ziesch, **Kai Wei**, Alexander L. Gerbes, Enrico N. De Toni (2018). The PI3K inhibitor copanlisib synergizes with sorafenib to induce cell death in hepatocellular carcinoma (HCC). Zeitschrift für Gastroenterologie. 2018; 56(05): e22. doi.org/10.1055/s-0038-1648607.

3. Wei Zhang, Gang Zhao, **Kai Wei**, Qingxiang Zhang, Weiwei Ma, Qiang Wu, Ti Zhang, Dalu Kong, Qiang Li, Tianqiang Song (2015). Adjuvant sorafenib therapy in patients with resected hepatocellular carcinoma: Evaluation of predictive factors. Medical Oncology. 2015; 32(4):107. doi.org/10.1007/s12032-015-0549-3.

4. Wei Zhang, Gang Zhao, **Kai Wei**, Qingxiang Zhang, Weiwei Ma, Tianqiang Song, Qiang Wu, Ti Zhang, Dalu Kong, Qiang Li (2014). Adjuvant sorafenib reduced mortality and prolonged overall survival and post-recurrence survival in hepatocellular carcinoma patients after curative resection: A single-center experience. BioScience Trends. 2014; 8(6):333-338. doi.org/10.5582/bst.2014.01120 **(Co-first author).**

5. **Kai Wei**, Meng Wang, Wei Zhang, Han Mu. Tian-Qiang Song (2014). Neutrophil–lymphocyte ratio as a predictor of outcomes for patients with hepatocellular carcinoma undergoing TAE combined with Sorafenib. Medical Oncology. 2014; 31(6): 969. doi.org/10.1007/s12032-014-0969-5.

11. CURRICULUM VITAE

Personal Information

Family name, Given name: Wei, Kai

Date of Birth: 22.12.1988

Place of Birth: Jiangsu, P. R. China

Citizenship: Chinese

Education

09/2016 – present	Hepato-Biliary Research Lab, Department of General, Visceral, and Transplant Surgery, Ruprecht-Karls-University, Heidelberg, Germany
09/2015 – 06/2016	Program student for Medicine, Ludwig-Maximilians-University, Munich, Germany
09/2012 – 06/2015	Master of Medical Science in Oncology, Graduate School, Tianjin Medical University, Tianjin, China
09/2007 – 06/2012	Bachelor of Medical Science, School of Medical Imaging Sciences, Tianjin Medical University, Tianjin, China

12. ACKNOWLEDGEMENT

EIDESSTATTLICHE VERSICHERUNG

1. Bei der eingereichten Dissertation zu dem Thema

Glutamine-Dependent de novo Synthetic Asparagine via ATF4/ASNS/eIF4F Complex Axes for Homeostatic Regulation in Hepatocellular Carcinoma responding to Endoplasmic reticulum (ER) stress

handelt es sich um meine eigenständig erbrachte Leistung.

2. Ich habe nur die angegebenen Quellen und Hilfsmittel benutzt und mich keiner unzulässigen Hilfe Dritter bedient. Insbesondere habe ich wörtlich oder sinngemäß aus anderen Werken übernommene Inhalte als solche kenntlich gemacht.

3. Die Arbeit oder Teile davon habe ich bislang nicht an einer Hochschule des Inoder Auslands als Bestandteil einer Prüfungs- oder Qualifikationsleistung vorgelegt. *

4. Die Richtigkeit der vorstehenden Erklärungen bestätige ich.

5. Die Bedeutung der eidesstattlichen Versicherung und die strafrechtlichen Folgen einer unrichtigen oder unvollständigen eidesstattlichen Versicherung sind mir bekannt. Ich versichere an Eides statt, dass ich nach bestem Wissen die reine Wahrheit erklärt und nichts verschwiegen habe.

Ort und Datum   Unterschrift

* Wenn dies nicht zutrifft, machen Sie folgende Angaben:

3. Die Arbeit oder Teile davon habe ich wie folgt an einer Hochschule des Inoder Auslands als Bestandteil einer Prüfungs- oder Qualifikationsleistung vorgelegt:

Titel der Arbeit:

Hochschule und Jahr:

Art der Prüfungs- oder Qualifikationsleistung: